Universitat de Girona
Escola Politècnica Superior

MAJOR PROJECT

CHEMICAL ENGINEERING DEGREE

Obtaining high-capacity absorption radiopaque surgical gauzes by using modified cellulose nanofibres

THESIS

AUTHOR: Jordi Rutllan Esteba

TUTOR: Marc Delgado Aguilar

EQATA Department

Chemical Engineering Area

JUNE 2019

“As in science and as in life itself, to advance, we must fail; and to fail, we have to keep trying. Only in this way the objective set will be reached.”

AGRAÏMENTS

Des de l'ESO tenia molt clar que allò que més m'agradava era la química i la tecnologia, és per això que sempre he tingut clar que el meu objectiu era poder cursar la carrera d'Enginyeria Química. Ara bé, el món de la medicina també m'ha cridat molt l'atenció, ja que des de ben petit he pogut viure la passió i he sentit la necessitat d'ajudar aquells que més ho requereixen. És per això que finalment, he enfocat aquest treball de final de grau en allò que més m'agrada, relacionant tot el que he après al llarg d'aquest petit viatge de quatre anys per poder-ho aplicar a allò que en aquests moments és el que més em desperta la curiositat per seguir investigant, l'enginyeria biomèdica.

Dit això, en primera instància m'agradaria expressar el meu sentit agraïment al Dr. Marc Delgado Aguilar per tots els coneixements que m'ha concedit, l'assessorament i la seva total disponibilitat en tot moment durant la realització d'aquest projecte.

A continuació, voldria agrair a tots els meus familiars, en especial atenció als pares i a l'Emma, per tots els esforços que han posat en mi, fins i tot en els moments més difícils, perquè hagin estat capaços de mantenir-me amb l'autoestima elevada; a l'Anna i a la Clara, perquè més enllà de les distàncies que ens separen sempre troben qualsevol moment per ajudar-me de la millor manera possible.

Finalment, també m'agradaria donar les gràcies a tot el personal del grup de recerca LEPAMAP, pel seu constant interès i motivació mostrada per tal que el treball esdevingués millor. Així com tampoc em voldria oblidar del Dr. Joan San Molina, qui des d'un inici ha cregut en mi i en les meves capacitats per tal de treballar en gran part en una línia de recerca en la qual encara no he desenvolupat al màxim els meus coneixements.

TABLE OF CONTENTS

FIGURES LIST

TABLES LIST

ABBREVIATURES

AN: A fungus named *Aspergillus Nigger.*

AT: Aerogel made with TEMPO nanofibres.

AE: Aerogel made with enzymatic nanofibres.

BNC: Bacterial nanocellulose.

BS: Bacterium named *Bacillus.*

CC: Carboxylic content of the nanofibres.

CD: Cationic demand of the nanofibres.

CNC: Crystalline nanocellulose.

CNF: Cellulose nanofibres.

DP: Degree of polymerization.

FE-SEM: Field emission of scanning electron microscopy.

HCl: Hydrochloric acid.

ICS: Wealth Catalan institute

JTH: Josep Trueta Hospital.

NaBr: Sodium Bromide

NaClO: Sodium Hypochlorite.

SS: Specific surface.

ST-ST: Stress – strain curves.

TEMPO: 2,2,6,6-tetramethylpiperidine-1-oxyl radical

TiO_2: Titanium dioxide.

VWT: Vertical wicking test.

WAT: Water absorption value.

WHT: Water holding time test.

1 INTRODUCTION

1.1 BACKGROUND

Climate change is currently one of the most debated issues in any part of the world. This is because day after day the global temperature of the planet increases unceasingly. Until someday, the effect caused by this environmental phenomenon become irreversible and we are no longer able to do anything.

The main cause of this change comes from the large quantity of greenhouse gauzes that are release, apart from automobiles, from manufacturing companies, etc. Every industry must have several basic services, for example boilers to generate steam, which is a source of pollution gauzes. If we also add the fact that many production processes release other polluting gauzes, the generated volume increases by time. However, this is not the only cause of the problem since we should also take into account the large amount of waste that we generate and we do not manage properly, either because we do not know how to do it or because we are not responsible enough and we throw them wherever. Of these generated wastes, some can be renewable or recyclable, but in proportion to the amount of waste that does not fit into these two previous groups is much greater. Consequently, at the time of wanting to manage these wastes, the only possible solution to extract any benefit is to incinerate them or deposit them in a dump. The first option, used to generate energy that could also be generated from renewable sources, produces a large amount of polluting combustion gauzes; on the other hand the second option is damaging to the environment, since it is necessary to have a large surface without inhabitants in its proximity, with specific geological conditions and where the waste will take thousands of years to decompose.

Although government agencies around the world are trying to establish new guidelines to solve it, it is not enough. For this reason, every day in the engineering fields, the application of what is known as green engineering is more important. It consists on the design and development of production processes or objects environmentally sustainable and economically profitable.

In order to continue with this tendency, it is very important to focus on improving the development of objects or materials most used, either by creating new products or by improving its properties, using materials from renewable sources to make more profits. Subsequently, once its useful life has been exhausted, the objects and material should be eliminated more easily and environmentally cleaner, such as the case of medical tissues.

1.2 OBJECTIVES

The present final degree work has been carried out in order to fulfil several objectives: the first and most important one is to try to improve the absorption capacity of conventional gauzes such as those that can be obtained from a pharmacy or those used in medical centres. The second main objective of this project is to find a possible substitute for the titanium threads which are sewn in surgical gauzes.

On the other hand, in order to substitute gauzes for a consumable easier to manage once their useful life ends, it will be evaluated the possibility to manufacture highly absorbent aerogels.

However, it is a secondary objective to improve some other properties of these type of medical fabrics, such as evaporation, capillarity and mechanical properties.

Therefore, the general purpose of this research is to aid biomedical companies sensitized and worried about sustainable development to improve constantly their products to be more competitive.

1.3 SCOPE

Taking into account the objectives set out above, the research will start by carrying out a type of market study to know the initial properties value to be exceeded. All types of analyses are going to be done on the reference gauze (provided by Josep Trueta's Hospital) and as well as on other gauzes that can be used in a surgery or can be bought in a pharmacy. More specifically, the studies that will be carried out are: water absorption tests, water holding time tests, capillarity tests and stress-strain tests.

Once the initial properties of gauzes are known, the research will proceed to the production of cellulose nanofibres, obtained from eucalyptus paper fibres. Subsequently, in order to improve the properties of the studied gauzes, part of the nanofibres produced will be infused to different gauze brands, while the rest will be used to produce aerogels. During this phase, we will also add some titanium dioxide and glycerol to some gauzes and only titanium dioxide to aerogels in order to prepare all the samples we need.

Once all the samples are ready, all the analysis mentioned above will be repeated to see if nanofibres have produced an improvement on gauzes and if there are differences between aerogels. However, clinical trials on gauzes and aerogels will be carried out to ensure the preservation of biocompatibility with the human body. In particular, antimicrobial tests will be done.

Finally, the effect of titanium threads substitution by nanoparticles of titanium dioxide will be checked by applying X-rays on different samples. This test will allow to determine if it possible to maintain the radiopacity of the surgical gauzes, using less quantity of a cheaper substances.

2 LITERATURE REVIEW

2.1 BIOMEDICAL ENGINEERING ON MEDICAL TISSUES

In engineering can be found many different specialities. In some of them, research have been done for many years but in others, as is the case of biomedical engineering, which is considered a relatively new discipline without a huge wealth of knowledge. However, within this specialty it is possible to find some branches where a lot of research has been dedicated and others where researchers are just beginning to focus. In the last case, the research applied to medical tissues could be an example.

To get an idea of which are the objects that could be found in this family, a classification has been made according to three different groups: quotidian consumables, special consumables and those that could be classified in either of the two previous groups. *Table 1* shows some of the examples that are part of each family.

Table 1: Classification of some consumable medical tissues in function of their uses.

QUOTIDIANS CONSUMABLES	SPECIAL CONSUMABLES	BOTH USES
Handkerchief	Patches	Gauzes
Wipes	Protective facial mask	Diapers
Strips	Surgical fields	Bandages

Even though it does not seem like, all of these useful objects, among others, are very used each day despite having a high cost and generating a huge amount of waste because they have disposable uses. In certain cases, depending on what they have been used for or the place where have been used, their waste management and subsequent elimination is much more complicated. For example, all those gauzes used in Primary Care Centres or hospitals have a special treatment, so they are considered a sanitary waste to prevent infections to other people because can contain pathogenic microorganisms.

Once again, this point of view allows us to see the importance of making an economical, sustainable and with greater applicability design; in order to make life easier for those people or institutions that use them daily, and those who subsequently have to manage the generated waste.

2.1.1 GAUZES, SUCH AN IMPORTANT TOOL FOR DOCTORS

Gauze, which is derived from the Persian word meaning "raw silk", is a thin, transparent fabric of synthetic or natural material used for different purposes. Gauzes are a type of mesh, with more or less threads, and the number of threads is what determines the quality of the gauzes. Today, it is possible to find meshes of many types and with different thread structures. Mainly, it distinguishes between cotton gauzes (woven fabrics) and unwoven gauzes or dressings (Medical Market, 2016).

Traditionally, cotton gauzes are the most widely used to cover and protect wounds without getting into contact with the air and all types of external agents. These are usually classified according to: number of threads, number of folds and size. On the other hand, as already stated, there are also non-knit gauzes. These are gauzes manufactured with 70% of viscose and 30% of polyester; without bleaching agents or surfactants; highly absorbent, soft and permeable to the air, which can be cut without leaving any threads (Medical Market, 2016).

Viscose is a viscous organic liquid used in the manufacture of rayon and cellophane. This was discovered in 1884 by the French scientist and industrialist Hilaire de Chardonnet (inventor of the first artificial textile fibre) and later patented by three British scientists, Charles Frederick Cross, Edward John Bevan and Clayton Beadle, in 1891. To produce it, cellulose from wood or cotton fibres is used. Then, it is treated with sodium hydroxide, and mixed with carbon disulphide to form cellulose xanthate, which is dissolved in more sodium hydroxide. Lastly, the resulting viscose is extruded through a small hole to make rayon (which is sometimes also called viscose) (Barnhardt Natural Fibers, 2019).

Figure 1: Many different types of medical wound dressings.

To get an idea of the importance of these consumables, according to the ICS, 2017 the Josep Trueta's Hospital (JTH) in Girona performed 10.281 major surgery interventions and 10.420 outpatient minor surgery interventions (42 surgeries/day) and according to the medical professionals consulted, in each of these operations the gauzes consumption can be established approximately to 100 per operation, that is about 500 gauzes per day (this approach is variable depending on the type of action to be performed and the patient to whom it is carried out). These statistics do not consider the amount of gauzes that are also consumed in other areas of a health care centre (external consultations, emergency rooms, etc.).

To understand better the importance of these tools, it is also needed to know why they are used exactly. The best-known function for most people is to clean all kinds of skin wounds that can be injured and prevent them from entering as long as possible with the air to avoid infections, as they are sterilized. But they do not only have this function, since putting ourselves in the skin of a surgeon a gauze is more than just an object to clean; professionals use them to detect if there is a bleeding in certain areas while they are doing an operation: if the gauze stays with its original white colour it means that there is no loss of blood, but if the gauze begins to stain of red, it means that in this point there is a bleeding. Therefore, it can be appreciated how it is not only an object to clean surfaces, but also a very effective visual indicator in the event of haemorrhages (Osorio et. al, 2012).

In addition, can be many different types of medical gauzes, but it should be noted that those that are used in surgery have a different peculiarity from others, so they incorporate a titanium metal thread into their structure to provide them with radiopacity. The reason is because in an intervention all the used gauzes are counted, this way, before the surgeon proceeds to the insertion closing, all the gauzes are withdrawn from the patient and recounted. If some of them are lost, it is immediately known (the gauzes size is very variable, you can use gauzes from 1 cm up to 30 cm depending on the intervention). If there is a lack of gauzes due to the fact that some has shifted to another area of the body during the operation, a visual search is first performed, but if they do not find it, then an X-ray radiography is performed and thanks to the thread of titanium can be easily removed.

After understanding all these exposed data and examples it is easily appreciated why they are so important throw-away objects. Looking to the volume consumed of this product for a single hospital in one year and taking into account the rest of hospitals around the world, it is entirely understandable the need of trying to improve the properties to extract the maximum performance possible, or at least, turn it into an easy product to manage once its useful life is over.

2.2 PAPER FIBRES, THE RAW MATERIAL

Before talking about the different types of nanofibres and their production, you must know better which raw material will be used, paper fibres, where cellulose, hemicellulose and lignin are the main constituents of the cell wall of the fibres. The morphology of fibres depends primarily on the composition and structural organization of these constituents. The chemical composition of fibre varies a lot depending on the type of wood and/or vegetable from which they come, since these materials are extremely heterogeneous. However, it contains non-polymeric minority compounds, which depending on their quantity and type industrial processes can be affected. The constituents of fibre together with their main chemical characteristics are described in *Table 2* (El Aboussi, 2016).

Table 2: Description of natural fibres constituents. Source: *El Aboussi, 2016*.

CONSTITUENTS	NATURAL STATE	MONOMER FORMED	DEGREE OF POLYMERIZATION	STRUCTURE
Cellulose	linear crystalline polymer	D-glucose	3000 – 10000	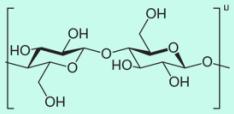
Hemicellulose	branched and amorphous heteropolymer	Pentose and hexose	150 – 200	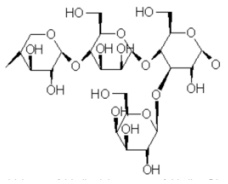
Lignin	amorphous three-dimensional macromolecule	Alcohols	100 - 200	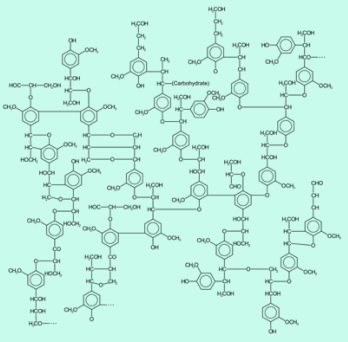
Extracts	Various	-	-	-

At histological levels, fibres have an empty central cavity, called lumen, and a cell wall divided into layers, as shown in Figure 2. Lignin is more concentrated in the middle lamella, which is the outer layer that connects the cell walls of the contiguous fibres. The rest of the layers of the vegetal wall, including the secondary wall

that is the thickest layer, also present a certain content of lignin but they are mainly constituted by cellulose and hemicellulose. As shown in the same figure, lignin of the secondary wall forms an amorphous matrix that protects polysaccharides from microbial degradation and enzymatic hydrolysis in general.

As entering into the fibre, cellulose and hemicellulose are exposed, which will give the ability to bind the fibres due to the surface density of the hydroxyl groups they present. The function of each component is clear: lignin acts as a natural adhesive of the fibres giving stability to the wood; cellulose, on the other hand, is the component that gives resistance to fibres. Finally, the hemicelluloses have the function of associating the lignin with the cellulose, creating links between both so that each one exerts its function and thus, ensure a good distribution of efforts (KTH, 2019).

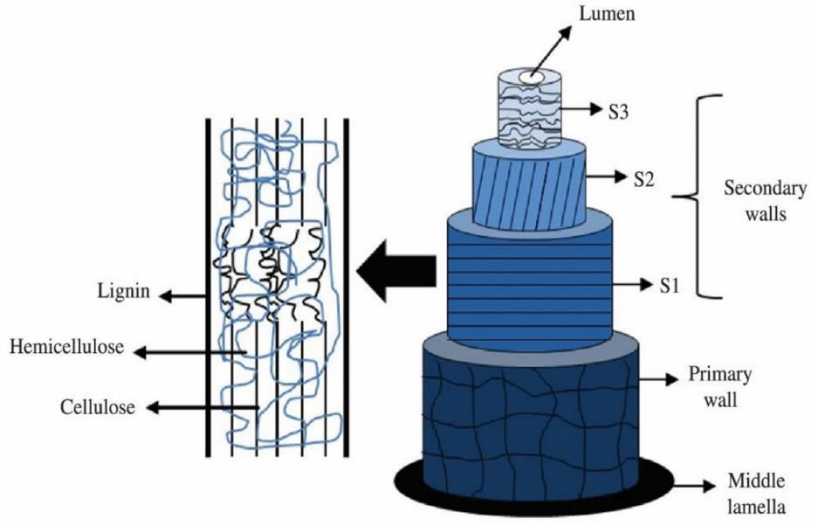

Figure 2: Layers distribution on a vegetable fibre. Source: El Aboussi, 2016.

2.3 CELLULOSE NANOFIBRES

Cellulose is the most abundant biological molecule in the earth, becoming the highest percentage of biopolymers on earth (Klemm, Heublein, Fink, & Bohn, 2005). This biological polymer is mainly synthesized in the cell walls of plants: approximately 33% of all the matter of plants and vegetables is cellulose. With the emergence and development of nanotechnology, cellulose, the most ancient and important natural polymer on earth revives and attracts more attention in the new form of ‘‘nanocellulose’’ to be used as novel and advanced material. Nanocellulose is described as the product or extract from native cellulose (found in plants, animals, and bacteria) composed of the nanoscaled structure material.

Generally, the family of nanocellulose can be divided in three types, (1) cellulose nanocrystals (CNC), with other designations such as nanocrystalline cellulose, cellulose (nano) whiskers or rod-like cellulose microcrystals; then also exists the (2) cellulose nanofibrils (CNF), with the synonyms of nanofibrillated cellulose (NFC), microfibrillated cellulose (MFC) or cellulose nanofibres; and finally (3) bacterial nanocellulose (BNC), also referred to as microbial cellulose. To have an idea of how they look like, all three types of nanofibres can be seen in Figure 3 (Lin & Dufresne, 2014a).

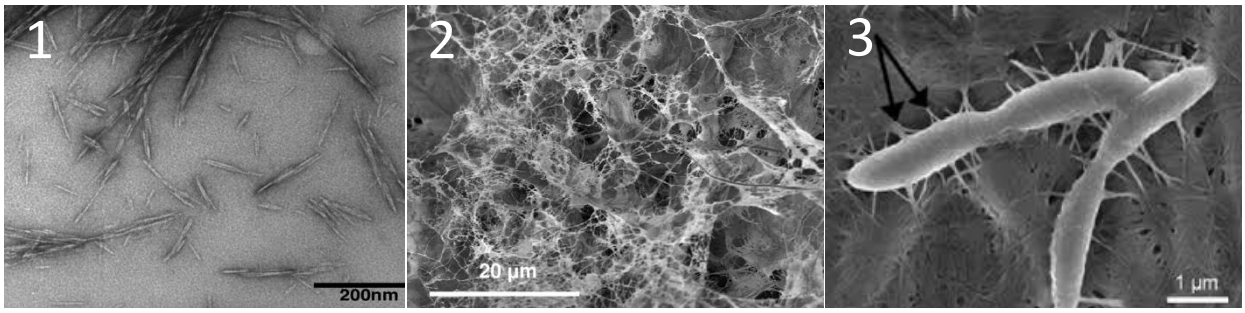

Figure 3: Structure of different types of nanocellulose: 1) CNC, 2) CNF and 3) Glucanobacter bacteria forming BNC. Source: Wallace & Venere, 2018; FARS news agengy, 2014; Lin & Dufresne, 2014 .

The sources for CNC and CNF extraction are wood, cotton, hemp, flax, wheat straw, sugar beet, potato tuber, mulberry bark, ramie, algae, and tunicin. As shown in Figure 3 (1 and 2), the production of CNC or CNF consist on a transformation procedure from the large unit (cm) to the small unit (nm). To achieve this change, chemically induced destructuring strategy, such as acid hydrolysis, is commonly performed for the extraction of CNC from native cellulose, through the removal of amorphous regions and preservation of highly crystalline structure. The released nanoparticles (CNC) present a diameter of 5–30 nm, and length of 100–500 nm (from plant cellulose), or length of 100 nm to several micrometers (from tunicate and algae celluloses). With microscopic observations and light scattering techniques, the morphology and dimensions of CNC can be assessed as elongated rod-like (or needle-like) nanoparticles, and each rod can therefore be considered as a rigid cellulosic crystal with no apparent defect.

Regarding the preparation of CNF, mechanically induced destructuring strategy is mainly applied, which involves high-pressure homogenization and/or grinding before and/or after chemical or enzymatic treatment. Multiple mechanical shearing actions can effectively delaminate individual microfibrils from cellulosic fibres. Different from rigid CNC, CNF consists of both individual and aggregated nanofibrils made of alternating crystalline and amorphous cellulose domains, which attributes the morphology of CNF with soft and long chains. Due to the entanglement of long cellulosic chains, it is not so easy to determine the length of CNF

(commonly regarded as higher than 1 μm) with microscopic techniques. Therefore, only the information of fibril width for CNF is generally provided in the studies, which varies from 10 to 100 nm depending on the source of cellulose, defibrillation process and pre-treatment.

Contrary to the production of CNC and CNF, the biosynthesis of BNC is a process of construction from tiny unit (Å) to small unit (nm). As shown in Figure 3 (3), BC is typically synthesized by bacteria (such as *Acetobacter Xylinum*) in a pure form which requires no intensive processing to remove unwanted impurities or contaminants such as lignin, pectin and hemicellulose. During the biosynthesis of BC, the glucose chains are produced inside the bacterial body and extruded out through tiny pores present on the cell envelope. With the combination of glucose chains, microfibrils are formed and further aggregate as ribbons (nanofibres). These ribbons subsequently generate a web-shaped network structure with cellulosic fibres (BNC), which has a diameter of 20–100 nm with different types of nanofibre networks (Lin & Dufresne, 2014a).

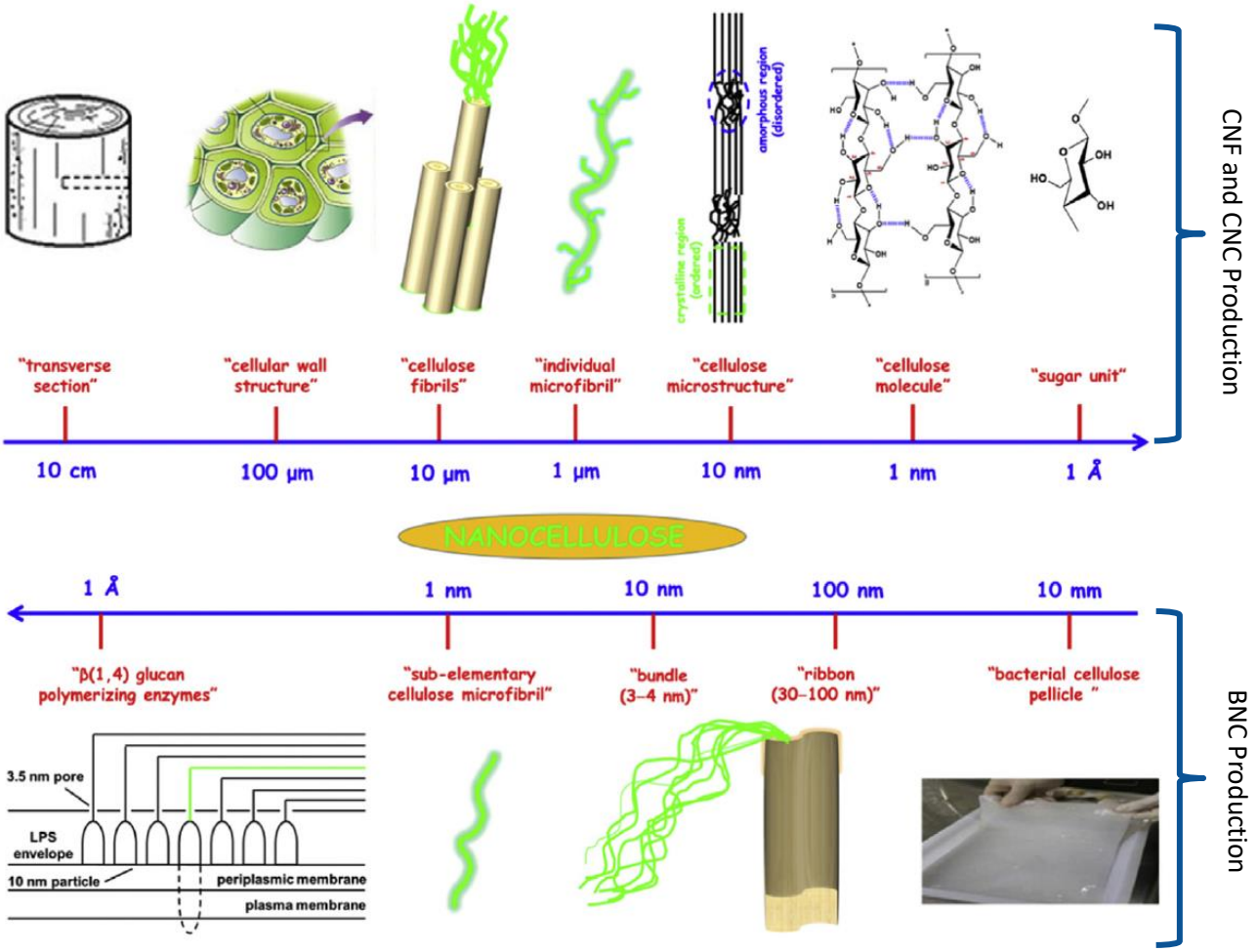

Figure 4: Scheme of the transformation process of nanocellulose depending on the method selected. ***Source:*** *Lin & Dufresne, 2014.*

2.3.1 PROPERTIES

As natural nanoscaled material, nanocellulose possesses diverse characteristics different from traditional materials, including special morphology and geometrical dimensions, crystallinity, high specific surface area, rheological properties, liquid crystalline behavior, alignment and orientation, mechanical reinforcement, barrier properties, surface chemical reactivity, biocompatibility, biodegradability, lack of toxicity, etc. (Österberg & Cranston, 2014).

All the properties of nanocellulose can be generally classified in three parts: visual physical properties, surface chemistry, and biological properties. Associated with the topic ‘‘biomedicine’’, the emphasis of this projects is mainly placed on the mechanical reinforcement, surface groups and charges, as well as various biological properties of nanocellulose applied on gauzes improvementc.

MECHANICAL PROPERTIES

The mechanical properties of nanocellulose can be characterized by its properties in both regions of the nanoparticle, the ordered (crystalline) and disordered (amorphous): cellulosic chains in disordered regions contribute to the flexibility and plasticity of the bulk material, while those in ordered regions contribute to the stiffness and elasticity of the material. The modulus of different types of nanocellulose is expected to result from a mixing rule between the modulus of the crystalline domains and the amorphous fraction (see Figure 5). Therefore, the stiffness and modulus of CNC with more crystalline regions should be higher than those of CNF and BC fibrils with both crystalline and amorphous structures (Lin & Dufresne, 2014a).

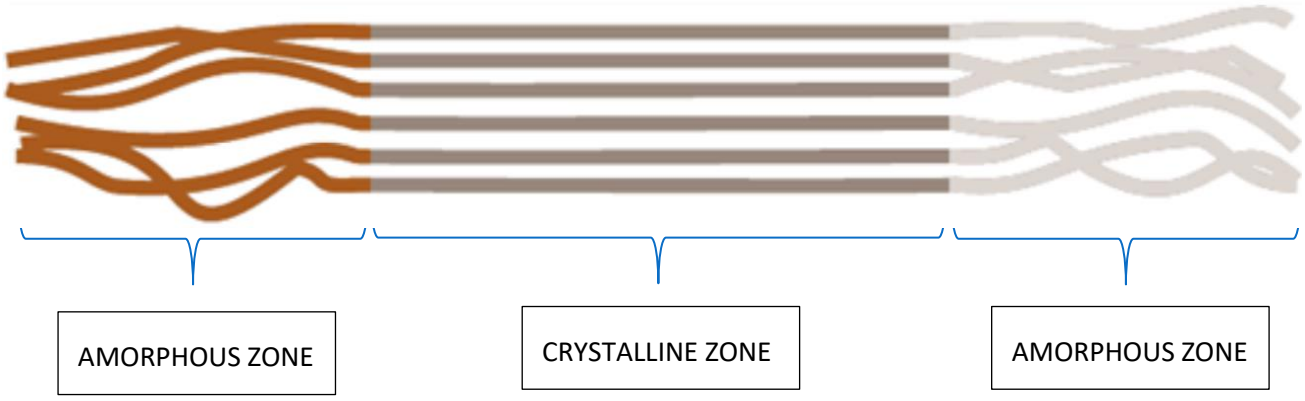

Figure 5: Scheme of the different zones distribution that exist on a polymeric cellulose chain.

Since 1930s, the elastic modulus of crystalline cellulose has been investigated either by theoretical evaluations or by experimental measurements (wave propagation, X-ray diffraction, Raman spectroscopy, and atomic

force microscopy). A broad range of values was reported, and it is generally accepted that the Young's modulus of crystalline cellulose (assimilated to the one of CNC) should be in the range 100–200 GPa, which gives specific values similar to Kevlar (60–125 GPa) and potentially stronger than steel (200–220 GPa). Recently, the elastic modulus of crystalline cellulose was investigated from atomistic simulations using both the standard uniform deformation approach and a complementary approach based on nanoscale indentation, which was reported as 139.5 ± 3.5 GPa, similar to Kevlar (Wu ' et al., 2013). In another study, Dri et al. performed the atomic structure model of cellulose in tandem with quantum mechanics to compute the Young's modulus of crystalline cellulose, which predicted the modulus of crystalline cellulose as high as 206 GPa, similar to steel.

Again, a broad range of values for the longitudinal modulus of cellulose microfibrils (involving both CNF and BC) was reported based on different theoretical and experimental strategies. The accepted average value is around 100 GPa for the modulus of cellulose microfibril. A three-point bending experiment using atomic force microscopy tips was performed on cellulose microfibrils to calculate the elastic modulus. The dimension of cellulose microfibrils was found to significantly affect the mechanical properties, and a value of 81 ± 12 GPa was reported to be the longitudinal modulus of pulp CNF (Cheng, Wang, & Harper, 2009). Recently, the modulus of BC was reported as 114 GPa through the analysis of a Raman spectroscopic technique, which involved the determination of local molecular deformation of BC via a shift in the central position of the 1095 cm^{-1} Raman band (Hsieh, Yano, Nogi, & Eichhorn, 2008).

Originated from these impressive mechanical properties, nanocellulose has been potentially used as a loadbearing element for various host materials. With the homogenous dispersion and strong interfacial adhesion, the presence of high-modulus nanocellulose can exhibit the promising nano-reinforcement allowing proper stress transfer from host material (matrix) to the reinforcing phase (nanocellulose).

CHEMICAL PROPERTIES

From a structural point of view, cellulose is a high molecular weight homopolysaccharide composed of b-1,4-anhydro-D-glucopyranose units (Figure 6). These units do not lie exactly in the plane with the structure, but rather they assume a chair conformation with successive glucose residues rotated through an angle of 180º about the molecular axis and hydroxyl groups in an equatorial position (Habibi, Lucia, & Rojas, 2010). The ability of these hydroxyl groups to form hydrogen bonds plays a major role in the formation of fibrillar and semicrystalline packing, which governs the important physical properties of this highly cohesive material (Kroschwitz & Seidel, 2004).

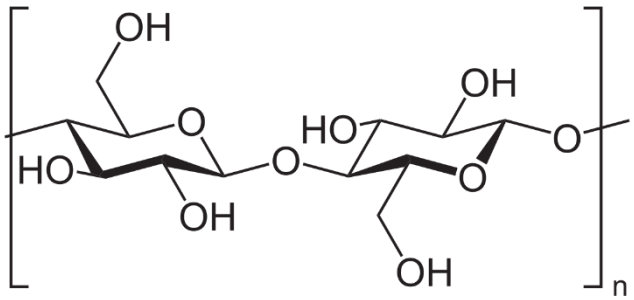

Figure 6: Chemical structure of cellulose monomer.

It is well known that the unidirectional parallel orientation of cellulose chains within the elementary fibrils, occurring during biosynthesis and deposition, induces the formation of crystals having hydroxyl functionality on one end, known as the non-reducing end (shown in pink in Figure 7), and hemiacetal functionality on the other, known as the reducing end (shown in green in Figure 7).

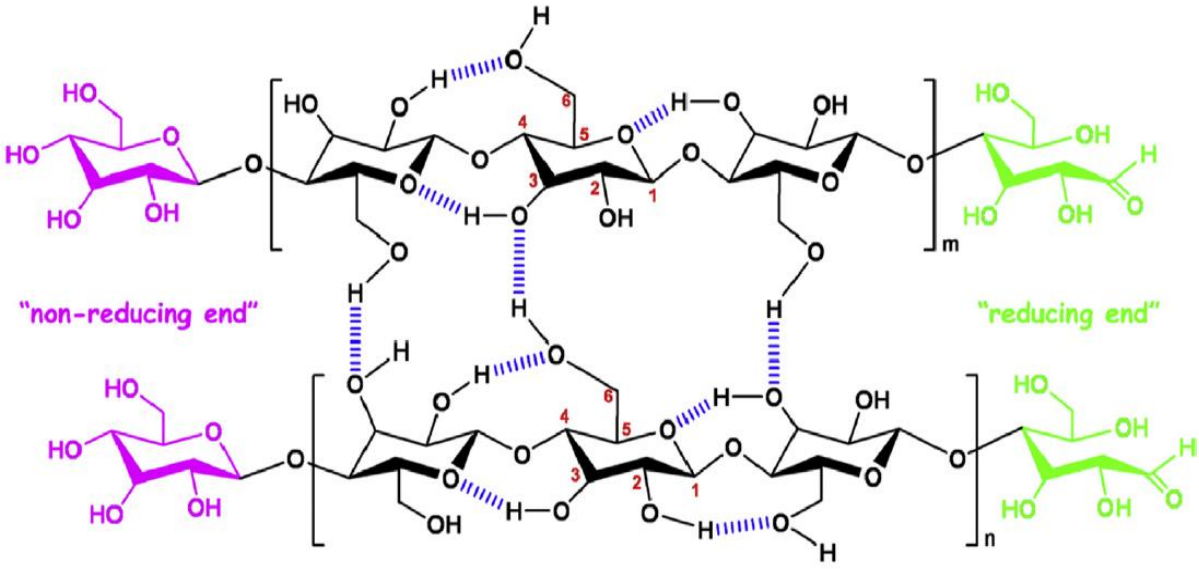

Figure 7: Schematic representation of chemical structure and intra-, inter- molecular bonds in cellulose. Source: Lin & Dufresne, 2014.

One of the most specific characteristics of cellulose is that each of its glucose unit bears three hydroxyl groups, which endows nanocellulose a reactive surface covered with numerous active hydroxyl groups. For each anhydroglucose unit, the reactivity of hydroxyl groups on different positions is heterogeneous. The hydroxyl group at the 6 position acts as a primary alcohol whereas the hydroxyl groups in the 2 and 3 positions behave as secondary alcohols. Indeed, the carbon atom which carries the hydroxyl group in the 6 position is only attached to one alkyl group, while the carbons with the hydroxyl groups in the 2 and 3 positions are joined

directly to two alkyl groups, which will induce steric effects derived from the supramolecular structure of cellulose and the reacting agent. It has been reported that on the structure of cellulose, the hydroxyl group at the 6 position can react ten times faster than the other OH groups, while the reactivity of the hydroxyl group on the 2 position was found to be twice that of at the 3 position (Hebeish & Guthrie, 1981). However, regarding the surface reactivity of hydroxyl groups from nanocellulose, the use of reactants or solvents may affect the reactivity of hydroxyl groups from different positions (de la Motte et al., 2011).

BIOLOGICAL PROPERTIES

When talking about biological properties we can refer to such different properties, but while talking about cellulose nanofibres for medical applications, the most important properties to focus on are: the biocompatibility of the material with tissues, the biodegradability of the material in determined conditions and also the toxicology of the material.

Biocompatibility is the ability of a foreign material implanted in the body to exist in harmony with tissue without causing deleterious changes, which is an essential requirement for biomedical materials (Dugan et al., 2013). Regarding the evaluation of cellulose biocompatibility, different studies provide various results due to the range of methodologies and sample preparations. According to some reports (Märtson, et al., 1999; Miyamoto, et al., 1989), cellulose can be generally considered to be broadly biocompatible, invoking only moderate (if any) foreign body responses *in vivo*. However, it is well known that cellulose is not readily degraded by the human body because it lacks cellulolytic enzymes, which will inevitably cause some incompatibility.

Hemocompatibility (or blood compatibility) is another significant property of biocompatibility, especially for blood-contacting biomaterials (gauzes) and artificial organs, such as artificial blood vessels, pumps and artificial hearts. Interestingly, recent study reported the regulation of blood metabolic variables by the presence of TEMPO-oxidized cellulose nanofibres. It seems that TEMPO oxidized cellulose nanofibres have both promising hemocompatibility and unique biological activities (Shimotoyodome et al., 2011).

Attributed to its biosynthesis procedure, BC is commonly regarded as a material possessing better biocompatibility than other types of nanocellulose. Some sources explain that subcutaneous *in vivo* implantations were carried out on mice and the worst results were the appearance of a mild and benign inflammatory reaction that decreased with time and did not elicit a foreign body reaction (Helenius et al., 2006).

For some applications (e.g. artificial heart valves or menisci), biocompatible, non-biodegradable materials may be acceptable whereas for other applications (e.g. artificial bone grafts), the bioresorbable material enabling tissue regeneration is preferable (Petersen & Gatenholm, 2011). In terms of biodegradation, cellulose may be considered as nonbiodegradable *in vivo* or, at best, slowly degradable, due to the lack of cellulase enzymes in animals. However, the form (i.e. crystallinity, hydration and swelling) of cellulose may affect the degree of degradation, absorption and immune response.

In an early *in vivo* study, Miyamoto et al. found that the degradation of cellulose and cellulose derivatives in canine specimens depended significantly on the cellulose crystalline form and chemical derivatization (Miyamoto et al., 1989). Recently, oxidized cellulose was rendered more vulnerable to hydrolysis and therefore potentially degradable by the human body. Based on this strategy, researchers attempted to enhance the biodegradability of nanocellulose through oxidation, such as the report of improving BC degradability *in vitro* (in water, phosphate buffered saline, and simulated body fluid) through periodate oxidation (Li et al., 2009; Luo et al., 2013).

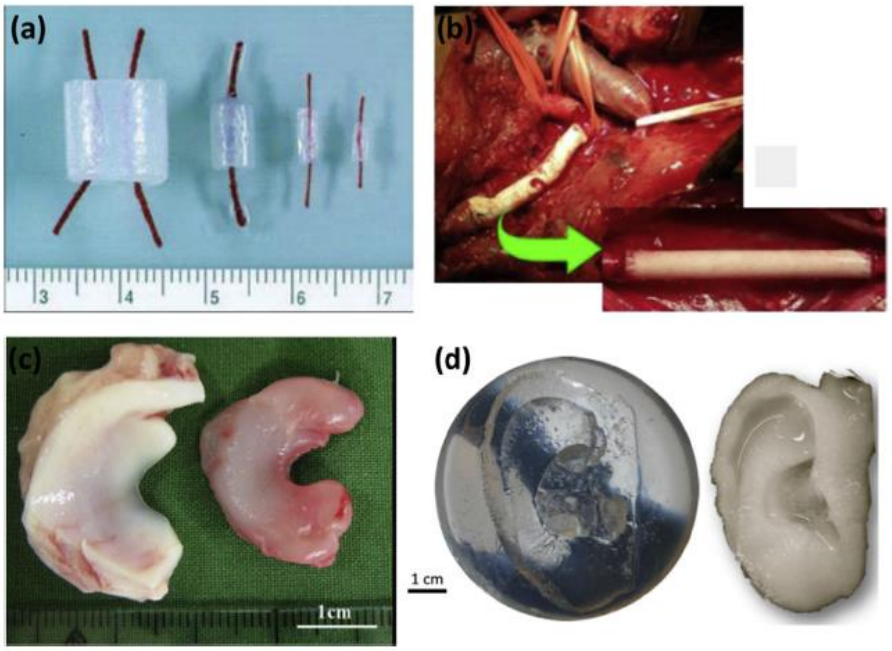

Figure 8: Examples of substitutes from nanocellulose: a) BASYC, BActerial SYnthesized Cellulose (BC tubes) with different dimensions. (b) Vascular prostheses made of CNF-polyurethane placed between the brachiocephalic trunk and the right common carotid artery in male patient. (c) Comparison between pig meniscus (left) and BC hydrogel (right). (d) Negative silicone mold used to guide the bacteria during culture to reproduce the large-scale features of the outer ear (left); and 3D implant prototype (1% effective cellulose content) produced in the shape of the whole outer ear according to the 3T MRI scanning technique (right). Source: Lin & Dufresne, 2014.

nanomaterials should be further emphasized. Since the beginning over twenty years ago, the nanotoxicology research for nanoparticles has built a comprehensive assessment system, such as for metallic nanoparticles (Au, Ag nanoparticles, quantum dot, etc.) and carbon nanotubes. However, the toxicology study of nanocellulose and nanocellulose based bio-composites is still restricted at a very preliminary stage (mainly on the level of cytotoxicity). Table 3 summarizes recent reports on toxicology experiments and conclusions for nanocellulose. On the whole, there is no evidence for serious influence or damage of nanocellulose on both cellular and genetic level as well as *in vivo* organ and animal experiments. However, the inhalation of plentiful nanocellulose (especially for CNC) may induce pulmonary inflammation due to the easy self-aggregation and none degradation of nanocellulose in the body of animals (Lin & Dufresne, 2014).

Table 3: Toxicological evaluation of cellulose nanofibres. Source: Lin & Dufresne, 2014.

TYPE	***EXPERIMENT CARRIED OUT***	***CONCLUSIONS***
CNC	Acute lethal test	Low toxicity potential
	Multi-trophic assays	Low environmental risk
	Animal experiments with fathead minnow and Zebrafish reproduction tests	
	In vitro rainbow trout hepatocyte assay	
	Respiratory toxicity of aerosolized CNC on the human airway with a co-culture of human monocyte-derived macrophages, dendritic cells and a bronchial epithelial cell line	Low cytotoxicity Somewhat **(pro-)inflammatory cytokines**
	In vitro gene mutations	No evidence of high toxicity
	In vitro and *in vivo* chromosomal tests	
	Skin irritation and sensitization tests	
	Animal experiments with rat feeding study (28 d)	
	Cytotoxicity evaluation with L929 cells	Low cytotoxicity at low CNC concentration
	Cytotoxicity evaluation with nine different cell lines	No cytotoxic effects in the concentration range (0–50 μg/mL) and exposure time (48 h)
CNF	Cytotoxicity evaluation with human monocyte and mouse macrophages	No evidence of inflammatory effects or cytotoxicity
	Kinetic luminescent bacteria test for acute environmental toxicity	

	In vitro genotoxicity with enzyme comet assay	No significant DNA damage
	Neurotoxicity and systemic effects with a nematode model	Low or no cytotoxicity
	In vitro pharyngeal aspiration study for pulmonary immunotoxicity and genotoxicity with mice	No DNA and chromosome damage Pulmonary inflammation
	Cytotoxicity evaluation with 3T3 fibroblast cells (including the test of cell membrane, cell mitochondrial activity and DNA proliferation)	No toxic phenomena for pure CNF Somewhat cytotoxicity for modified-CNF (with PEI or CTAB surface modification)
	Cytotoxicity evaluation with bovine fibroblasts cells	Low cytotoxicity at low CNF concentration (0.02–100 μg/mL)
	Effects of gene expression in vitro	Reduction of cell viability and affection of the expression of stress- and apoptosis-associated molecular markers at high CNF concentration (2000–5000 μg/mL)
	Cytotoxicity evaluation with human dermal fibroblasts	No evidence of cytotoxicity for pure CNF Improved cytocompatibility of EPTMAC-modified CNF
BC	Cytotoxicity evaluation with osteoblast cells and L929 fibroblast cells	No evidence of cytotoxicity
	Cytotoxicity evaluation with human umbilical vein endothelial cells	No evidence of toxicity in vitro and *in vivo*
	Animal experiment with C57/Bl6 male mouse	
	In vitro immunoreactivity with human umbilical vein endothelial cells	Non-toxicity and non-immunogenicity
	In vivo intraperitoneal injection study with BALB/c male mice	

Abbreviations: *PEI, polyethyleneimine; CTAB, cetyl trimethylammonium bromide; EPTMAC, glycidyl trimethylammonium chloride.*

2.3.2 CNF MEDIATED BY AN OXIDATION REACTION

As said, there are different methods to make CNF. One of them is the oxidation reaction; so in order to develop it well for the correct CNF formation previously it should be understood how this type of reaction works. Only this way it will be able to comprise what is taking place in each moment and when nanofibres with suitable characteristics can obtained.

The oxidation reaction is between the raw material, the natural cellulose fibres, and sodium hypochlorite (NaClO), commercially known as bleach. During the reaction, what takes place is the exchange of the primary alcohols present in the amorphous ramifications of the cellulosic structure by carboxylic groups. Since these last molecules are bigger than the primary alcohol ones, the polymer chain breaks into different parts, giving rise to fractions of lower size that is what really interests.

Subsequently, the nanofibres solution reacts with the sodium hydroxide (NaOH) formed in the oxidation reaction from the union of sodium bromide (NaBr) and hydroxyl groups released. Therefore, in this last reaction, the hydrogens of carboxylic groups are exchanged for sodium atoms, what concludes with the obtaining of cellulose molecules of lesser size charged negatively. The adopted final structure by the cellulose fibres causes an increase on the repulsion between chains, so it is reflected on the increasment of the surface area from the general structure. As well as, a better distribution is achieved and all these improvements will allow molecules to capture more water.

However, in normal conditions it will take lot of time to achieve the appropriate performance of the reaction. Therefore, the help of some catalyst product is needed and that is the TEMPO catalyst (2,2,6,6-tetramethylpiperidine-1-oxyl radical), the additive chosen in order to achieve the expected performance, effects and improvements to the properties and uses of cellulose fibres with less time than it will normally take.

Catalytic oxidation using TEMPO has opened a new field of efficient and selective conversion chemistry of alcoholic hydroxyl groups to aldehydes, ketones and carboxyl groups under mild conditions. Many related studies have been extensively carried out in the last two decades, and have been reviewed in detail (Adam, Saha-Möller, & Ganeshpure, 2001; Isogai, Saito, & Fukuzumi, 2011). The efficient conversion of primary hydroxyl groups to carboxylates via aldehydes is hypothesized to proceed according to the mechanism shown in Figure 9 (Bailey, Bobbitt, & Wiberg, 2007; Goldstein & Samuni, 2007).

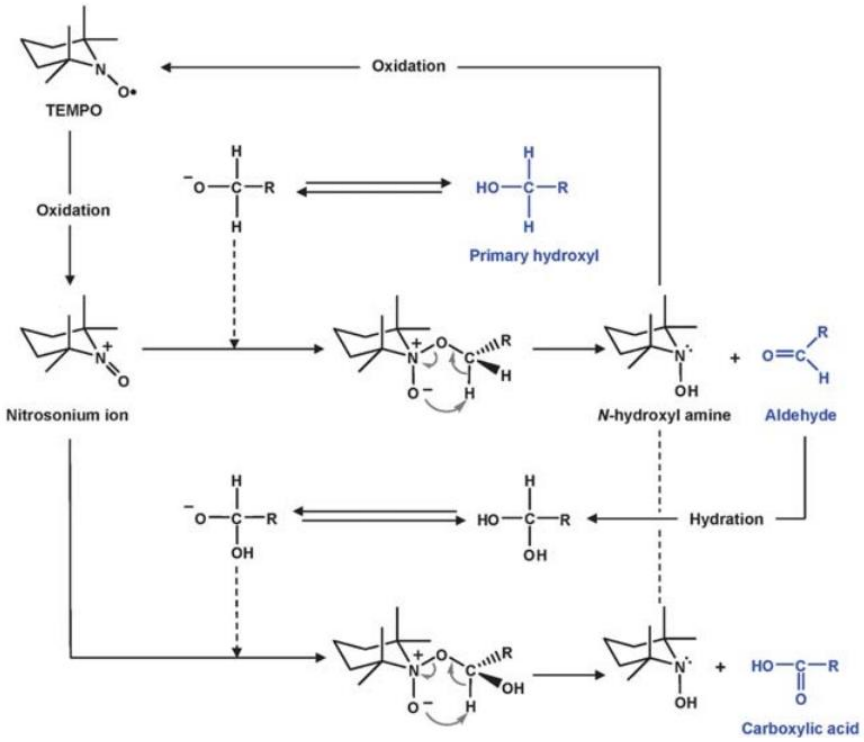

Figure 9: TEMPO-mediated oxidation of primary hydroxyls to carboxyl groups via aldehydes. ***Source:*** *Isogai et al., 2011.*

According to the scheme shown in Figure 10, the C6 primary hydroxyls of cellulose are expected to be oxidized to C6 carboxylate groups by TEMPO/NaBr/NaClO oxidation in water at pH 10–11. The oxidation process can be monitored from the pattern of aqueous NaOH consumption, which is continuously added to the reaction mixture to maintain the pH at 10 during the oxidation. When TEMPO/NaBr/NaClO oxidation is applied to native celluloses such as cotton linters, bleached Kraft pulps and bacterial cellulose, even under harsh oxidation conditions or for extended reaction times, almost no or only small amounts of water-soluble products are obtained (Isogai, Akira & Yumiko, 1998).

The oxidized products have almost homogeneous chemical structures of sodium (1 / 4)-b-D-polyglucuronate or Na salt of cellouronic acid (CUA) consisting of D-glucuronosyl units alone. Hence, the C6 primary hydroxyls of celluloses can be entirely and selectively converted to C6 sodium carboxylate groups by TEMPO-mediated oxidation. It is confirmed that C6-carboxylate groups are formed by not only the oxidized TEMPO but also NaBrO and/or NaClO present in the TEMPO/NaBr/NaClO system at pH 10 (Figure 10)(Isogai et al., 2011).

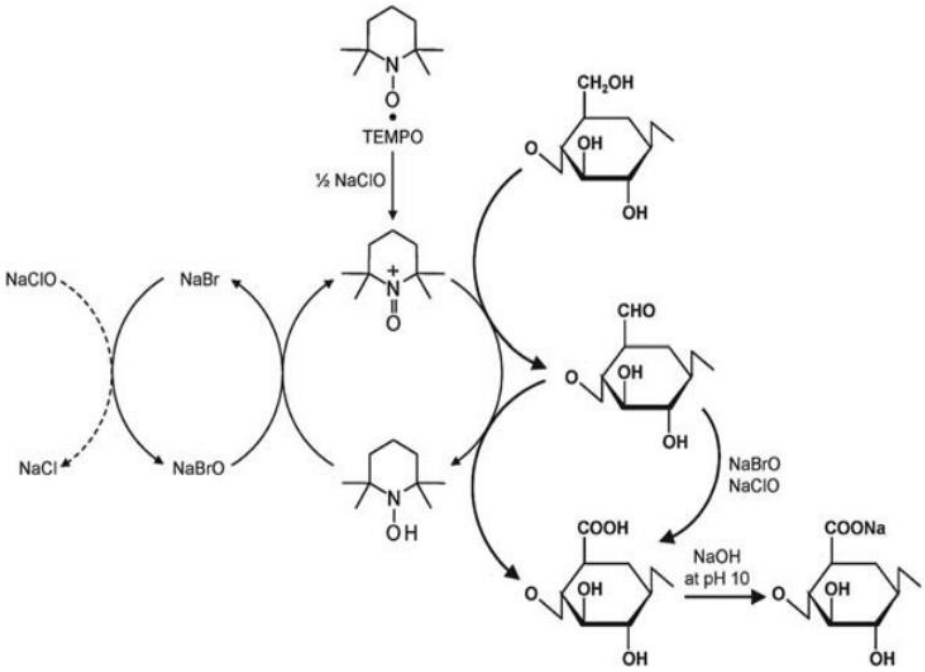

Figure 10: *Regioselective oxidation of C6 primary hydroxyls of cellulose to C6 carboxylate groups by TEMPO/NaBr/NaClO oxidation in water at pH 10-11. Source: Isogai et al., 2011*

2.3.3 CNF MEDIATED BY AN ENZYMATIC REACTION

Another reaction mechanism used for the nanofibres production is the enzymatic method. As its name says it is based on the use of enzymes to reduce the large polymeric cellulose fibres to nanometric fibres. Nowadays, exists more than 5.500 different types of enzymes, but if we focus on looking for a particular class to act on cellulose fibres this will be the glycoside hydrolase class. When entering into this family, they stand out on one side the endo-cellulases: enzymes who break the amorphous structure of cellulose into polysaccharide chains; and also the exo-cellulases: enzymes that cut 2-4 units at the end of the polysaccharide chains, releasing for example the cellobiose (Celodev, 2018b).

Then, once you know the different types of enzymes that can be used, it is need to determine which one is most useful for our requirements: Exo-cellulases work progressively either from the reductive termination or from the other, something that does not interest us since what is needed is to work in the amorphous zone of fiber to shorten the length of the fibers. Despite all, it is important to take into account that enzymes involved in cellulose degradation are not capable of completely degrading cellulose and complete hydrolysis requires the synergistic action of three types of cellulases (Celodev, 2018):

1. Endoglucanases (EGs): which randomly cut the cellulose chains mainly at the level of the amorphous zones generating new ends of chains.
2. Cellobiohydrolases (CBHs) or exoglucanases: which act in a processive way on the free ends of cellulose chains releasing cellobiose.
3. β-glucosidases (BGLs): which hydrolyse cellobiose and, to a lesser extent, soluble cellodextrins, into glucose. This enzyme plays a key role because it reduces the inhibition of Cellobiohydrolases and endoglucanases by cellobiose. It therefore has the major role of regulating the rate of hydrolysis.

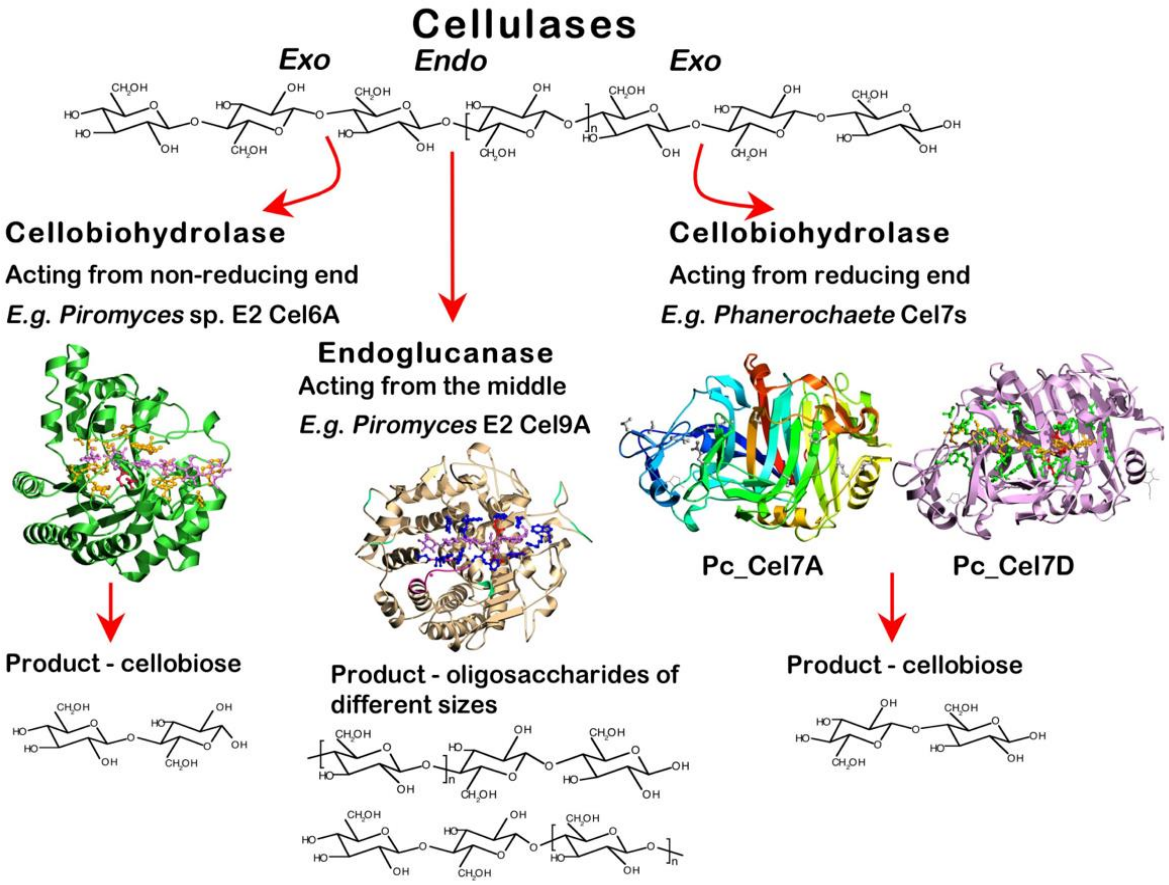

Figure 11: Scheme of the three different types of cellulases that can be used for enzymatic hydrolysis reactions. Source: Celodev, 2018.

So, according to Henriksson, Henriksson, Berglund, & Lindströ, 2007 the best enzymes to use for this application are the endoglucanase because when these types of enzymes are added to the treated fiber solution, act by cutting the polymeric chain of cellulose through carbon 1 and 4 (see the enzymatic hydrolysis mechanism on Figure 12).This enzymes will help us to achieve the desired effect and significant improvement of the properties and uses of cellulose fibres. At the same time, the use of enzymatic pre-treatment may also

have lower processing cost by lowering the number of passes through the homogenizer, and has advantages from the environmental point of view as compared with chemical methods mentioned before.

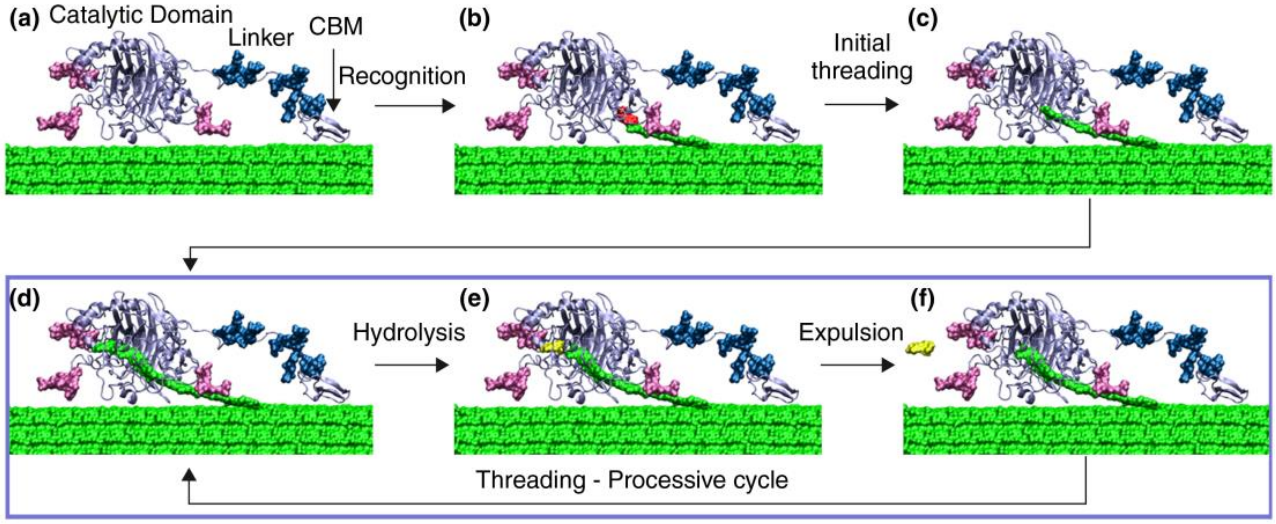

Figure 12: Evolution of phases on the enzymatic hydrolysis of cellulose chains. Source: Celodev, 2018.

Usually, before giving rise to the incorporation of the enzyme, mechanical pre-treatment must be applied to raw material fibres in an aqueous solution. This pre-treatment helps the dispersion of fibres in the solution by promoting a better action of the enzyme.

Regarding the development of the reaction, the amount of enzyme added to the solution is very important because these type of substances have a high cost, this means that the minimum and most exact amount possible to get the maximum performance (usually it is used to use a concentration between 80 - 320 g/tonne depending on the application they are going to be used for) should be use. If a higher amount is added, some enzyme will be wasted uselessly; but if less amount than the necessary is added, the expected performance will not be achieved and therefore the quality of the fibres will not be adequate.

2.4 IMPROVEMENT OF ABSORBENCY ON MEDICAL TISSUES

Once known the two materials to be used, that are, the cotton gauzes and the nanofibres of cellulose, a study of different options available will be done in order to improve the properties of gauzes. Next, more specifically, it explains the possibility of obtaining gas with a high specific surface and also the possibility of producing super-absorbent aerogels.

2.4.1 PRODUCTION OF HIGH SPECIFIC SURFACE GAUZES

As mentioned above, one of the options to improve the properties of gauzes comes from the addition of CNF to their structure. But first, the fact why nanofibres can be easily added to the threaded structure of gauzes should be understood.

Gauzes made of cotton, have between 70% - 90% of cellulose on their composition (Textile Learner, 2019); while TEMPO nanofibres are nano-cellular structures with negative electric charge. Well, it is this electrical property that allows the CNF to connect easily with the cellulose molecules present in the cotton filaments. Specifically, CNF binds to the structure of gauzes by means of some attractive interaction between molecules.

The fundamental point of molecular interactions is to understand the forces coherently associated with each of the individual molecular species involved, which in turn is based upon the basic physical forces involved. However, the most important molecular interactions have been recognized. They are hydrogen bonds, van der Waals, and electrostatic interactions, among which the hydrogen bond is the strongest and most well-known of the intermolecular forces. These intermolecular interactions are coherent intermolecular forces of a physical nature, and it is these forces that lead to cooperative interactions between the same and/or different molecules and on which most supramolecular structures are formed (Zhang & Cresswell, 2016).

The first type of link, despite being one of the most important types of molecular interaction, is a weak link type compared to covalent and ionic bonds. The interaction is established between a hydrogen atom linked to an electronegative heteroatom, called a hydrogen donor (in our case, the oxygen of the hydroxyl groups of the cellulose molecule of gauzes), and a second atom electronegative that acts as acceptor (the oxygen atoms present in the carboxylic groups of the structure of the nanofibres that have been negatively charged). The hydrogen that takes part in the electronic exchange has a positive charge and interacts electronically with the electronic pairs of the acceptor (Arunan et al., 2011). However, the hydrogen bonding is not just an electrostatic interaction, but it has characteristic forces commonly associated with the covalent bond. The strength of the hydrogen bond depends primarily on the atoms of the donor and the acceptor and its chemical environment (Emsley, 1980; Steiner, 2002).

Van der Waals forces are interactions between molecules without affecting their molecular structure and can be repulsive or attractive depending on the distance between the interacting non-bonded atoms and molecules. These type of forces are weaker than chemical bonds that unite atoms in chemical compounds (Zhang & Cresswell, 2016). They are divided into three types: dipole-dipole forces, induced dipole-dipole

forces, and induced dipole-induced dipole forces. For the CNF interaction, only the dipole-dipole forces take place.

All these forces, theoretically, end up giving rise to the infusion of nanofibres over the gauzes and between them. Further on, it will be evaluated whether or not these theories are fulfilled.

2.4.2 PRODUCTION OF SUPER-ABSORBENT AEROGELS

Aerogel is a broad term used to talk about an extraordinary group of materials that have been used since the 1960's in space travel, but are now finding uses across a whole range of industries. Aerogel is not a specific mineral or material with a set chemical formula-rather, the term is used to encompass all materials with a specific geometrical structure. By definition, "an aerogel is an open-celled, mesoporous, solid foam that is composed of a network of interconnected nanostructures and that exhibits a porosity (non-solid volume) of no less than 50%" (Thomas, 1960).

In general terms, aerogel is created by drying a gel, in a very low temperature environment. First the gel is created in a solution, and then the liquid component is removed via supercritical drying, which removes liquid slowly in order to maintain the structural shape. This liquid component is then replaced by air. Aerogel was first created in 1931 by Samuel Stephens Kistler, with carbon aerogels first introduced in the 1980's (Thomas, 1960).

Figure 13: Transition metal oxide aerogels including an iron oxide (rust) aerogel (top). Source: Aerogel.org

Though aerogel is technically a foam, it can take many different shapes and forms. The majority of aerogels are composed of silica, but carbon, iron oxide, organic polymers, semiconductor nanostructures, gold and copper can also form aerogels (some examples are shown on Figure 13). However, within the aerogel structure, very little is solid material, with up to 99.8% of the structure consisting of nothing but air. This unique

composition gives aerogel an almost ghostly appearance; hence it is often referred to as 'frozen smoke' (Aerogel.org, n.d.).

One of the best known and most useful physical properties of aerogel is its incredible lightness. It typically has a density between 0,0011 to 0,5 g/cm^3, with a typical average of around 0,020 g/cm^3. This means that aerogel is usually only 15 times heavier than air, and has been produced at a density of only 3 times that of air. For many years, aerogel was in the Guinness book of world records as the 'solid with the lowest density', before being ousted recently by the metallic micro-lattice and then aerographite. Further desirable properties of aerogel are: low mean free path of diffusion, high specific surface area (for a non-powder material), low thermal conductivity, low sound speed, low refractive index, low dielectric constant (Thomas, 1960).

2.5 SUBSTITUTION OF TITANIUM THREADS

Titanium as a metal is not free in nature, but it is the ninth element in abundance in the earth's crust and the fourth most abundant metal, present in most igneous rocks and sediments derived from them. It can be found in many types of different ferric minerals, but those that most interest us are mainly the anatase minerals (TiO_2) and brookite (TiO_2), from which important deposits are found in Australia, the Scandinavian region, states United and Malaysia (Krebs, 2006).

Figure 14: (A) Schematic representation of a Titanium dioxide molecule. (B) Titanium dioxide in the form of whitish powder, commercial form. (C) A titanium crystal bar, high purity 99,99%. Sources: 123RF Limited, 2019; Amazon.in, 2018.

Approximately 95% of the titanium is consumed as titanium dioxide (TiO_2). a permanent white pigment used in paints, toothpaste, medicines, plastics and, even, in meals. In paintings they are used in reflectors because they reflect the infrared radiation very well, an example is the varnish for tile of hospitals, reducing the rates of infection by lethal bacteria. In addition, it is a substance that is considered to be physiologically inert, that is why it is used in titanium prostheses, consisting of pure titanium snails that have been superficially treated to improve their osteointegration; or it can be used for medical implants to manufacture artificial heart pumps

and pacemaker boxes. Even some titanium compounds may have applications in cancer treatments. For example, titanocene chloride in the case of gastrointestinal and breast tumours (Buettner & Valentine, 2012).

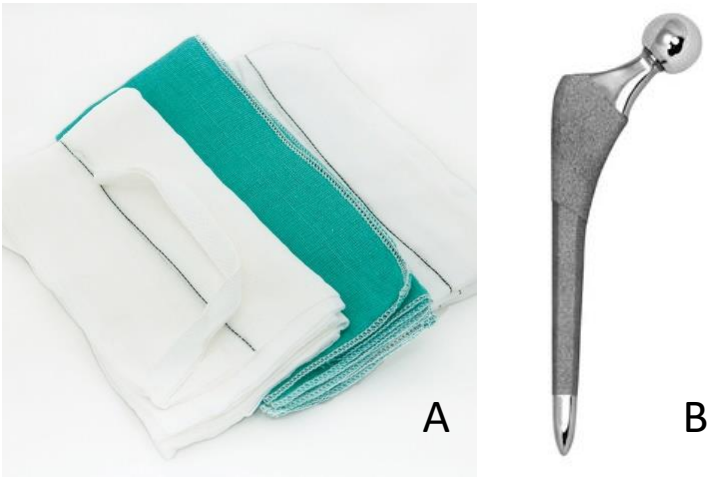

Figure 15: Examples of titanium applications on medicine: (A) Surgical gauzes with titanium threads woven in the middle. (B) Femur protheses made of pure titanium. Sources: Alibaba; TEXPOL.

Currently, however, the surgical gauzes are equipped with a titanium filament woven in its same structure so that it provides an important and very useful radiopacity capacity in the event of losing one during an operation, as explained initially, taking advantage of the inert property of the material.

However, despite being one of the most abundant materials, obtaining it purely is complicated and costly (Sŏng, Younossi, Goldsmith, & United States. Air Force., 2009), that is why the solution studied to reduce the cost and retain its applicability is to replace the titanium filament for TiO_2 nanoparticles. Theoretically, these particles are easier to achieve because it is like the titanium is in its natural state. Therefore, only eliminating the bargain of the mineral should be enough to have them. Also, because they are particles that contain titanium atoms in their structure the radiopacity properties of titanium should be preserved. Although, it may also be that by adding so much in the gauzes as in the Aerogels give us extra resistance thanks to the links that can be established between the oxygens of the dioxide and the CNF.

3 MATERIALS AND METHODS

3.1 MATERIALS

Once all the learned all the information detailed in the literature review, it is necessary to establish what the required materials have been and to know the steps carried out in order to carry out: the fabrications of the two different types of nanofibres and their subsequent characterization, infusion of CNF on gauzes, production of CNF aerogels and finally the trials carried out in each of the samples prepared.

3.1.1 PRODUCTION OF CNF

Bleached Kraft hardwood (*Eucalyptus globulus*) pulp (BKHP) was kindly provided by Torraspapel S.A. (Spain), originally with 16 µm of diameter and 700 µm of length, according to the supplier. Then, to perform the TEMPO mediated oxidation different reagents were required: the TEMPO catalyst and sodium bromide (NaBr) were both obtained from Sigma-Aldrich, Barcelona, Spain; NaClO was obtained from commercial bleach, so it was bought on a supermarket considering its NaClO content (7,5 w/w).

Otherwise, the enzymatic hydrolysis was performed using the commercial enzyme cocktail Novozym 476, kindly provided by Novozymes A/S (Denmark), that contains 2% of endo-b-1,4-glucanases with an activity factor of 4500 CNF-CA/g of cellulose (tested over a CMC substrate). All the reagents required for conducting enzymatic hydrolysis were also supplied by Sigma Aldrich.

Finally, all the suspensions were made in distilled water and as well as, to bring the pH of both reactions to a basic medium, a concentrated sodium hydroxide (NaOH) was required. Even thought, a diluted solution of hydrochloride acid was made to maintain de pH of the enzymatic reaction in acid conditions.

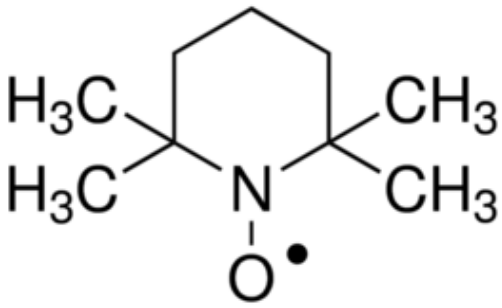

Figure 16: Chemical structure of TEMPO catalyst.
Source: Yoshida, 2009.

3.1.2 CNF INFUSION

Next, to perform the infusion of CNF on gauzes a starter infusion kit was required. The kit includes a high-quality resin catch pot complete with a vacuum gauge, two valves and connectors and re-usable silicone rubber resin infusion connectors (5m). Also supplied with the kit was a complete set of vacuum bagging consumables selected specifically for resin infusion including a vacuum bagging film, an infusion mesh, a plastic spiral diffusor and sealant tape (90 m were required approximately to prepare all samples).

Therefore, a small quantity of a biocompatible glycerol from Labkem was required in order to provide more flexibility to the gauzes after the lyophilization process. Lastly, some quantity of TiO_2 nanoparticles was also required to try adding radiopacity to gauzes and aerogels. These nanoparticles were provided by Sharlau, S.L.

Figure 17: Components of the infusion kit.
Source: Easy Composites, 2019.

3.2 METHODS

3.2.1 CELLULOSE NANOFIBRES PRODUCTION

When producing nanofibres, it has been taken into account that the whitened and dried eucalyptus pulp acquired from Torraspapel, S.A. presents a quantity of water associated with the fibre to has to be determined to be able to calculate which is the percentage of fibre and humidity on the BKHP.

For this determination, IDM IR-35 humidity analyser from Denver Instrument has been used and it has been worked on according to the PNT-63.1EP15. This device gives the percentage of dry mass (%D) of the fibre analysed by means of a thermogravimetry, it consists of a thermal resistance that applies heat to the fibre

until all the water has been evaporated and the weight keeps constant. Dryness is a very important parameter since it is necessary to know the dry weight of fibre that is available for subsequent processes.

Figure 18: IDM IR-35 humidity analyser from Denver Instrument.

MECHANICAL PRE-TREATMENT

The next step was to disintegrate the BKHP. The aim was to get the fibre separated by applying mechanical work to a suspension of fibres and water without damaging its morphology. Therefore, the disintegrator ENJO Process from Papelquimia, S.A. was used, following the ISO 5263 standard. It should be noted that this device has a maximum load capacity of 30g. of dry fibre per batch and is usually load together with a volume of approximately 2L of distilled water. To determine these 30g. consistency value was used, so to determine the necessary wet grams the Eq. 1 was followed.

Eq. 1

$$30\ of\ dry\ BKHP * \frac{100\ wet\ gr}{\text{X gr dry}} = \boldsymbol{y\ gr\ of\ wet\ BKHP}$$

Once the paste was weighed, it was soaked for 4 hours and later it was torn into the disintegrator, along with the distilled water, at 30.000 revolutions for 20 minutes. After this time, the fibres suspension was washed with distilled water and filtered with the vacuum pump up to three times. In the end, consistency again determined.

Figure 19: Disintegrator ENJO Process from Papelquimia, S.A.

At this point, there are two different roads to choose according to the requirements of the application: the first one is passing the fibres already decayed by a refining process, or proceed directly to the preparation of reagents to initiate the reaction. As far as this research is concerned, the reaction was proceeded directly. But in any case, the refinement process is explained if it is considered necessary for other projects.

So, if you want to apply the refinement process, you would use a refine machine, such as the IDM PFI (Figure 20), following the ISO 5264-2 standard.

Figure 20: IDM PFI.

The PFI works at a consistency of 10% and with 30g. of dry fibre and the maximum load to be introduced is 300 g. This device consists of two parts: a cylindrical container where the suspension is homogenously distributed by its wall and a toothed refining grinder that carries out the shear action on the paste. Both parts rotate in the same direction but at different speeds, in this case the pulp is refined to 4.000 revolutions.

REACTION

In this part, both types of reaction process will be explained. First of all the TEMPO-mediated oxidation is descript, followed for the enzymatic reaction.

The main objective of the oxidation reaction catalysed by TEMPO is to oxidize the primary alcohol of the cellulose chain to convert it into carboxylic acid. The oxidation degree is determined by the amount of sodium hypochlorite (NaClO) added. The steps followed to carry out the reaction are detailed below:

First of all, because it was planned to oxidize all the disintegrated fibres, they were brought to a consistency of 1% in a container big enough for the quantity it was treated with. When preparing the assembly to perform the reaction, it must be kept in mind that this chemical treatment must be constantly stirring and at a basic pH, exactly at pH 10.

Then, the TEMPO catalyst and sodium bromide (NaBr) were added and the reagents were stirred until the total disintegration. For 1 g of cellulose, 0.016 g of catalyst and 0.1g of sodium bromide should be added. The amount of oxidizing agent added is determined by the mmols we want to oxidize the fibre. These vary between 5, 10 and 15 mmol and are added dropwise until the millilitres measured are exhausted. For this project, eucalyptus fibres were oxidized at 15 mmol:

Eq. 2

$$\text{X } gr\ cellulose * \frac{15\ mmol\ NaClO}{1\ g\ cellulose} * \frac{74{,}44\ gr\ NaClO}{1000\ mmol\ NaClO} * \frac{100\ gr\ bleach}{7.5\ gr\ NaClo} * \frac{1\ mL\ bleach}{1.04\ gr\ bleach} = \boldsymbol{y\ ml\ bleach}$$

By incorporating NaClO, the reaction begins, but it is not conditioned at that time. It is for this reason that afterwards, the sodium hydroxide was added at a concentration of 0.5M until the pH was constant at 10. When a constant value of pH was observed during certain period of time, it means that the reaction was over, and the stirring was already stopped. At the end of the oxidation, the fibres of the aqueous suspension were filtered again and washed repeatedly by using as before the vacuum pump to remove the remaining NaOH and achieve a neutral pH.

Regarding the enzymatic reaction, the objective is to use an enzyme in order to reduce the length of fibres. In this case, the performance of the reaction is based on the amount of enzyme added to the suspension; below are detailed the followed steps to carry out this type of reaction:

As well as in the oxidation reaction, all the pulp prepared initially was taken to react, so it was brought to a consistency of 5%. Compared to the other reaction, when preparing the assembly, it must be taken into

account that the prepared suspension must be introduced in a heated reactor with enough capacity to heat up to 90ºC, with constant stirring and resistance to acid pH. Despite that, the initial conditions were 50ºC with non-stop stirring and the commented pH was achieved with a solution of HCl at a concentration of 0.5M.

Then, knowing the desired degree of fibrillation the enzyme was added into the reactor. According to Tarrés et al., 2016, the amount of enzyme to use can vary between 80g and 320g per ton of fibres depending on the requirements. In this case, to obtain the maximum possible performance the proportional amount to the 320g / Tn had been added. In order to know accurately the amount of enzyme despite the use of the Eq. 3.

Eq. 3

$$\text{X } gr\ cellulose * \frac{320\text{gr endoglucanase}}{1.000.000\ g\ cellulose} * \frac{100\ ml\ enzym}{2\text{ gr endoglucanase}} = \boldsymbol{y\ ml\ enzym}$$

Once on the initial conditions described above and the enzyme had been added, the reaction started; then the stationary state was conserved for at least 2 hours. After this time, to stop the enzyme work, the reactor temperature was increased up to 80ºC; however, a neutral pH was achieved by adding the same solution of NaOH (0.5M). This change of conditions is carried out in order to denature the enzyme, because only this way it will be able to counteract the effect of this protein and end the reaction.

MECHANICAL FINAL TREATMENT

Once the reaction was complete, the fibres were still not in the desired nanometric size, that is why mechanical efforts were applied, in order to achieve a greater resizing of the fibre. This mechanical action was carried out on a homogenizer NS1001L PANDA 2000-GEA, GEA NIRO, Parma, Italy (Figure 21).

Figure 21: Homogenizer NS1001L PANDA 2000-GEA.

Since it works at consistencies of 1 - 2%, it has had to re-check the consistency of the fibre slurry and dilute it again with distilled water. Finally, the solution was passed through the homogenizer repeatedly to obtain a consistent gel. The number of cycles vary depending on the degree of oxidation applied. To achieve consistent nanofibres from treated eucalyptus at 15 mmol, 3 passages were required at 600 bar.

It is necessary to know, that the nano-fibrillation takes place when the solution passes through the narrow pipes of the equipment with a pressure of 600 bar, action that increases the formation of new hydrogen bridges between fibres and the water on the suspension. The formation of new links increases the adsorption capacity of the fibre and its specific surface.

After finishing the process, the gel shown in Figure 22 was obtained.

Figure 22: Gelatinous appearance of recently produced CNF.

3.2.2 CHARACTERIZATION OF NANOFIBRES

Already produced the CNF, they had to be characterized and compared to the parameters established by Serra et al., 2017. In this way, it could be certified that the produced nanofibres had the correct morphology and would provide us with the expected properties. The methods used to determine each of the parameters are described below:

CATIONIC DEMAND

Cationic Demand (CD) was determined by means of a colloidal evaluation in excess, using a Mütek PCD04 load analyser provided by BTG, S.L. (UK). Firstly, the surface absorption of a polymeric substance called poly-DADMAC (Mm = 107 KDa) was carried out on the surface of the CNF. The excess of the remaining poly-DADMAC adsorption was assessed with PES-Na, another standard anion polymer facilitated by BTG.

Exactly, 0.04g of CNF (dry weight) are diluted in distilled water and dispersed by stirring at 3000 rpm for 10 min with a pulp disintegrator. Then, 10 mL of sample are measured and mixed with 25 mL of poly-di-allyl methyl ammonium chloride (poly-DADMAC) for 5 minutes using magnetic agitation. After that, the mixture was centrifuged in a Sigma laboratory centrifuge (model 6K15) lasting 90 minutes at 4000 rpm.

Figure 23: Mütek PCD04 load analyser provided from BTG, S.L.

After all this time, a sample of 10 mL of the supernatant is extracted and introduced into the Mütek load detector, the solution of the anionic polymer selected by the evaluation was added (PES-Na), until the detector showed a signal of 0mV. Finally, the volume of PES-Na consumed in the valuation was noted and used to calculate the value of the cationic demand by means of the following equation:

Eq. 4

$$\boldsymbol{Cationic\ demand} = \frac{(\boldsymbol{C_{poly-D}} * \boldsymbol{V_{poly-D}}) - (\boldsymbol{C_{PES-Na}} * \boldsymbol{V_{PES-Na}})}{\boldsymbol{W_{sample}}}$$

$\mathbf{C_{poly\text{-}D}}$ → Concentration of poly-DADMAC	$\mathbf{V_{poly\text{-}D}}$ → Volume used of poly-DADMAC
$\mathbf{C_{PES\text{-}Na}}$ → Concentration of PES-Na	$\mathbf{V_{PES\text{-}Na}}$ → Volume used of PES-Na
$\mathbf{W_{mostra}}$ → sample weight [g]	

CARBOXYLIC GROUP CONTENT

The Content of carboxylic groups (CC) was determined by doing a conductimetric evaluation. In the practical implementation, between 50-100g of dry CNF have been weighted and mixed with a solution of 15 ml HCl (0.01 M). In this way the protons of hydrochloric acid will be exchanged with the sodium atoms that are attached in the carboxylic groups of the CNF. Then the mixture was stirred for a short period of 10 minutes and was finally evaluated with a NaOH solution (0.01 M). Parallel to the titration, the conductivity of the mixture [mS/cm] was analysed by using a conductometer, to observe the reduction, stabilization and increase of the conductivity of the sample.

All the data acquired allowed us to create a titration curve where: the point where a greater presence of acid has been detected will correspond to the excess of hydrochloric acid, while the point where the lowest acid

content is detected will correspond to the concentration of COOH groups. Numerically, the content of carboxyls can be determined through the following equation:

Eq. 5

$$\boldsymbol{CC = 162 * (V_2 - V_1) * c * \left[w - \left(36 * (V_2 - V_1)\right)\right]} = \frac{mmol\ de - COOH}{g\ de\ CNF}$$

V_1 i V_2 → Equivalent volumes of NaOH added to the solution [L].

c → Molar concentration of NaOH.

w → Weight of the dried CNF sample used [g].

DEGREE OF POLYMERIZATION

The degree of polymerization is defined as the number of times that the monomeric unit that forms the polymer chain is repeated. The degree of polymerization of the cellulose fibres was determined from the intrinsic viscosity (η) of the fibres dissolved in cuproethylene diamine at 25ºC. The intrinsic viscosity refers to the contribution of the solute of a solution to its viscosity. Thus, comparing the viscosity of the solvent with the viscosity of the solution, it is possible to know the contribution to this property that the solute imparts. A viscosity increasement is noticed when the degree of polymerization of the solute is greater. This methodology is only valid for linear polymers, excluding those that have branches or non-linear morphologies.

Thus, for the determination of the viscosity, the dissolution of the fibres in cuproethylene diamine was carried out in accordance with the UNE 57-039-92 standard and was carried out in a capillary viscometer at low concentration, being the viscosity of the solution close to the solvent one.

From the initial model proposed by Staudinger, Mark-Houwink Sakurada formulated the Eq. 6. But, since the behaviour of this equation is exponential, natural logarithms are usually applied to obtain a first-order polynomial mathematical expression:

Eq. 6

$$\boldsymbol{\eta = K * M^a}$$

Eq. 7

$$\boldsymbol{\ln \eta = \ln K + a * \ln M}$$

The slope of the line represented in Eq. 7 corresponds to the term a. Also, K can be determined since it corresponds to the independent term of the equation. The values of both constants depend directly on the solvent and solute used to determine the viscosity. Despite most polymers have values of a between 0.5 and 1, the values of the constants K and a were estimated at 2.28 and 0.76, respectively.

FIBRILLATION PERFORMANCE

The fibrillation performance (Yield) was determined by centrifuging a solids content of 0.2% in the CNF sample. Centrifugation took place at 4500 rpm along 20 min in order to properly separate the nano-metric fractions of the material, retained in the area of the supernatant, of those non-nanometric solids that remained in the bottom of the container. Once the centrifugation had finished, the solids remaining at the bottom of the container were duly weighed, leaving them to dry at 105ºC until their weight was constant. In order to calculate the performance of the fibrillation Eq. 8 below was followed:

Eq. 8

$$\boldsymbol{Yield}\ (\%) = \left(\mathbf{1} - \frac{\boldsymbol{weight\ of\ the\ dried\ sediments}}{\boldsymbol{weight\ of\ the\ diluted\ sample} * \%\ \boldsymbol{solids}}\right) * \mathbf{100}$$

WATER RETENTION VALUE

The water retention value (WRV) determines the amount of water associated chemically to fibres; it is an indicator of their hydration and swelling capacity. This parameter was determined doing also another centrifugation from a determined volume of CNF sample, that sample was extracted firstly from the division of another CNF sample in two identical portions. CNF samples were centrifuged at 2400 rpm for 30 min (the containers with which the centrifugation was carried out were previously weighed). In this way what is achieved is to eliminate all those water molecules that have not been linked to the cellulose structure, while the nanofibres are retained in the surface of a nitrocellulose membrane that have to be at the bottom of the container (the diameter of their pores was 0.65 µm).

Once the centrifugation was completed, based on the methodology described by TAPPI UM 256, the CNF retained in the nitrocellulose membrane was recovered and they are dried at 105ºC for 24h. Finally, using the following expression we are able to calculate the percentage of water retained by cellulose nanofibres:

Eq. 9

$$\boldsymbol{WRV}\ (\%) = \left(\frac{\boldsymbol{W_w - W_d}}{\boldsymbol{W_d}}\right) * \mathbf{100}$$

W_w → weight of wet sample W_d → weight of dry sample

SPECIFIC SURFACE AREA

The specific surface area (σ) was theoretically determined by the content of COOH groups and cationic demand. So, it should be taken into account that for the calculation of this value, certain considerations have been made:

1. The adsorption of the poly-DADMAC takes place as a single-layer adsorption.
2. The poly-DADMAC has a cylindrical geometry. Its surface was previously calculated by calculating the surface of its monomer and its degree of polymerization, considering the distance between the links and assuming its circular geometry described. The results of the calculation of dimensions were a length of 4,849 Å and a diameter of 5,427 Å, thus obtaining an area of 535.87 nm2.

Once all of these points have been reached, it is only needed the application of the mathematical expression that follows:

Eq. 10

$$\sigma_{CNF} = (CD - CC) * S_{poly-DADMAC}$$

DIAMETER

The Diameter (d) of CNF was calculated assuming that nanofibres also have a cylindrical geometry and that their density is close to 1.5 g/cm^3 according to bibliographical sources. Their diameter can be easily calculated by means of Eq. 11:

Eq. 11

$$d = \frac{\rho * m^2}{4 * g}$$

3.2.3 INFUSION OF CNF ON GAUZES

When finishing the production of cellulose nanofibres, including its characterization, it was preceded by the final preparation of all the necessary samples. Following, the assembly applied to infuse the CNF on the gauzes, extracted from the same company who facilitated the materials (Easy Composites, S.A., UK), is explained. Note that for each type of gauze studied, up to 5 samples were infused.

The assembly of the infusion system starts by weighing the dry gauze to be infused, because later they will also be characterized. Then since they are thickness-less, a single unit was placed, open by its half, at the centre of a metal base and stickled with tape. Next, it was placed just above the plastic infusion mesh. This mesh is used for two reasons: it helps to distribute the CNF more homogeneously throughout the surface of the gauze, it also increases the contact and the absorption of the CNF with the gauze when pressurized.

Next, in front of the two long edges of the sample, a rubber connector was placed. In addition, in one of them was installed in a spiral plastic tube that acts as a diffuser, thus avoiding that there is a single-entry point and that the CNF solution is distributed in the best possible way. Then, sealant tape was stuck around the assembly in order to attach a piece of the bagging film that covered the entire surface. In this case, since the vacuum pump used is powerful, a single sealant tape was not enough to guarantee the tightness of the system, forcing to place a second strip on the film. Finally, only the inlet and outlet holes were made between the film and the connectors, in order to connect the suction and extraction tubes.

Figure 24: Ultra Turrax IKA T25 digital used to mix all CNF solutions.

Then, the CNF solution was prepared to infuse. About 200 ml of the TEMPO-CNF mother solution at 1% consistency was diluted to 0.5%, obtaining a final infusion volume of 400 ml per sample. Also, in the necessary cases, it was added 0.3% of glycerol per dry weight of CNF and 10% of TiO_2 per dry weight of CNF. To mix the solution, the Ultra Turrax IKA T25 digital was used for 1 minute: a homogenizer that shakes at high speeds. As a result of this strong agitation bubbles of air appear to the solution. To avoid this problem, the Sonicador Qsonica 700 was used. Its main mechanism of action is to shake the suspension by means of ultrasounds, so that the bubbles that were previously mentioned were removed.

Finally, the final assembly of the infusion system was only done: the suction tube (which was connected to the diffuser) was placed inside the vessel with the CNF solution, and the other tube was connected to the liquid catch pot. The metal clamps were placed in each of the tubes and the infusion started. When creating the vacuum, it was previously verified that there were no leaks of pressure. To regulate the infusion speed, the suction valve was opened with caution, leaving the output valve completely open.

Below you can see some images that shows how the assembly is structured (Figure 25) and how the final assembly looks like Figure 26:

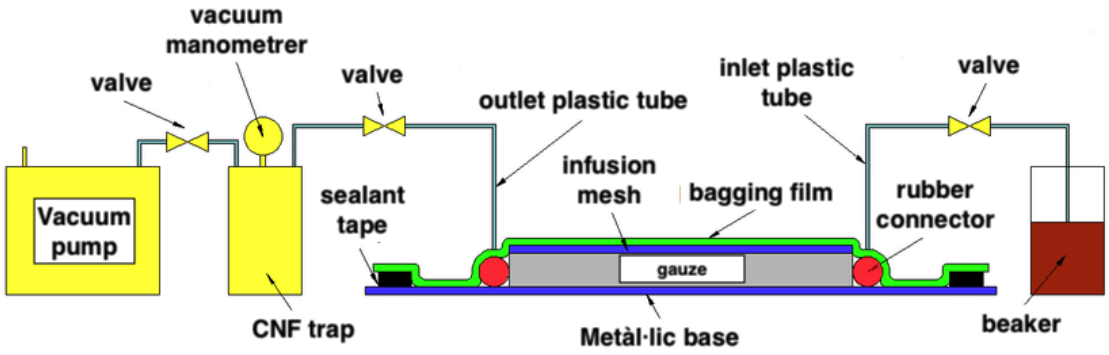

Figure 25: Schematic structure of the infusion system.

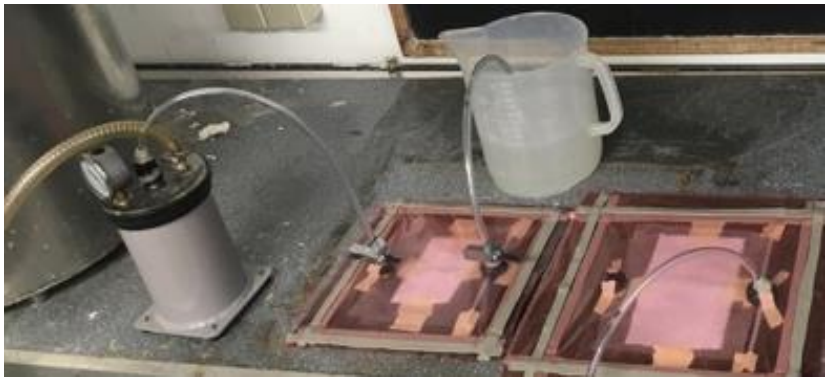

Figure 26: Real aspect of the final infusion assembly.

After the infusion of CNF, the sample was removed carefully and placed in the freezer, on a cardboard base previously covered with plastic wrap. Once frozen, the sample was introduced into the freeze-drying machine at -60ºC, with the aim of sublimate the water it contained without damaging the gauze structure. The samples were kept in the lyophilizer from Coolvacuum Technologies between 1 and 0.5 days, since having very little amount of water did not require a high lyophilization time. After that time they were stored in a sealed bag.

3.2.4 AEROGELS PRODUCTION

The other analysed product are aerogels, sponges with 100% of CNF composition. To produce these substances, solutions of 0.3% and 0.6% on CNF were made (enzymatic CNF and TEMPO-CNF), from mother's solutions at 1% of consistency. As with the infusion, Ultra Turrax was used for 1 minute to mix the solution. The solutions were distributed in different Petri metallic dishes of 20 cm and kept in the freezer.

In total, to prepare 15 samples (3 aerogels of each type) 3 Kg of 1% mother solution were consumed. It is necessary to take into account that three samples of TEMPO-CNF aerogel at 0,3% had been also added with 10% of TiO_2 on CNF dry weight, to observe whether some radiopacity on aerogels.

Once the samples were frozen, about 3 samples per cycle, were introduced to the lyophilizer at -60ºC. After a week the lyophilized samples were stored also in a sealed bag.

Figure 28: Lyophilizer from Coolvacuum Technologies working.

Figure 27: Lyophilized aerogel TEMPO (0,3%).

3.2.5 CHARACTERIZATION OF GAUZES AND AEROGELS

To know if the treatment applied to gauzes and the aerogels production was effective some different tests have been already done. As well as, these analyses will provide valuable information to distinguish between the different types of gauzes, infused and none infused, and aerogels.

Before knowing how each of the trials have been carried out, it must be known some decisions taken before starting the analytical process, since acquiring blood was not bureaucratically easy. However, keep in mind that the differences between blood and water are minimum. Blood is a liquid only composed of plasma and several kinds of cells. These blood cells (which are also called corpuscles or "formed elements") consist of erythrocytes (red blood cells, RBCs), leukocytes (white blood cells), and thrombocytes (platelets). By volume,

the red blood cells constitute about 45% of whole blood, the white cells about 0.7% and the plasma about 54.3%. As seen the majoritarian component is plasma, which is basically 90% H_2O. Therefore, considering de difficulties of acquiring blood and knowing that it is approximately 50% water composed it was decided to use water instead of blood for doing all tests.

Also, before starting the description of each test done, it should be known which are the gauzes and aerogels selected for the research, the nomenclature established, their characteristics and what tests have been performed on each type of sample, because unfortunately, in some cases, there was not enough sample quantity to carry out all the tests. In the Table 4 you can find detailed all the necessary information mentioned above:

Table 4: General description of the samples, nomenclature established and tests carried out in each one.

MATERIAL	DESCRIPTION	WOVEN / NON-WOVEN	CNF CONSISTENCY [%]	NOMENCLATURE	WATER ABSORPTION TEST (WAT)	WATER HOLDING TIME (WHT)	VERTICAL WICKING TEST (VWT)	STRESS-STRAIN CURVES (ST-ST)	ANTI-MICROBIAL TEST
Gauze	from JOSEP TRUETA'S HOSPITAL	woven	-	G-0	✓	✓	✓	✓	✓
Gauze	Infused w/ TEMPO-CNF	woven	0,50%	G-CNF	✓	✓	✓	✓	X
Gauze	Infused w/ TEMPO-CNF + Glycerol	woven	0,50%	G-GLI	✓	✓	✓	✓	X
Gauze	Infused w/ TEMPO-CNF + Glycerol + TiO_2	woven	0,50%	G-TiO_2	✓	✓	✓	✓	✓
Gauze	from TEXPOL	woven	-	GTEXPOL-0	✓	✓	✓	X	X
Gauze	from TEXPOL infused w/ TEMPO-CNF	woven	0,50%	GTEXPOL-CNF	✓	✓	✓	X	X
Gauze	from GASPUNT	non-woven	-	GGASPUNT-0	✓	✓	✓	✓	X
Gauze	from GASPUNT infused w/ TEMPO-CNF	non-woven	0,50%	GGASPUNT-CNF	✓	✓	✓	✓	X
Gauze	from ORTOPEDIA Y CIRURGIA	woven	-	GORTO-0	✓	✓	✓	✓	X
Gauze	from ORTOPEDIA Y CIRUGIA infused w/ TEMPO-CNF	woven	0,50%	GORTO-CNF	✓	✓	✓	✓	X
Gauze	from TEXPLA	non-woven	-	GTEXPAL-0	✓	✓	✓	X	X
Gauze	from TEXPLA infused w/ TEMPO-CNF	non-woven	0,50%	GTEXPAL-CNF	✓	✓	✓	X	X
Aerogel	made of TEMPO-CNF	non-woven	0,60%	AT-0,6	✓	✓	✓	X	X
Aerogel	made of TEMPO-CNF	non-woven	0,30%	AT-0,3	✓	✓	✓	X	X
Aerogel	made of TEMPO-CNF and TiO_2	non-woven	0,30%	AT-0,3-TiO_2	✓	✓	✓	X	✓
Aerogel	made of ENZYMATIC-CNF	non-woven	0,60%	AE-0,6	✓	✓	✓	X	X
Aerogel	made of ENZYMATIC-CNF	non-woven	0,30%	AE-0,3	✓	✓	✓	X	X

WATER ABSORPTION TESTS

The water absorption value (WAV) is the most important parameter studied in this research. For surgeons it is the most helpful parameter when talking about surgical gauzes because it provides essential information to know how much water or blood is able to absorb the fabric. Well, WAV was done according to the standard BS 34491 (1990) known as ''Static immersion test'' for fabrics (like bandages, gauzes and cotton for medical applications) with high capability of water absorption.

First, for each lyophilized sample two squares of 5x5 cm were cut. Then, dry samples were weighted and soaked in a filled beaker with distilled water for a minute then hanged for two minutes and weighted another time; up to 5 absorption cycles were performed on each sample.

The water absorption percentage (W) was obtained by Eq. 12. Each test was repeated five times and the mean values for sample were reported.

Eq. 12

$$WAV = \frac{M2 - M1}{M1} * 100$$

M1 = Weight of the dry sample

M2 = Weight of the wet sample

WATER HOLDING TIME TESTS

Regarding to the drying time of samples, it was determined based on T-PACC method. First of all, three circular cuts (3.5-inch diameter) of each type of fabric samples were prepared and weighed. Then, the samples were wetted (sprayed) with approximately 1CC of distilled water and weighted another time. The reduced weight of samples due to water evaporation was measured every 15 min. until the weight measuring differences between three successive measurements reached to a non-significance level. Finally, and the mean value was reported.

VERTICAL CAPILLARITY TESTS

To determine the wicking rate, three samples for each type of fabric were cut (in ribbon shape) with dimensions of 170 mm x 25 mm and placed straight in a beaker containing distilled water. The height of wicked water in different times (1, 5, 10 and 15 min.) was recorded as wicking ability factor. At the end, the mean value was reported.

Figure 30: Water evolution by capillarity during the VWT.

STRESS – STRAIN CURVES

The last essay realized in university laboratories has been the stress test. This type of test has been carried out to measure the maximum load and deformation of different types of gauzes, because the addition of nanofibres has been able to modify some other property than absorption, such as resistance and elasticity.

To perform this test, a Starrett thickness gauge and the Hounsfield dynamometer shown in Figure 31 were used. In addition, a computer is necessary to install Metrotech software in order to extract the results of the analysis.

Figure 31: On the left the Starrett thickness gauge and on the right the Hounsfield dynamometer used to perform the stress-strain curves.

A very important parameter is the size of the test tubes, both length and width. In this case, the prepared test tubes were 15mm wide and 50mm long. The methodology followed was the following one:

Firstly, the thickness meter was used to find out the average thickness of each sample. Next, with the distance between the jaws previously configured at 50mm, the analysed test tube was placed between trying to make it perfectly stretched. However, it must be said that due to the type of samples analysed, it was difficult to

place them completely smooth, since once infused they have hard-wrinkling wrinkles unless an important pre-existing force is applied. Finally, a reset on the force and the extension was done and immediately after that the tests began automatically. When all the samples where tested, all the results were reported.

ANTIMICROBIAL TESTS

The antibacterial and antifungal activity of gauzes and aerogels has been analysed by the growth of a bacterium (*Bacillus*, BS) and a fungus (Aspergillus Nigger, AN) following the UNE-EN1104 standard. The objective of this analysis is to verify if the treatments applied to the materials inhibits or promotes the appearance of microorganisms around it.

First, before placing the samples in the growth medium, it had to be inoculated; BS and AN had to be incorporated into different bottles. Below it is explained how each of the processes was carried out, since each microorganism must be treated as they require:

In order to inoculate the BS, firstly, the medium had to be removed from the fridge were was stored and immediately placed in the autoclave with the corresponding program that applied for 20 minutes a temperature up to 121ºC, so that the medium left liquid. Meanwhile, the area of the hood was sterilized to ensure work in an unpolluted area. When the program finished, the bottle was cooled down to approximately 60ºC due to the fact that if you work at higher temperatures the bacterium may not reproduce. Then, the bottle and the strain with the bacterium had to be brought below the bell. Finally, with a micropipette, 1mL of the bacterium was added and it was introduced into the bottle. Then, the bottle was closed and mixed slightly with hands.

When inoculating the AN on the other bottle with medium, the procedure followed was the same as inoculating the medium with BS, the difference is how to inoculate it. Once the medium has cooled down to 60ºC, a turpentine with the Bunsen flame was sterilized and gently slid through the surface of the AN strain. Once the turpentine was impregnated, it was only necessary to enter it in the medium to disperse the fungus. Finally, the action was repeated a couple of times, the bottle was covered with the inoculated medium and also slightly mixed with the hands.

Next, to prepare the qualitative analysis we used the two previously inoculated mediums and several samples with the different bactericidal agents (JTH infused gauzes with glycerol and TiO_2 and aerogels only with TiO_2). The procedure begins dropping approximately 50mL of the inoculated medium with the appropriate microorganism inside a Petri dish under the hood, with the extractor and Bunsen on to prevent contamination.

The medium was allowed to cool until it became solid and then three circular treated samples, about 2cm, were placed with the help of previously sterilized tweezers in the middle of the correspondent Petri dishes. Once positioned, the plate was covered and placed on the stove at 30ºC for 5 days for the bacteria and 7 days for the fungus. The effect of these microorganisms on non-treated samples was also analysed.

RADIOPACITY TESTS

In order to observe whether the last consumables produced have radiopacity or not, X-rays have been performed on different samples with the Multi Fusion Max RX machine from Siemens Healthineers. Concretely, a gauze with a 0,5% CNF infused, glycerol and TiO_2, an aerogel made with 0,3% of nanofibres and TiO_2 and an untreated gauze were tested.

4 RESULTS AND DISCUSION

Following the methodology explained above, it is proceeded to discuss the results obtained. Firstly, the nanofibre properties will be evaluated to know if the production is correct. Subsequently, the results obtained in the characterization of the gauzes will be evaluated to determine whether the desired properties have been improved.

4.1 EVALUATION OF CNF CHARACTERISTICS

As mentioned in point 2.3, there are many types of cellulose nanofibres depending on the pre-treatment applied to fibres. Each type of CNF can be used for various applications depending on their intrinsic properties. In this work, it was decided to use TEMPO oxidation cellulose nanofibres to produce gauzes and some of the aerogels, although some CNF were produced by enzymatic hydrolysis to prepare the rest of aerogels. The last type of treatment has a better quality/cost ratio (13,66€/Kg CNF) compared to the other treatment, which results in CNF with a much higher mechanical performance, but by contrast its cost increases exponentially since the TEMPO catalyst is very expensive for the treatment (205,73 – 175,39€/Kg CNF depending on the degree of oxidation). Otherwise, oxidizing the fibre makes it more polar, which is interesting in this study to achieve more affinity surface to create future hydrogen bonds. On the other hand, the enzymatic hydrolysis applies a methodology based on bioprocesses and therefore, possibly it is a process more respectful with the environment. However, there has been no analysis of the life cycle of these methodologies to compare their environmental effects. It should be noted that there are parameters that are considered crucial when it comes to obtaining good properties, such as: the consistency of the paste, the pH, the chemical composition of the fibre, the temperature (only for enzymatic) and the dose of catalyst/enzyme (Maestre & Delgado-Aguilar, 2016).

Currently, there is still a lot of controversy surrounding the dosing of these reagents. With regard to the production of TEMPO-CNF the doubt was in what degree of oxidation was the most optimal for obtaining better quality nanofibres. For this reason, Serra et al. conducted a study showing how much NaClO is the best to add in order to obtain the desired results. In this study, CNF was analysed with an oxidation degree of between 2 - 15 mmol NaClO. In their results can be seen independently of the analysed parameter that the best results are shown by the nanofibres produced with 15 mmol NaClO. For this reason, in this work, it has also been decided to apply this degree of oxidation to the fibres (Maestre & Delgado-Aguilar, 2016).

About E-CNF production, some researchers decided to apply to the suspension of pulp amounts of 200 to 30.000 g/tonne of enzyme; others decided to apply lower doses, of 80 g/Tn. However, Wang et al., (2004) showed that low dosage such as 1 mg of enzyme per gram of fibre was enough to observe a reduction in the degree of polymerization of cellulose chains.

The conditions established in this work to develop nanofibres treated by enzymatic hydrolysis (E-CNF) were based on the results obtained by Tarrés et al., 2016. Regarding the temperature, it is known that the kinetic reaction of the enzyme depends on it, like most biochemical reactions. Knowing that the enzyme used in this work undergoes its denaturalization at 80 ° C, Tarrés et al., 2016 made changes in the reaction temperature in order to know its relationship with the final mechanical properties of a paper with 3% of E-CNF. It was determined that the optimum reaction temperature was 50 ° C. On the other hand, as far as the reaction pH, Tarrés et al. determined that this type of enzyme showed its maximum activity at pH values of about 5. Finally, they determined that the efficacy of endo-β-1,4-glucanases improved when working at a consistency of the paste 5% by weight.

Otherwise, Tarrés et al., 2016 studied the relationship between the reaction time and the amount of dosed enzyme with respect to the breaking length of a paper formed with 3% of the resulting E-CNF (Figure 32). The dose of enzyme ranged between 80-320 g/t and the reaction time between 2 and 4 hours.

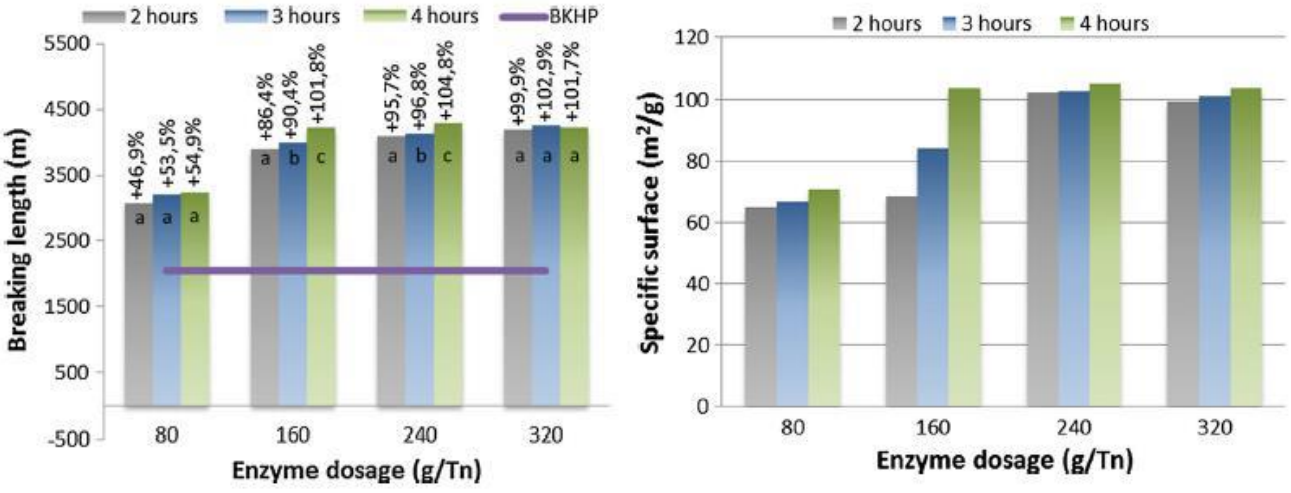

Figure 32: Evolution of the break length (left) and the specific surface (right) of different papers reinforced with E-CNF regarding increments in dosing of the enzyme and reaction time. Source: Tarrés et al., 2016.

Although, according to Tarrés et al., 2016 the best option to obtain a greater specific surface and breaking length would be to apply a dose of 160g/Tn. during 4 hours, it was decided to apply the dose of 320g/Tn. for 2 hours; as Figure 33 shows a lower degree of polymerization is achieved, that means, a shorter length of fibres (more nanofibres), taking into account that as seen before the difference from the other properties at different dosage varies minimally.

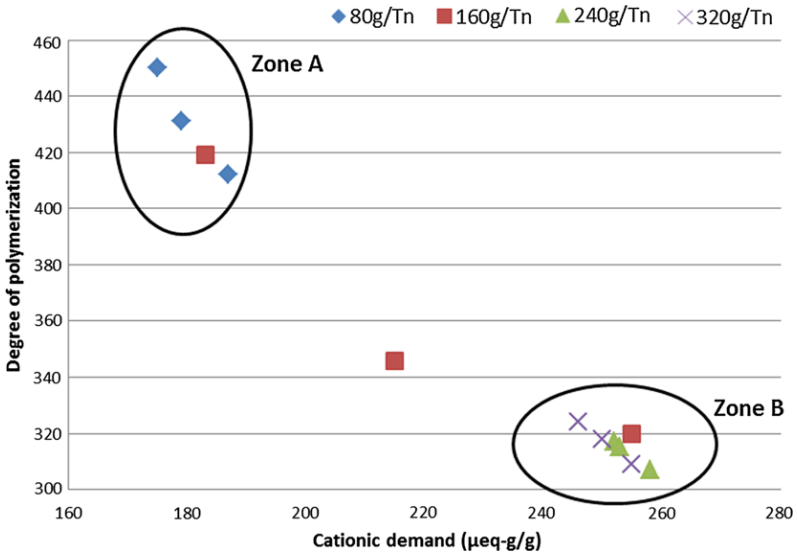

Figure 33: Correlation between the degree of polymerization and cationic demand of CNF. Source: Tarrés et al., 2016.

Once both types of CNF were obtained, it was decided to perform a characterization of these to assess whether the results obtained were similar to those found by Serra et al., 2017. In this case, the characterization performed was based on determination of the cationic demand, the polymerization degree, the yield, the water retention value, the specific surface area and the diameter (Table 5).

Table 5: Characterization of both types of CNF produced.

CNF	CD [µeq·g/g]	CC [µeq·g/g]	DP	Yield [%]	WRV [g/g]	SS [m^2/g]	∅ [nm]
TEMPO 15mmol	2031,47	1392	197	98,88	11,4	311,4	8,56
Enzymatic 320g/Tn	226,20	42,1	309	38,9	6,3	89,7	29,7

Table 6: Reference values for the CNF characterization. Source:(Serra et al., 2017).

CNF	CD [μeq·g/g]	CC [μeq·g/g]	DP	Yield [%]	WRV [g/g]	SS [m^2/g]	∅ [nm]
TEMPO 15mmol	2043	1392	197	98,88	11,4	317,0	7,89
Enzymatic 320g/Tn	260	42,1	309	38,9	-	-	-

Initially, comparing both characterizations, huge differences can be notice. As found in the literature research, it is normal that cationic demand is so much higher in TEMPO-CNF, because they last with an electrical charged structure due to the oxidation reaction. So, apparently, TEMPO-CNF should be able to form better structures thanks to this property. As well as, there is a lot of difference between the carboxylic content of each type, because TEMPO nanofibres have been made through an oxidation reaction where hydroxyls groups from cellulose change to carboxyl groups, then is normal to have more quantity in the first type of nanofibres.

Regarding the degree of polymerization, it is seen that enzymatic nanofibres have a higher value for not a long difference; this fact is due to the reaction mechanism applied. So, if an enzymatic reaction is performed the nanofibres will always result large than TEMPO-CNF. For this application, it is interesting to have the lowest DP possible in order to have the same length in all the nanofibres. Now, evaluating the values obtained for the SS and the diameter a great difference is observed, too. Concretely, TEMPO-CNF have a specific surface and a diameter 3,47 times higher than E-CNFs and a diameter. Curiously, both parameters have the same relation because they are calculated theoretically doing the same considerations as Serra et al., 2017; so, to know exactly the real values the diameters should have been measured using the scanning electron microscopy (with a gold layer to have more resolution). Unfortunately, in this case the real measure was taken using a SEM with a silver layer instead and consequently it was not possible to take pictures at nanometric scale without burning the samples. Focusing on the water retention value, it is seen that apparently TEMPO have a better absorption capacity, since they have a better CD, DP and SS. WRV is one of the most important parameters to consider when choosing which type of CNF is better to produce for this application, because it has a lot of influence at the end. Considering all the differences commented an idea is given to know apparently which samples are going to have better absorption, evaporation and wicking capacity.

Finally, comparing the obtained results with the literature values on Table 6, an insignificant deviation can be appreciated on some values. Therefore, it is considered that nanofibres have been correctly prepared and that they are ready to use for the desired application.

4.2 PHYSICAL PROPERTIES EVALUATION OF GAUZES AND AEROGELS

After certifying the quality of the CNF, the sample preparation and tests performed, the results obtained are exposed and commented according to a specific order. Note that this order will only be followed for the exposition of the physical analysis results. Firstly, the JTH gauzes will be compared, since they are the gauzes that have been established as the reference and the main focus of research. Secondly, the same gauzes will be compared with gauzes from other manufacturers, whether they are woven or non-woven. Then, a comparison of the aerogels will take place only between themselves. Finally, a general comparison will be made to compare all the cases, as well.

4.2.1 GAUZES COMPOSITION

The first question that was raised when initiating this research was whether the cellulose nanofibres would attach to the fibre of the gauzes. The literature has shown that they should join together through hydrogen bonds and Van de Waals forces, but to proof this, as previously said some of the samples were analysed by means of scanning electronic microscopy (SEM). The results are shown in Figure 34 and Figure 35.

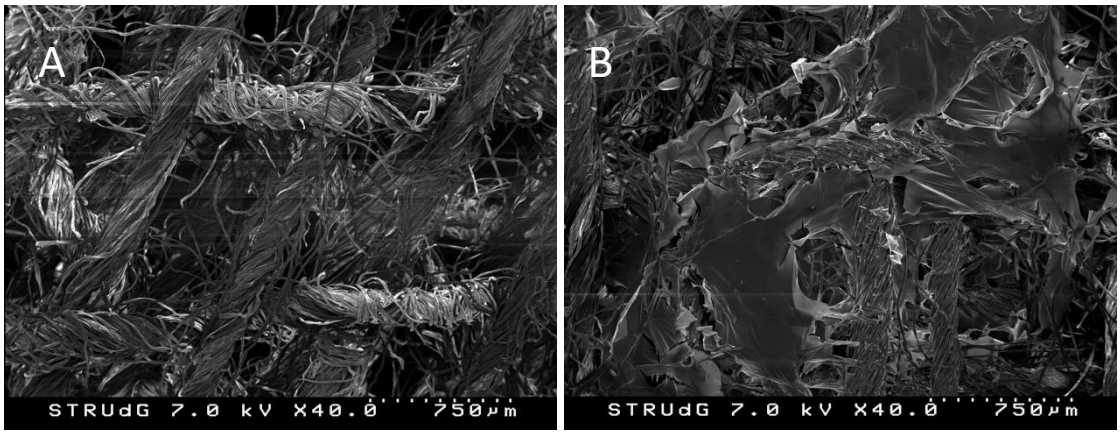

Figure 34: Comparison of woven gauzes through FE-SEM: (A) Untreated JTH gauze, (B) Treated JTH gauze.

As shown in Figure 34 (A), only the lattice of cotton filaments can be appreciated. When comparing with Figure 34(B), the presence of a kind of fabric attached to the structure of the woven gauze is clearly observed. This

new structure, which arises from nanofibres, first attaches to cotton threads and then builds a 3D network between them.

When comparing Figure 35 (A and B) the starting gauze, does not show any substance apart from the basic filaments. However, when compared to the gauze that has been properly treated, as well as with the swanned gauzes, the presence of the 3D network of nanofibres attached to the consumable can be seen.

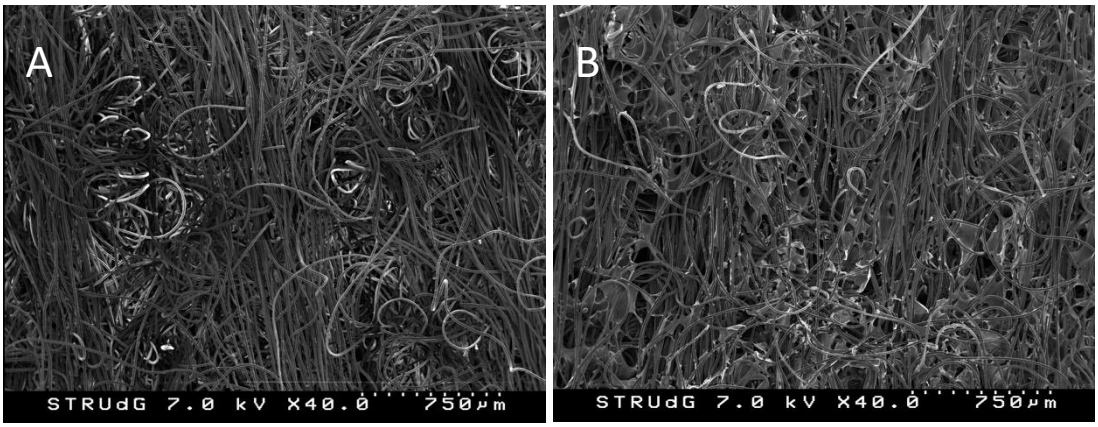

Figure 35: Comparison of non-woven gas through FE-SEM: (A) Untreated GASPUNT gauze, (B) Treated GASPUNT gauze.

If both gauzes are compared, it is possible to see an obvious difference between woven and non-woven gauzes. In the first case, each of the beams is clearly formed by a large quantity of cotton filaments and placed in the knitting direction. On the other hand, the non-woven gauzes have a huge disorder, since any fibre orientation has been given. This structural difference has some influence on the infusion of nanofibres, because then the woven gauzes can build much more extensive networks due to the available space between filaments. Contrary, the non-woven gauzes, they do not have the capacity to form large networks without adhering immediately to another thread.

Once the presence of the nanofibres in the gauzes is really certified, its composition has been calculated by means of a gravimetric analysis. Moreover, the same analysis was carried out with those gauzes which were also infused with glycerol and TiO_2 in order to observe the composition variation. At the end, the results obtained (see Figure 36) demonstrate the presence of CNF after the infusion process. Even though, in any case, the maximum amount of CNF that JHT gauzes have been able to withhold is approximately 0,05g per gauze (the initial weigh of gauzes ranges 1,3 and 1,4g). As seen in the graphic, this amount represents a very small percentage of the total. In spite of, only with a percentage between 3.5% and 4.3%, changes in the structure and properties can be apparently noticed.

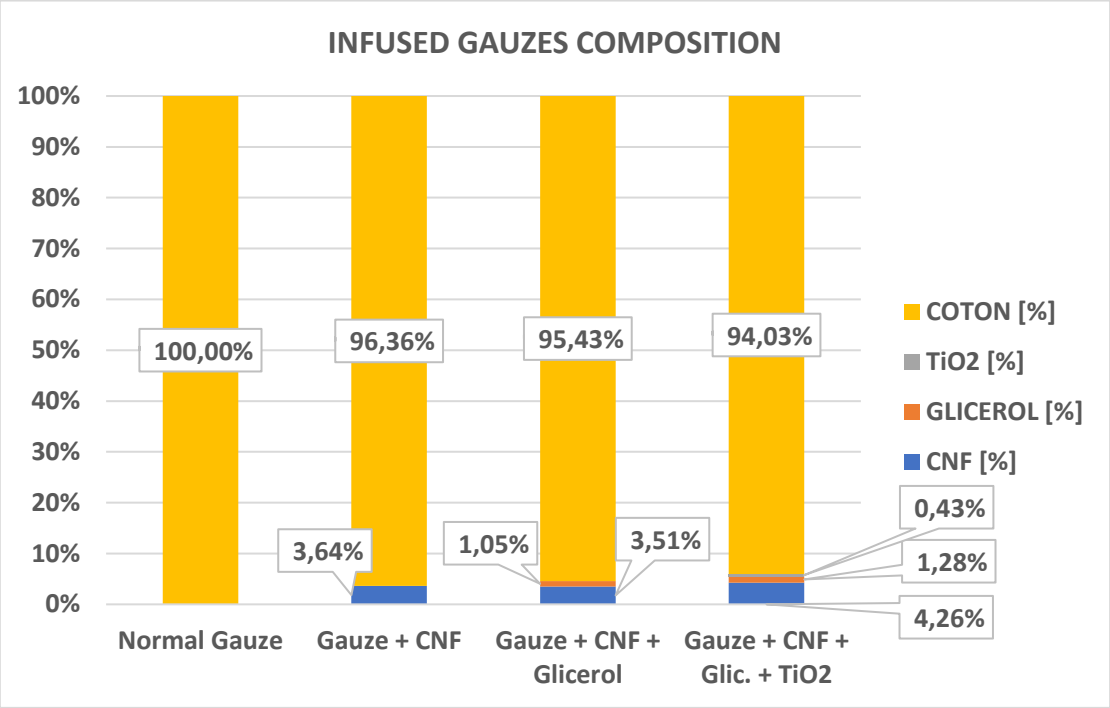

Figure 36: Composition comparison between JTH treated gauzes.

Finally, by focusing on the additives, different aspects are detected. Glycerol is theoretically placed between the cotton filaments and the nanofibres networks, then the internal forces of the same consumable diminish, and an improvement in the final malleability of the product can be noticed. During the research, its infusion has only been certified through the gravimetric method since with SEM it is impossible to distinguish it from cellulose. Regarding the TiO_2, a great change is already observed at first sight; so initially, those gauzes that have only been infused with CNF show their cotton threads white and transparent and the nanofibre networks that have been formed look bright against light. When titanium dioxide was incorporated, these structures formed by the CNF show a whitish colour. By using both analytical methods mentioned above a certain amount has been detected, as well as Figure 40 shows. However, despite being in very small quantities, they already cause changes in their final appearance and properties, since the amount added in their respective gauzes is very low, around 1% for glycerol and 0, 5% for TiO_2.

4.2.2 WATER ABSORPTION TESTS RESULTS

From all the different tests that have been carried out on each product, the most significant one is the water absorption test. The results allow us to establish whether or not gauzes meet with the conditions for which they were modified. Below all the results obtained on the WAT are described following the methodology set above:

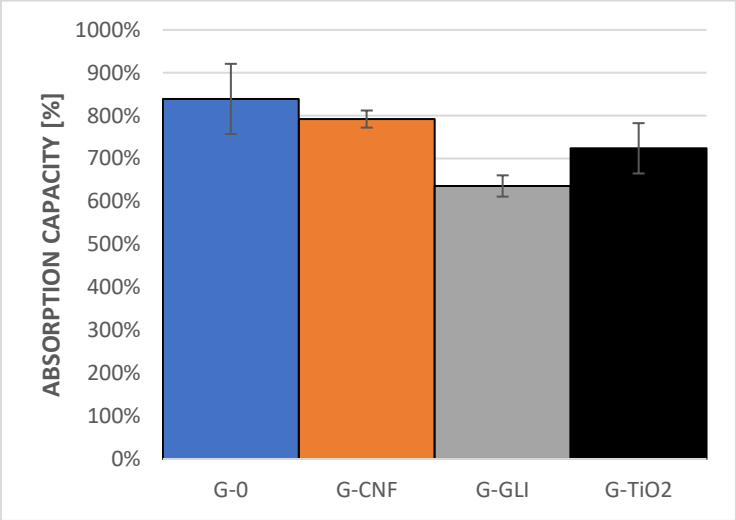

Figure 37: WAV comparison between JTH treated gauzes.

Even though theoretically, CNFs should increase the specific surface of the gauzes and consequently their absorption capacity, this is not what the results reflect on Figure 37. So, the most noted change is that treated gauzes show a deterioration in the absorption capacity when adding nanofibres, this drop is about 5,6% from its initial capacity. This difference is due to two causes: observing Figure 38 (A), when the CNFs are infused, they need a structure where to link themselves. This structure is the one made by the cotton threads and, hence, it shows some affinity with the CNFs (thanks to -OH groups and Van der Waals forces). However, the surface of these cotton filaments is more limited and lower than those from the CNFs. Therefore, once the surface of the cotton filaments is swamped, the CNFs need to start joining other structures or, in this case, build new structures with itself. Then, lots of three-dimensional framework are generated, creating networks between filaments. if we compared the achieved structures with the ones from other research (Figure 39) it is observed that CNFs take up all the free space between and into the cotton beams. Finally, this end limiting a lot the useful space of the entire gauzes where water should have been hold and absorption capacity is lost. Although, taking into account the deviation shown by the reference samples (G-0) and comparing it with G-CNF one, can be that sometimes the absorption capacity remains the same or increases minimally. Despite that, even in the best situation, the biggest positive difference possible would be insufficiently large to consider that the treatment has been worthwhile.

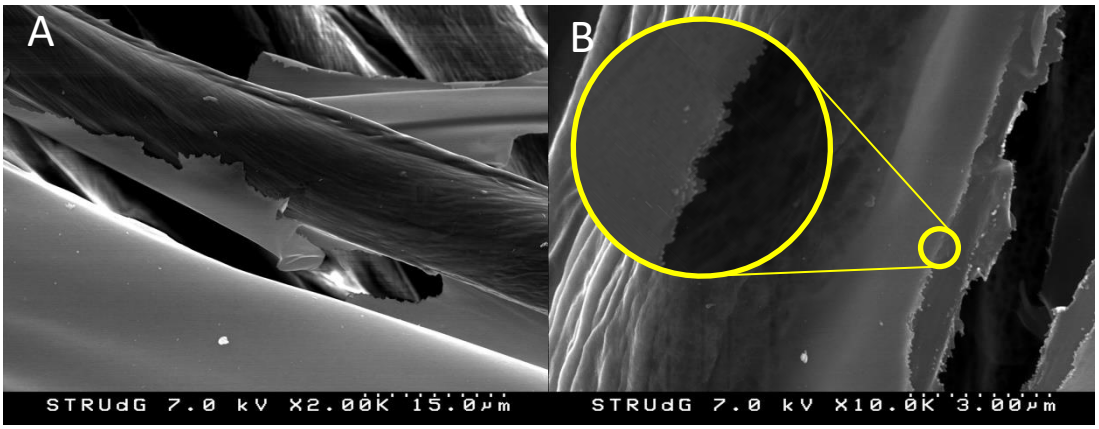

Figure 38: (A) shows the CNFs surrounding a cotton thread and (B) shows the moment when CNFs build the structure to extent themselves.

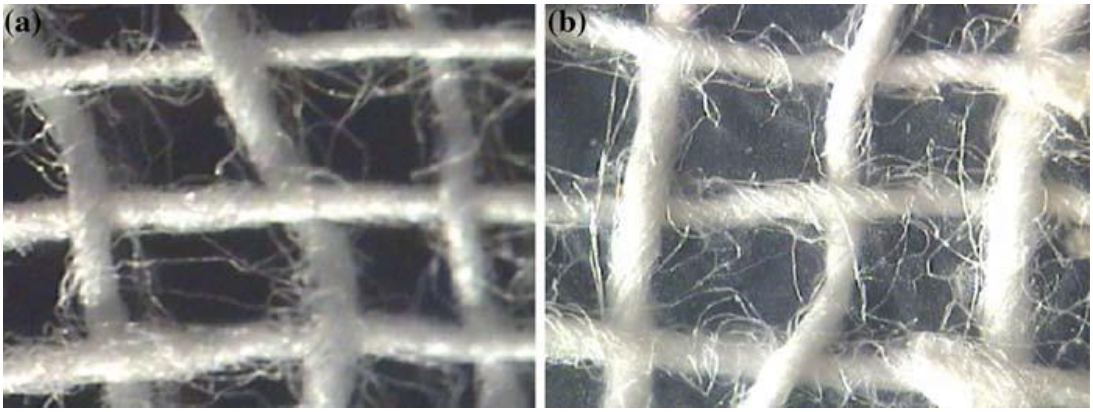

Figure 39: Microscopic images of a bacterial nanocellulose cotton gauze after 6 days in a culture media (x40): (a) untreated, (b) treated. Source: Meftahi et al., 2010.

Next, if those results cited above compared with the gauzes with glycerol (G-GLI), the reduction of the ability to absorb liquids is even more abrupt, their initial properties diminish about 24,2%. This happens because glycerol is a hydrophobic substance, although it is necessary to improve the movement of the gauzes. Unlike the results of G-GLI, by adding as well TiO_2, the gauzes show a slight recovery of their absorption capacity. The G-TiO_2 sample increases a 13.83% its absorption capacity, despite that in global terms the difference between G-0 remains negative with a loss of 13,7% of its starting capacity. Taking into account that those gauzes have better malleability, due to the glycerol addition, and according to its deviation in front of JTH untreated gauzes, the results are not so bad. This unexpected phenomenon happens because, as seen in Figure 40, titanium dioxide nanoparticles are cover by nanofibres instead of only being attached to the CNF structures. So, surprisingly CNF show a greater affinity for TiO_2 nanoparticles instead of cotton. This means that, the more CNF attached to TiO_2, the more cotton surface will be exposed, and this will cause that absorption increases slightly depending on the area of fibre that is uncovered.

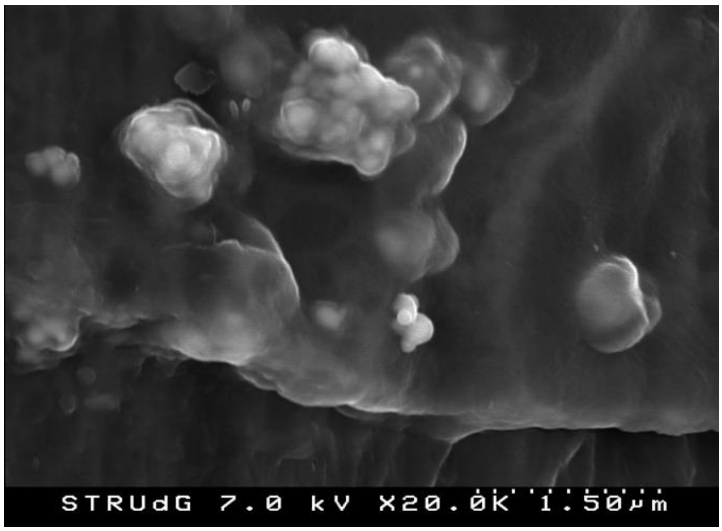

Figure 40: FE-SEM image of a G-TiO_2. Interphase between the cotton thread and the CNF layer with TiO_2 attached.

Next, on Figure 41, comparing the results obtained from the JTH gauzes with the others from different suppliers, the same behaviour as in Figure 37 is observed. The addition of CNF causes a deterioration on all the products absorption capacity. In this case, the worst change has been done by the one that had the second biggest WAV without treatment, the Texpol woven gauze. Now, with regard to non-infused gauzes, the best result is offered by Gaspunt's non-woven gauzes (1142% WAV) due to the porosity of the samples; followed by a minimal difference for Texpol woven gauzes (1126%). On the other hand, the worst results are clearly those from the "Ortopedia y Cirugia" gauze which have a WAV around 774%. This result is caused by the number of threads and the way that this consumable has been sewn, given that they reduce the global specific surface of the sample. Finally, focusing only on the results of all the treated gauzes it can be seen that there is no difference between the treated samples from the JTH and Gaspunt. Both consumables, despite having different sew manufacturing process, have a WAV around 800%. Possibly they have the same specific surface after the treatment; but unfortunately, there has not been time to perform a full characterization to know it in detail.

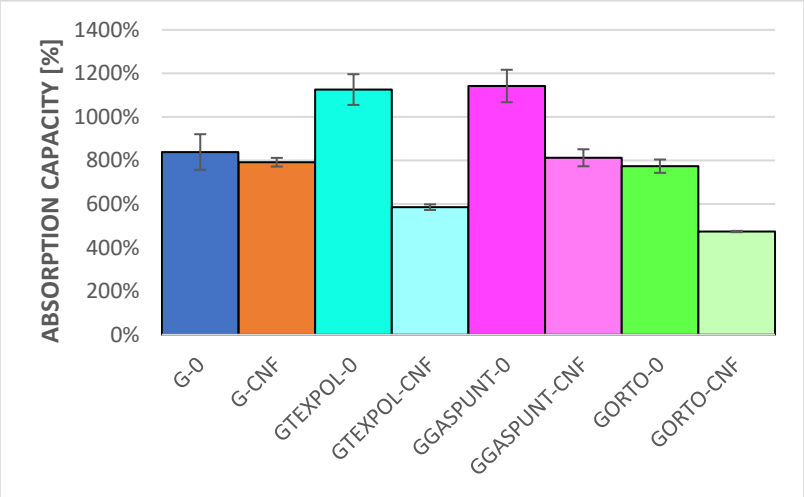

Figure 41: WAV results comparison between gauzes from different suppliers.

At first sight, on the comparison between aerogels it is possible to see how the aerogels produced by TEMPO-CNF have a better water absorption capacity than aerogels produced by E-CNF. Numerically, there is a difference of approximately 1.350% between AT-0,3 and AE-0,6, while the difference between AT-0,3 and AE-0,3 is still greater, specifically 2.750%. This dissimilarity is explained through its structural organization (Figure 43). The enzymatic aerogel has a large structural disorder due to the presence of cellulose chains of different lengths, as certified with their DP value due to their reaction mechanism. Whereas, the structure of aerogels made with TEMPO-CNF exhibits almost a crystalline structure, because both are very well structured due to the equal dimensions of the nanofibres.

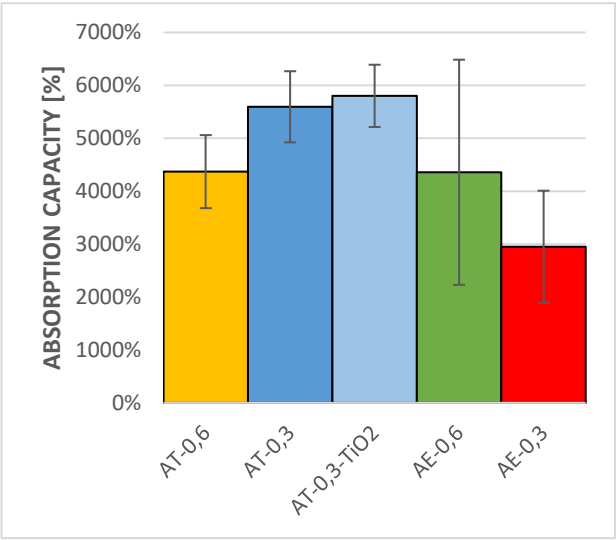

Figure 42: WAV results comparison between aerogels made by different types of CNF.

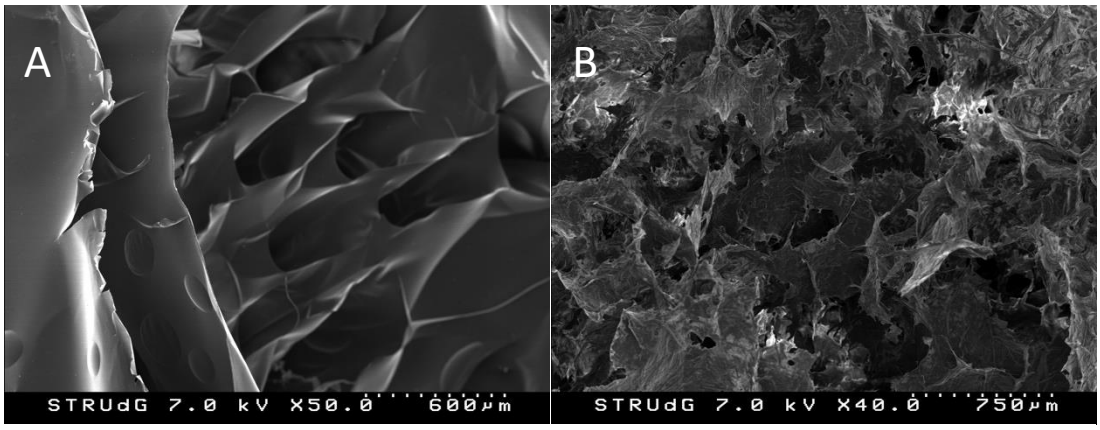

Figure 43: Comparison of the internal structural organization between AT-0,3 (left) and AE-0,3 (right).

Now, only discussing about the aerogels produced with TEMPO-CNF, given that all the analysed samples have shown a better absorption capacity, it is observed that both AT-0,3 samples have a WAV clearly higher than the AT-0,6 samples. This first difference is also due to the structural organization of each type of aerogel, because when comparing both images (Figure 43(A) and Figure 44) it can be appreciated that the first sample has less porosity than the second one. This last affecting directly the properties of each aerogel, because those that have been manufactured from TEMPO-CNF, with a consistency of 0,3%, are 1,28 times greater. However, the AT-0,3 are not the samples that have been able to withstand more water, those have been the AT-0,3-TiO_2 ones. The aerogels made with TEMPO-CNF (0,3% consistency) and 10% of TiO_2 to CNF dry weight, shown an improvement of 3,7% in front of the AT-0,3. This property improvement, which have also been observed in the G-TiO_2 samples, is due to the same fact. The aerogels with titanium dioxide added are more porous, consequence of the coating that CNFs due to the titanium dioxide nanoparticles during the infusion process.

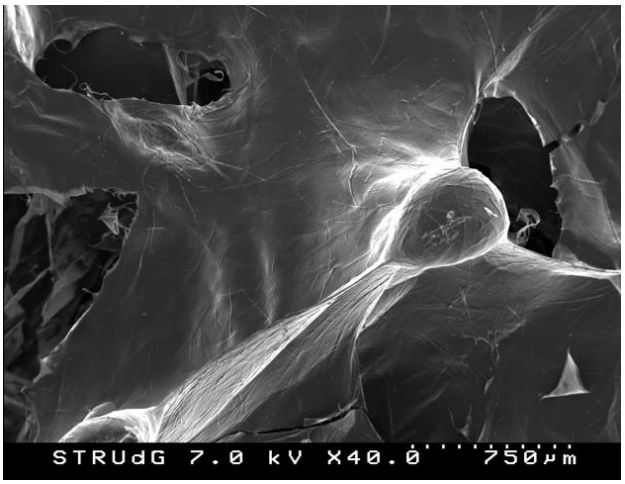

Figure 44: Internal structural organization of an AT-0,6.

About AT-0,3 results it is important to expose some appreciation done when testing. Before starting the experiment it was observed that half of the samples prepared showed a type of anisotropy, because they had some CNFs with spontaneous orientation in some directions, as it is exposed on Figure 45. After the analysis those samples that were a little bit orientated had the best WAV. As well as, those samples seemed to have a better resistance than the others. So, looking at what Chen et al., 2019 says, it could be possible to improve the structure organization of aerogels by: first, applying a carboxylic acid before ending the oxidation reaction to crosslink more the CNF. Then, to make this crosslink effective, freezing the sample in the same direction to give the fibres the same orientation. The final result should be an aerogel better structured than the one on Figure 43, which offers better absorption properties and above all improved stress resistance.

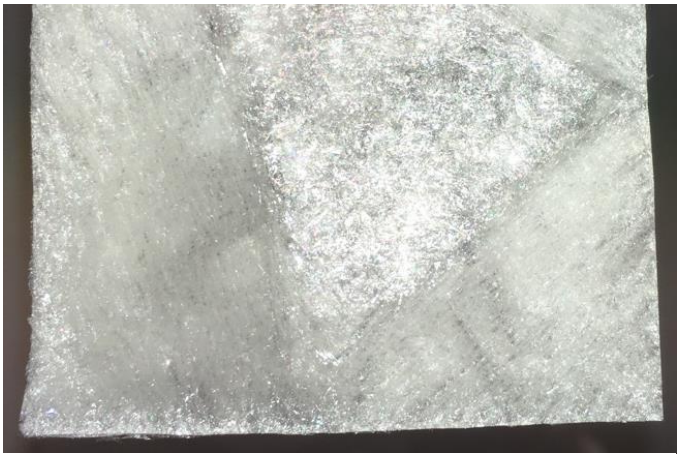

Figure 45: TEMPO aerogel at 0,3% of CNF consistency with some fibre orientation.

Also, note the variability of AE samples, there have been samples with higher WAV that the AT-0,3-TiO_2 (6.500%). This deviation is due to the weakness that these types of consumables have shown along all the tests, despite having one of the largest absorption capacities. To have an idea of their weakness, they do not have enough resistance to hold their own weight once all the water was absorbed. So, they end breaking by its half, despite of having been treated with the maximum care. The weakness that show this type of aerogel is directly related to its structural instability, as reflected in Figure 43 (B). Lastly, only one single cycle from five could be performed on each AE sample. To counteract this problem, the method explained above could be tried.

Ending the analysis of the water absorption cycles, all the reported results are compared in the same graphic (Figure 46). It can be seen that there is an extremely large difference between gauzes and aerogels. So, the

minimum possible difference is 2.5 times (AE-0,6 respect GGaspunt-0), but if looking to highest WAV it is found that the minimum difference from gauzes is about a 5 times greater capacity.

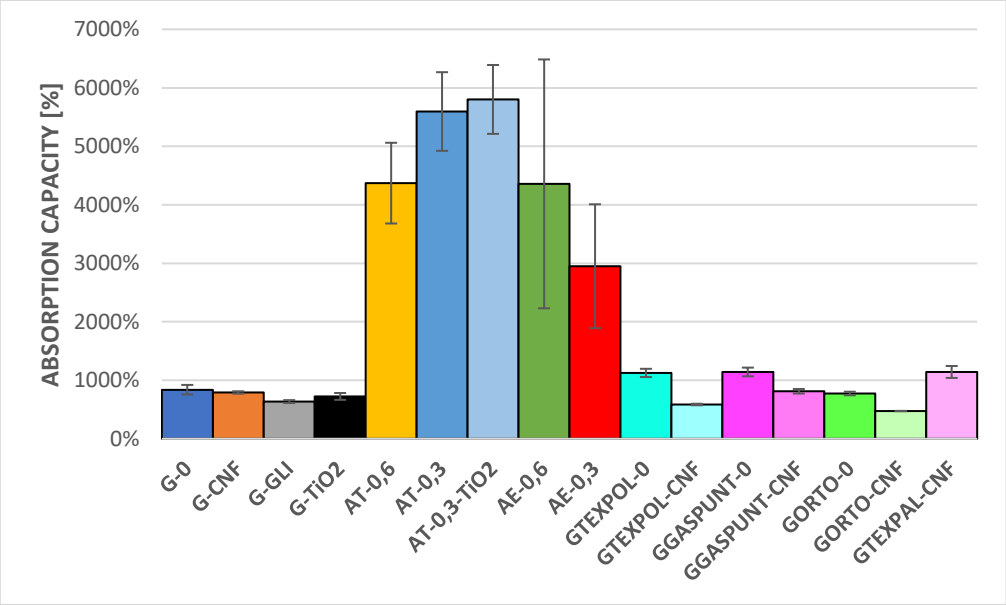

Figure 46: General comparison of the obtained WAV results.

4.2.3 WATER HOLDING TIME RESULTS

As Meftahi et al., 2010 says, moisture retaining of wound surface (preserving wet condition during wound care) accounts for a very important criterion in modern active wound dressing. For this reason, the results obtained from the water holding time tests will provide the information need to establish which consumable is the preferable from that application.

Firstly, in Figure 47, a comparison has been made with the results of all the JTH gauzes tested. In them, it is seen the opposite behaviour in front of the results obtained in WAV. Specifically, when adding CNF to the gauzes, they suffer an increase of 16,2% over the original gauzes. Then, when the other two additives are added, to provide to the final product a better applicability, the evaporation speed is reduced despite been for a very small difference. In case of the G-GLI it is 0,97 times lower from G-CN and G-TiO_2 have 0,82 times less capacity to evaporate liquids.

According to Silberberg (2006), for molecules of a liquid to evaporate, they must be located near the surface. They have to be moving in the proper direction, and have sufficient kinetic energy to overcome liquid-phase intermolecular forces. From here, some of the factors that have more influence on the evaporation capacity are discussed in order to explain why those treated samples have better evaporation. The first factor to

mention is the concentration of the substance that evaporates in the air, because if it already has a high concentration on the substance where it will be evaporated, then the substance given will evaporate slower. But, during all the experiments the air had around a 70% of RH and therefore this is not the cause of this improvement, since air was not saturated. In case of the concentration of other substances in the air it happens the same, because there was no other substance that prevent evaporation. Next, as far as the air flow through its surface is concerned, if a forced air flow is moving over the substance all the time, then the concentration of the substance in the air is less likely to go up with time. This fact encourages a faster evaporation because the air will displace the water vapor molecules on the interphase in favour of evaporation, due to an increase in the concentration gradient of the molecules. However, during the experiment, there was no forced flow at any time to cause an increase of the evaporation rate. Now, focusing on the intermolecular forces, it is known that the stronger the forces that keep the molecules of a liquid are, more energy will take to evaporate them. This factor is only important to consider when trying to understand why G-TiO_2 has a worse evaporation rate. As explained previously, nanofibres seem to prefer the TiO_2 nanoparticles than the cotton threads and due to this phenomenon, the evaporation capacity is a little bit minor.

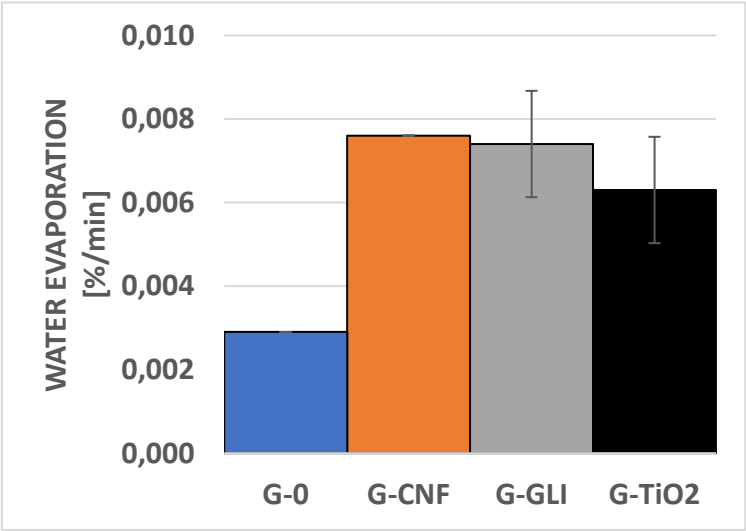

Figure 47: Comparison of the WHT results between treated and untreated gauzes from the JTH.

Regarding to pressure, evaporation is faster if there is less pressure on the surface that keeps the molecules moving between them, but throughout the entire study the atmospheric pressure had not changed at any time. Also, if the temperature of the substance is higher, the molecules will have a higher average kinetic energy to evaporate more quickly. But, as happens with the pressure and the other parameters mentioned so far, it has not been modified at any time while testing. Oppositely, when adding CNFs density increases even

though that is in a very slight way, since the added mass of nanofibres is minimal in relation to the volume of the gauze and it can affect minimally to gauze's evaporation. Hence, the last parameter remaining to evaluate, the specific surface, is the most important one since the product that has a larger surface area will evaporate faster than others. That happens because the surface from which the molecules can escape is much greater. Infused gauzes have a larger specific surface compared to the original ones and they are able to leave out water more quickly. However, as already has been mentioned, the evaporation descends when incorporating glycerol and titanium dioxide. This is due to the fact that the forces of interaction between water and these substances are greater and no extra energy has been provided to the particles linked to them, then it costs more to evaporate them.

Following, in the comparison with other gauzes from different distributors, it has been observed that the highest evaporation rate is show by the Texpla gauze with an evaporation speed of 0,0085 %/min for the original one and 0,0094 %/min for the infused one. This type of gauzes are the ones that are supposed to have a higher specific surface than the others, so the results are logical. Contrary, the minimum value is showed by the untreated JTH gauze, which is 0,34 times lower than the best gauze. The reason why this happens is due to their lower number of cotton threads and layers, what makes that also this type of gauzes have a lower specific surface. As well, it is important to amend that the gauzes from Gaspunt and "Ortopedia y Cirugia" have an abnormal behaviour. This is probably because in some cases the number of samples provided was not enough to do a correct study. In addition, the infusion method applied in this research is not enough mature and sometimes is difficult to end with the same quantity of CNF infused on gauzes. An example of this turmoil is the Figure 49.

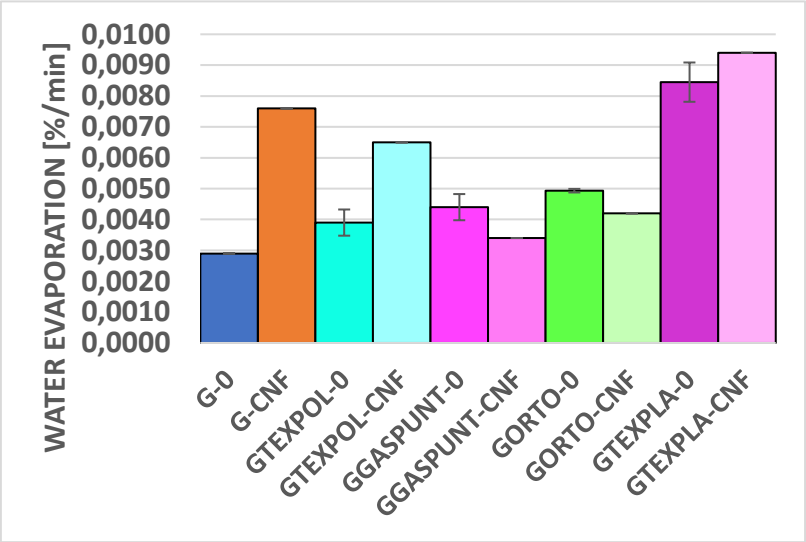

Figure 48: Comparison of the WHT results between treated and untreated gauzes from distinct suppliers.

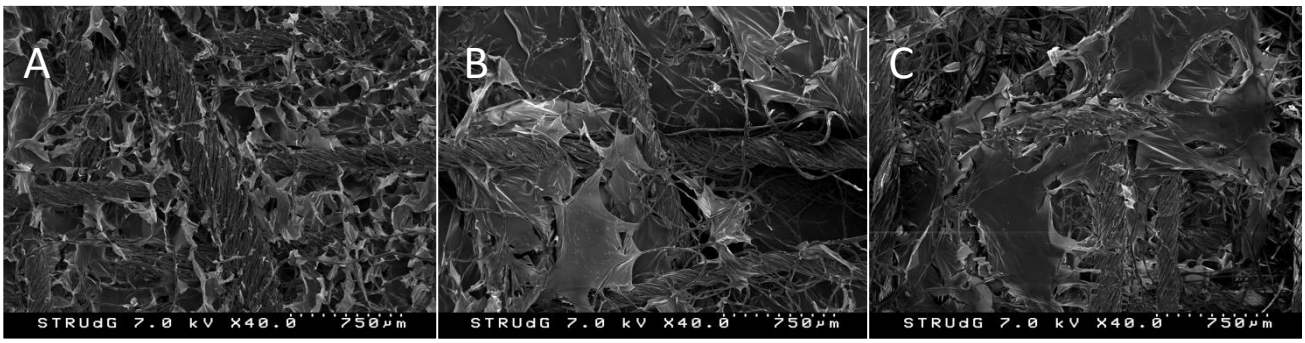

Figure 49: Comparison of three gauzes of the same brand infused exactly in the same way. This comparison gives an idea about how difficult can be to obtain improved gauzes with a similar CNF content.

When comparing the results from the aerogels, some difference between WA results can be noticed. Now, all the aerogels with a 0,3% of CNF in their composition, have a better ability to evaporate water. Numerically, AT-0,3 are a 58,5% better than AT-0,6 and AE-0,3 have an evaporation capacity 1,35 times higher than AE-0,6. This fact occurs because samples with a CNF content of 0,3% have less quantity of nanofibres in the same volume, so when they get distributed and lyophilized, the result is a more porous aerogel with a higher specific surface. Then, it is easier to evaporate whatever. However, the samples of AT-0,3 produced also with TiO_2 suffer some deterioration, because the affinity of the CNF with the titanium nanoparticles builds a structure with bigger pores than the normal one. That reduction on the evaporation ability is approximately of 8%, such a small reduction.

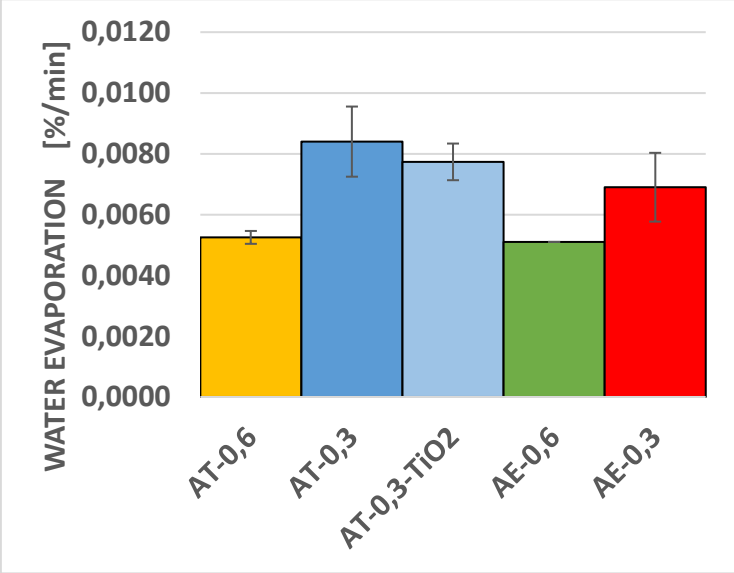

Figure 50:Comparison of the WHT results between aerogels made with different types of CNF.

Next, looking from Figure *66* to Figure 68 (attached into the annex), the evaporation evolution in front of time is evaluated. A uniform behaviour in the vast majority of samples is observed as was expected; while time draws on, more water is evaporated. Whereas, the evaporation speed decreases until in the long run they reach an almost stationary phase. The only samples that stand out for having a different behaviour are the non-woven gauzes by Texpla. These, instead of reducing their evaporation rate, keeps it constant. Even, in case of the only infused sample, the speed increases slightly by time.

Finally, when unifying all the results of the WHT test in Figure 51, this behaviour from the GTEXPLA gauze is also noted. Compared with the AT-0,3 aerogels, which have the second-best result, Texpla gauzes are almost 12% faster evaporating liquids. But, unlike the results of the WAV, the overall behaviour has been more balanced, because the largest difference shown is the one from the original JTH gauze in front of the GTEXPLA-CNF, which is 3,24 times slower. To sum up, it is observed that the greater the specific area of the sample the more evaporation capacity will be achieved, as explained in the first comparison.

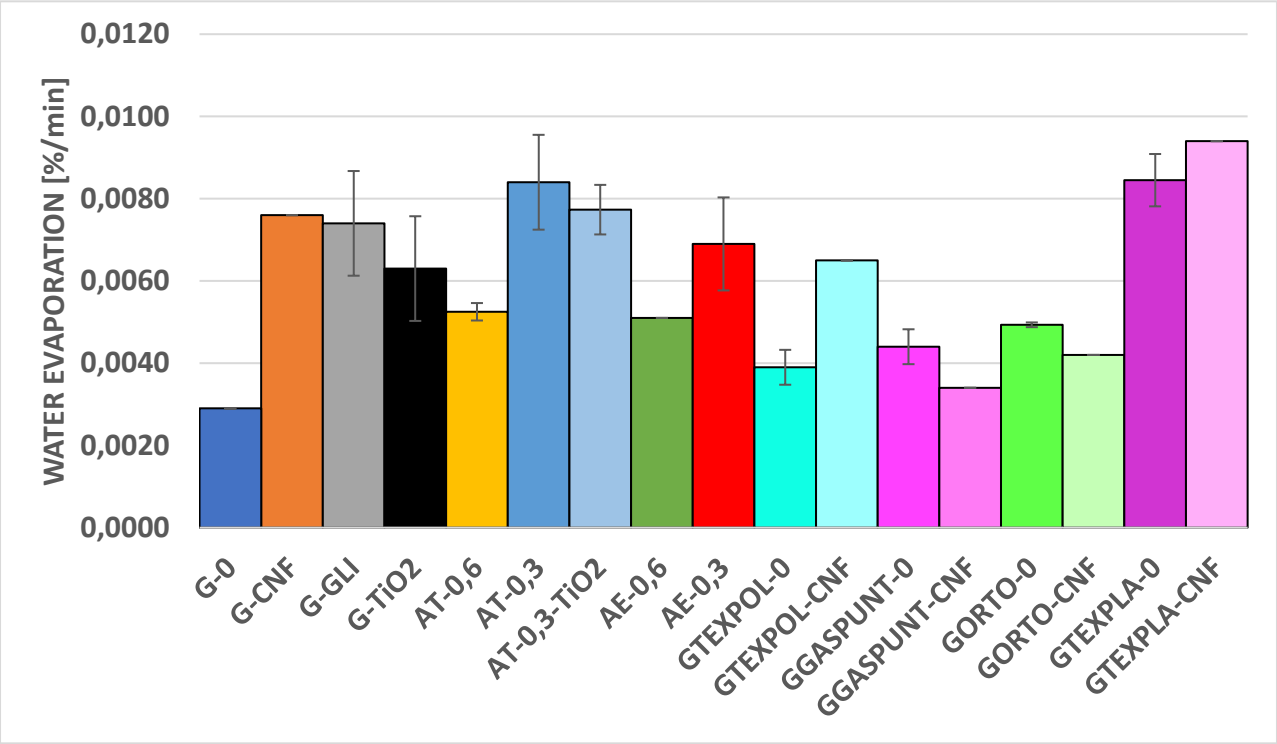

Figure 51: General summary of all the WHT tests.

4.2.4 VERTICAL CAPILLARITY RESULTS

When a dry porous medium contacts a liquid reservoir, the liquid is transported into the porous medium driven by capillary force. This phenomenon is known as capillary penetration. Capillary penetration in porous media is commonly observed in phenomena such as water absorbing into paper and rising damp in concrete walls. Recently, capillary penetration has attracted increasing scientific and industrial attention, owing to the high value of its diverse contemporary applications including paper-based microfluidics, medical diagnosis, energy harvesting devices, advanced textile engineering, cooling devices, architectural conservation, and oil recovery. Capillary penetration has also been utilized as an inverse method to determine the effective properties (e.g., the pore size distribution and porosity) of porous media in both numerical and experimental approaches. Capillary penetration in porous media shares a similar dynamic mechanism with capillary flow in hollow tubes, with both processes resisted by viscous forces (Liu, Wu, Gan, Hanaor, & Chen, 2018).

Looking at Figure 52, it is observed that treated gauzes have a slight improvement in their wicking ability. Although, when adding progressively the additives used in the study, this capacity has been negatively affected in a very light way. Concretely to the addition of TEMPO nanofibres, an improvement of 22% on the untreated gauzes from the Josep Trueta Hospital has been observed. The capillarity increases because when the CNF have been added, they act providing more entrances to the water to rise. As well, these entrances have smaller radius than the original ones; so, the smaller the capillary radius is, the most capillarity is obtained. On the other hand, as said before, when adding glycerol and also TiO_2, the improvement of properties only rises up to 8,5% and 1,5%, respectively. So, unfortunately, these improvements noticed are not enough to considerer that the infusion operation is feasible.

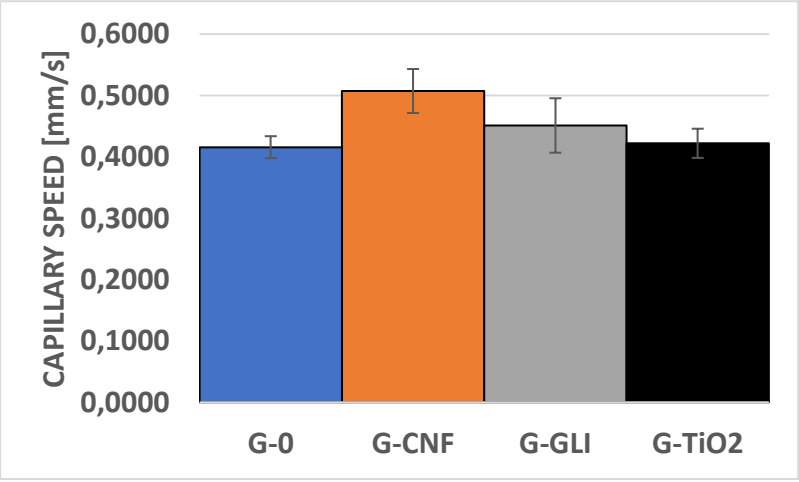

Figure 52: Results comparison from the VWT applied on the gauzes from the JTH.

By comparing the same gauzes from JTH with the other treated gauzes, it is seen the same behaviour in all of them. The consumables show an improvement in their wicking ability due to the same reasoning explained above. Moreover, this improvement ranges between 22% and 27% in all cases. This results not seem to be the best ones; in spite of, if they are compared to the results from Meftahi et al., 2010 research there is such a very small difference, because their manufactured BNC gauzes showed a wicking improvement of 30%. Considering that prior value, it is possible to affirm that the CNF gauzes seem more viable than the BNC ones. So, the last ones require a week to be correctly manufactured and the CNF gauzes require 2h or even less (if the CNF have been previously prepared and characterized).

Numerically, the best result of all the untreated gauzes is shown by Texpol gauzes with a capillary speed of 0,4868 mm/s, followed by a tinny difference for the non-woven gauzes of Gaspunt (0,4559mm/s) and Texpla (0,4317 mm/s). What looks reasonable because the non-woven fabrics theoretically offer more and smaller capillary entrances for water to rise up through the samples. Regarding the samples treated, exactly the same behaviour is observed, since the same order has been kept. The reason of this is due to the similar improvement that all the samples have suffered.

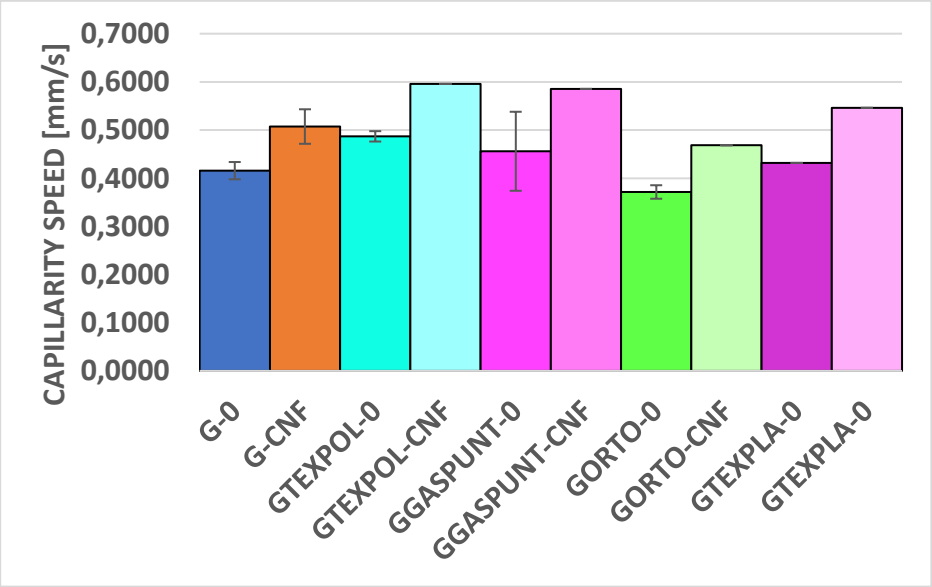

Figure 53: VWT results from the analysis of all the evaluated gauzes.

Now, looking at the results about aerogels shown in Figure 54, it has been clearly distinguished that enzymatic aerogels have the best wicking capacities. As an example, to have an idea of the experienced speed (0,6592mm/s for AE-0,6 and 0,7592 for AE-0,3), after 15 minutes from the beginning of the test they were able to travel at least 12,5 cm minimum from the 17 available. Whereas, the other samples arrived maximum

to 5 cm. This huge difference is due to the internal structure and CNF organization while they are manufactured. Enzymatic aerogels have the most pored structure and as well as they don't have the same length of nanofibres, as seen in Figure 43. This fact ends providing to AE better conditions to absorb water by capillarity. Specifically, the minimum difference between AE and AT is from 0,38mm/s (137%) and the difference between AE samples is from 15%, such a small difference taking into account that the difference between AT rises to 50%. When comparing TEMPO aerogels, it is observed that the highest the concentration of CNF is, the highest capillarity is obtained. The AT-0,6 have been the faster ones, in spite of, the AT-0,3 have been the slowest. The reason why this happens, is because aerogels at 0,6% of CNF content seem to be less organized than the AT-0,3 ones; so, they probably have little more entrances than the second ones. In addition, when TiO_2 was introduced, the results continued decreasing until 22%. and the worst case is from AT-0,3-TiO_2. This phenomenon is due to the preference of CNF for titanium dioxide nanoparticles, then the consumable has les capillary access. As well, supposing that TiO_2 nanoparticles have a total spherical shape, they can be an impediment to water rise.

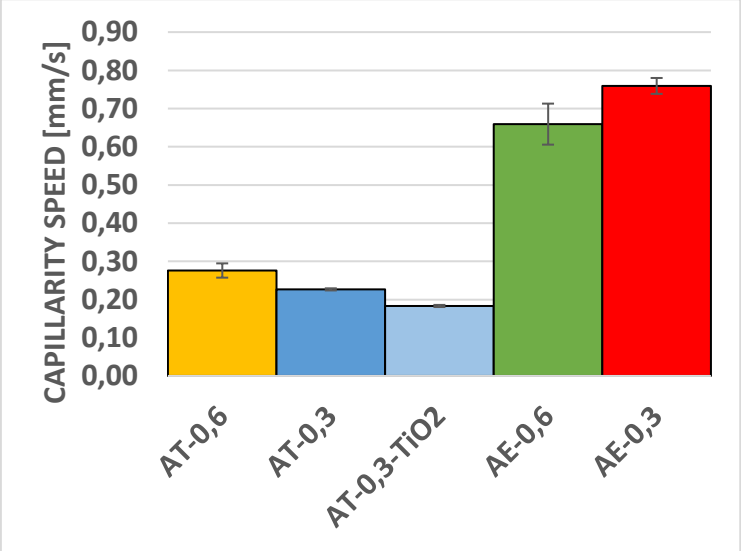

Figure 54: Aerogels comparison in function of their VWT results.

Regarding the evolutionary graphics of speed and distance over time, attached on the annexes (from Figure 69 to Figure 74, is verified that the general behaviour of all consumables analysed is practically the same. The capillarity speed of all the samples was maximum during the first instants. Then it decreased a lot until it got stopped at a very small velocity. Once at this speed, normally, the behaviour remained constant for the rest of time. This happens because it is at the beginning when the adhesion forces created by the liquid on porosities and fibres are stronger, compared to the forces of cohesion. But, once these forces are equated,

the speed diminishes dramatically and almost the liquid is no longer moving. Even though, when the speed is not less than 0,2 mm/s, the liquid continues progressing slowly through the porosities and fibres. Logically, with the displacement graphics it can be also certified that the speed is higher at the beginning, because it coincides with the moment when the water traverses more distance.

Lastly, when compiling all the results in the summary (Figure 55), it is observed that the enzymatic aerogels are those that have the best wicking capacity, followed by the best gauzes (GTEXPOL and GGASPUNT). The lowest values are surprisingly those from the AT aerogels, concretely the worst consumable is the AT-0,3-TiO_2. All the other values range between 0,5 mm/s and 0,3mm/s. In spite of that, the most important thing is that independently of which type of gauze is selected, the wicking ability is improved.

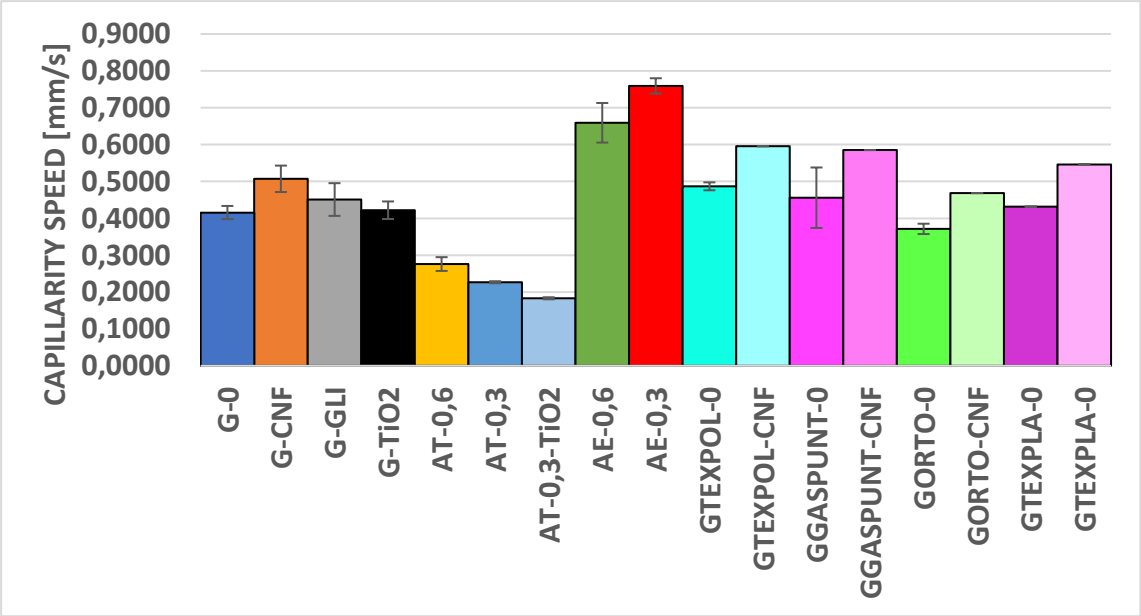

Figure 55: Global summary of all VWT results.

4.2.5 STRESS-STRAIN CURVES

Different from what have been exposed until now, are the results obtained from the stress-strain, because some changes have been introduced. Before but, it is necessary to keep in mind that in this case no aerogels have been evaluated, due to the weakness they showed along the water tests. Despite, almost all the gauzes have been evaluated.

Figure 56 is a comparison between all the tests that have been carried out in the JTH gauzes. Apparently, it is observed that G-CNF are able to support greater efforts compared to the reference gauzes. But, considering the deviations that show each type of gauze on Figure 58, the improvement of 23,6% could as well decrease

considerably to the point where there is no improvement or even the results are worse. A cause can be the way some samples have been tested. When adding CNF, the gauzes have more wrinkles and they show some increment of their internal stress, too. All these facts difficult the colocation of the sample before starting the test and also the forces applied will not be equal in all the gauzes surface forces.

When evaluating the samples with CNF and glycerol, it is observed that they are 1,10 times better than G-0, such a small improvement. Despite, comparing its value to the G-CNF one, the effort is negatively affected a 10,7%. Adding TiO_2, the results show that the gauzes support fewer large efforts than the others. If the deviations are considered, hypothetically could be that treated gauzes from JTH get worse when infused. By contrast, the addition of additives has not provided enough better elasticity properties to considerer that there have been a good improvement. This small elasticity gain is for two reasons: the first one is dues to the placement of glycerol on the gauzes structure. Glycerol binds in the interphase between cotton and CNF, reducing the inner tension experienced by the sample by containing only nanofibres. The other reason is due to the TiO_2, since the CNFs show a greater affinity to cover these molecules. So, there is less amount of CNF which increases the internal tensions into gauzes.

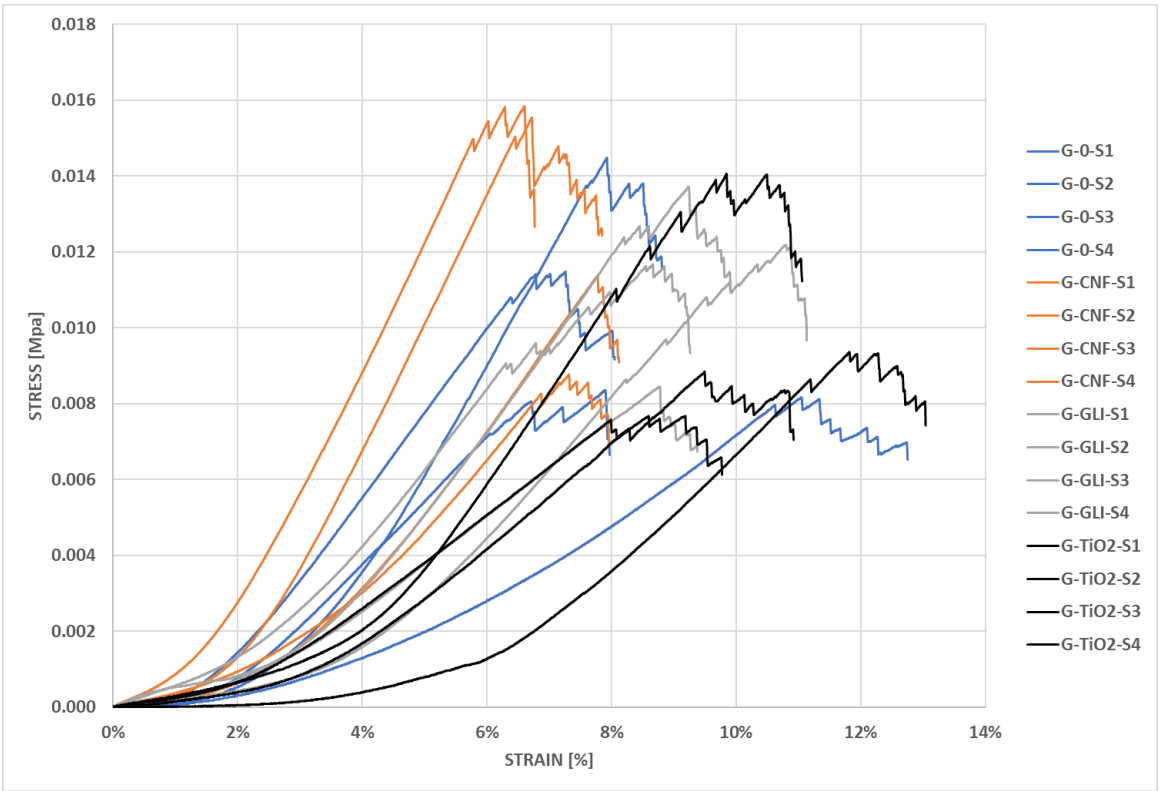

Figure 56: ST-ST curves for treated and non-treated JTH gauzes.

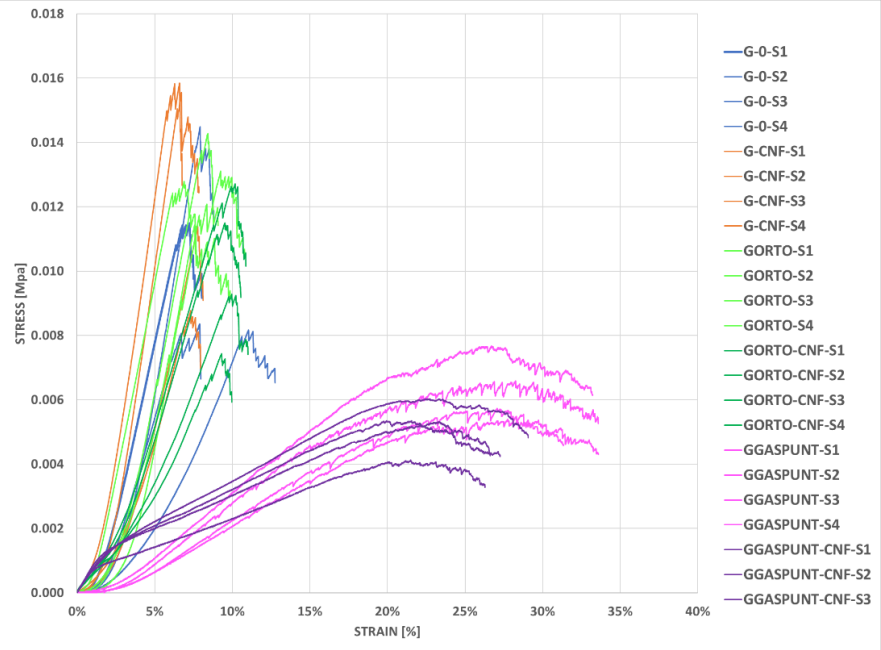

Figure 57: ST-ST curves for treated and non-treated gauzes from different suppliers.

Then, when evaluating the results presented in the Figure 57, there is a clear difference between woven gauzes and non-woven gauzes. Both woven gauzes (JTH and "Ortopedia y Cirugia"), before being treated are 1,64 and 2,03 times more resistant than the GGASPUNT. This difference is also due to the different internal distribution that each one has. Looking again on Figure 34 and Figure 35, observe how all the cotton threads of woven gauzes have an organized and oriented structure; whereas the non-woven gauzes have a free distribution along all the surface. So, the more oriented and organized the fibres are, the more resistance they will have. However, half of the beams from the woven gauzes are in the test direction, so this is also better for these samples. In spite of, non-woven gauze due to its composition (70% viscose and 30% polyester) and distribution must exceed a minimum elongation to start traction. In addition, since Gaspunt gauzes bring polyester in their composition, it will provide the gauze more flexibility, because its polymeric chains are longer and stronger than the cellulose ones.

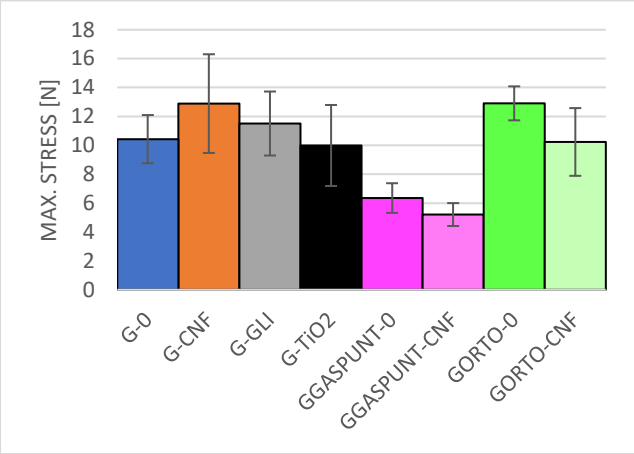

Figure 58: Maximum stress tolerated for each sample.

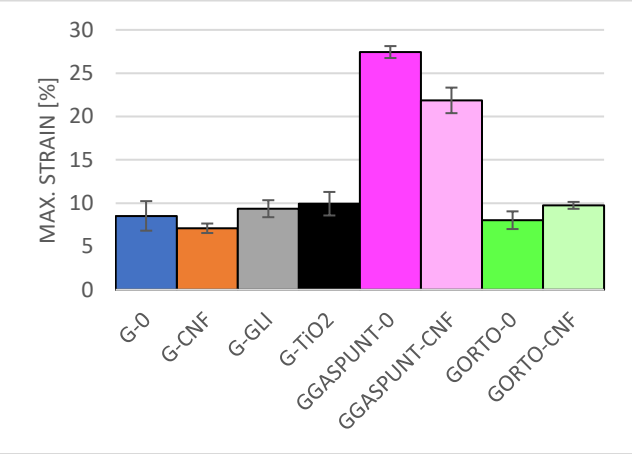

Figure 59: Maximum strain tolerated for each sample.

4.2.6 ANTIMICROBIAL TEST

With regard to the antimicrobial test, one week after the bacterium and fungus were inoculated, the results are showed in Figure 60 and Figure 61. In any case, the behaviour has been the expected because no inhibition rings can be appreciated. So, it means that these consumables do not segregate any unexpected antibiotic substances.

Probably, a fact to mention is that aerogels seem to have more quantity of bacterium and fungus grown, because all they structure is made by CNF, which are easier for the microorganisms to eat. Instead, gauzes are made by cotton filaments (long cellulose chains), which are worse to be eaten and grow up. Although, under any circumstances this assessment can be taken as true since this analysis is qualitative. In order to verify the statement, a quantitative analysis should be carried out, counting the number of colonies of each type of microorganisms.

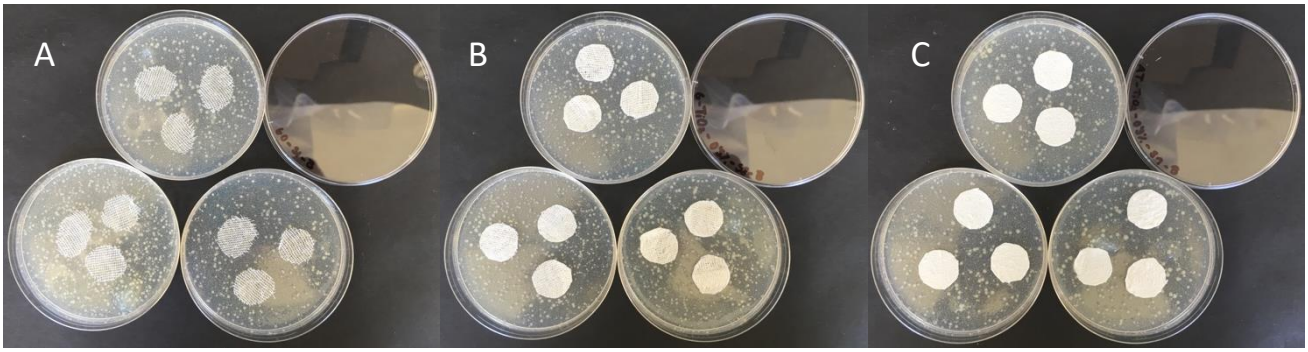

Figure 60: Antimicrobial tests results after the inoculation of a bacteria (Bacillus): A) JTH gauzes without treatment; B) JTH gauzes with TEMPO-CNF, glycerol and TiO_2; C) TEMPO-CNF aerogels at 0,3% of consistency.

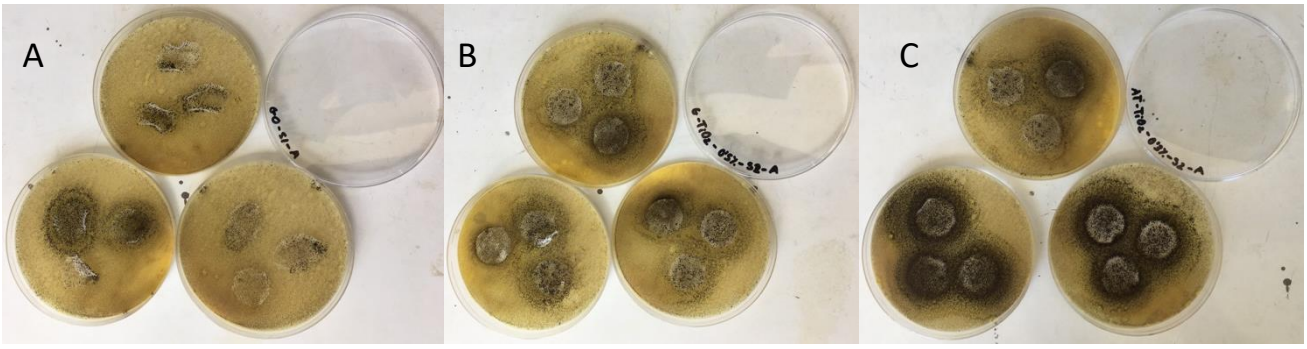

Figure 61: Antimicrobial tests results after the inoculation of a fungus (Aspergillus Niger): A) JTH gauzes without treatment; B) JTH gauzes with TEMPO-CNF, glycerol and TiO_2; C) TEMPO-CNF aerogels at 0,3% of consistency.

4.2.7 RADIOPACITY RESULTS

Finally, the last test carried out to the manufactured consumables was the radiopacity test. First of all, the samples took a radiography with a less sensible RX machine than the exposed in page 45, in order to see if it was already able to appreciate something. The first radiography taken is showed on Figure 62 (B) and nothing can be observed at a first glance.

Then it was decided to make use of a new RX machine, which is supposed to have more precision and sensibility to radiopacity. Looking on the results from Figure 62 (B), unfortunately, no radiopacity was detected at any time. Casually, the silhouette of the blanch can be appreciated minimally, but this is due to the optical properties of materials. According to the professionals who did the radiographies there are a lot of polymeric materials which shape can be detected without having radiopacity properties. Due to this fact, some coins where placed next to the samples to see the difference between a real radiopacity material and the gauzes. But definitely, any improvement is seen with the addition of the TiO_2. This phenomenon probably happens because the titanium dioxide nanoparticles have a diameter too small to avoid being detected by the RX. So, it cannot be said that there is no titanium dioxide; as it is possible to see in Figure 63, both, gauzes and aerogels have TiO_2 particles attached in their structure. Also, in the same figures, it can be appreciated how unexpectedly the CNF cover the TiO_2.

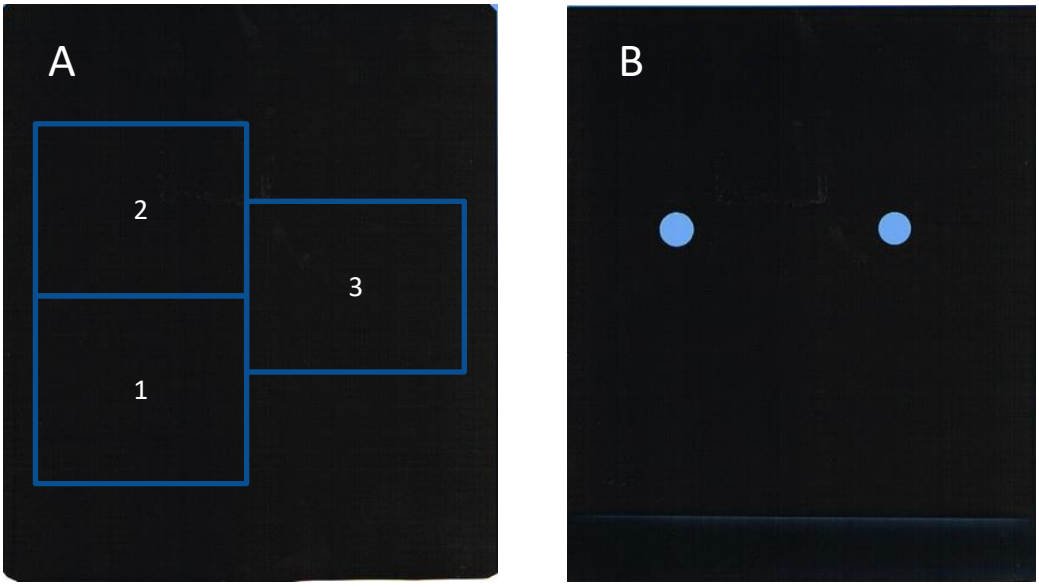

Figure 62: (A) Radiography done with the old RX machine [(1)G-0, (2) G-TiO_2, (3)AT-0,3-TiO_2]; (B) Radiography done with the new RX machine, where can be only observed the circular shape of the coins to compare the results.

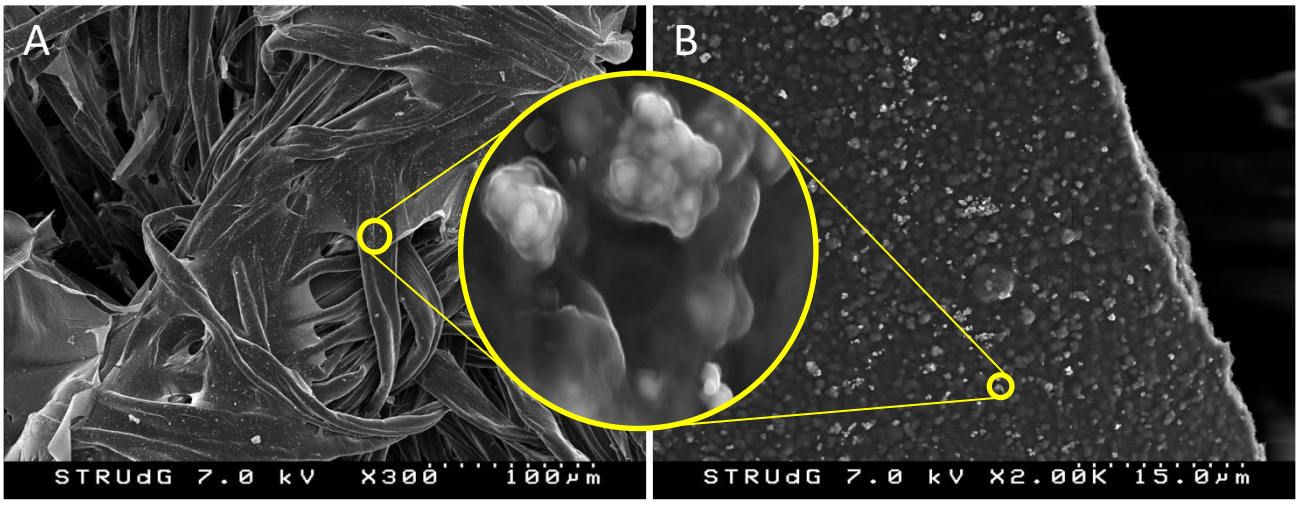

Figure 63: Samples analysed through FE-SEM: (A) G-TiO_2; (B) AT-0,3-TiO_2

5 CONCLUSIONS

The present work was set with the main objective of developing gauzes with greater absorption than those used habitually at Josep Trueta Hospital, in Girona. This way, it would be possible to increase its performance and at the same time reduce its consumption. After completing all the analyses, it can be concluded that the addition of TEMPO- CNF does not improve the absorption of these consumables. Specifically, gauzes have suffered an average decrease of 27% with respect to their initial absorption capacity.

The other main objective, related to the applicability of surgical gauzes, was to try to replace the titanium filaments that are sewn on them. The idea was to substitute them with nanoparticles of titanium dioxide; a substance which contains the same metal, has very good optical properties and has a lower production cost. Achieving these objective gauzes would become economically much more compatible in front of other fabrics, but it has not been this way, since the X-rays realized in the different consumables do not show any radio-optic signal. Additionally, the infusion of TiO_2 has not provided any notable benefits: it helped to the water absorption; but the shape of its particles and their interaction with the CNFs, ended getting worse evaporation and wicking capacity.

However, other objectives have been developed along the project and all of them have received many answers. The first one came from the idea of replacing gauzes using another consumable constituted entirely by CNFs, the aerogels. At the end, results have revealed a great potential in favour of the aerogels, as regards the absorption of liquids. These consumables have been able to improve absorption by nearly 600% from JTH gauzes, which was a totally unexpected fact, although it was known that these materials were highly absorbent. Nevertheless, these products also showed weaknesses. Being their structures made from nanometric fibres joined by hydrogen bonds and Van der Waals forces. When they are soaked into water, they must be carefully treated; as these links are not strong enough to withstand their own weight and they end breaking easily. This means that its applicability is low, but fortunately as discussed in the results, there are studies that try to improve its resistance. If this product continues to develop it would be very positive for medicine.

In order to know if the nanofibres improved gauzes and aerogels properties, other parameters were investigated, too. Firstly, with regard to antimicrobiologic test results, no inhibitory action was observed on the samples. Therefore, if in the future it is desired that these types of products have some antimicrobial application, then should be studied which is the best substance with to achieve this.

Regarding evaporation, its initial value has been increased in the vast majority of samples. This has a positive and a negative point of view depending on the desired application: if we are interested in developing a fabric able to evaporate certain substances faster, then the addition of nanofibres is positive. But if what interests us is to preserve better certain substances (e.g. moisture in tissue burns), then the application of CNFs would not be necessary.

The other property analysed was their wicking ability. Since improving this parameter means that they would be able to transport liquids more quickly wherever it was desired, or even to detect faster a liquids presence (e.g. as a bleedings detectors) due to this phenomenon. Finally, it was detected that by adding nanofibres to gauzes, its capillarity increases between 22% and 27%. Important results considering its applicability. With regard to aerogels, it was discovered that the enzymatic aerogels with a 0,3% of CNF content, had the best capillarity from all the samples with an absorption speed almost of 0,75mm/s. However, the results from the TEMPO aerogel with a 0,3% of CNF content, were the worst with a maximum absorption speed of 0,18mm/s. All these dissimilarities exhibit the importance of which type of CNF is used and also its quantity, to obtain the best performance.

Regarding the traction trials, initially it was thought that nanofibres had to improve the mechanical properties of gauzes. Actually, it has been observed how that is not true, since they become slightly weaker and they neither do not gain elasticity. When analysing some samples with FE-SEM it has been possible to observe how the infused CNFs form a 3-D structure that increases internal tensions and rigidity. Nevertheless, if the

Definitely, if some of the designed consumables have to be chosen, the best option would be the non-woven gauzes. This type of gauze, thanks to its internal organization and the materials with which they are produced, are those that have shown a more balanced behaviour throughout all the tests carried out. Nevertheless, if the only property that interests is the absorption capacity, then aerogels are the best option.

6 BUDGET

The costs associated with carrying out this work are detailed in Table 7, Table 8 and Table 9. The budget will be divided into three sections: the first, the cost of equipment; the second, the cost of the material; and finally the labours costs. The cost of supplies, that is, the costs of water and electricity, will also be determined.

The cost of the equipment is shown in Table 7, which details the initial value, that is, the price of the equipment, and the final value of the equipment. With these two values you get the annual amortization (AA).

Table 7: Cost of equipment.

For the CNF production			
Instrument	Initial Value [€]	Final Value [€]	AA [€/Year]
Analytical Balance	450	67,5	38,25
Stirrer	1.200	180	102
pH-meter	100	15	9
Vacuum Pump	800	120	68
Homogenizer	20.000	3.000	1.700
To produce gauzes and aerogels			
Ultra Turrax	3.000	450	255
Sonicador	5.800	870	493
Freezer	1.000	150	85
Lyophilizer	12.000	1.800	1.020

The initial value was found doing research, however, for the final value it should be taken into account that it is 15% of the initial value. In this work, an average life of the 10-year for each equipment has been assumed. So, to find the annual amortization both values have been subtracted and divided by the 10 years of their useful life. The same equipment that have been used in various activities has been only taken into account once and always where they were used for the first time.

Following in the materials and reagents used for the realization of the work, Table 8 shows the price of each component, the units used and the final price. The components that have been contributed by the LEPAMAP group, such as the BKHP and microorganisms, are not taken into account in the cost of materials and reagents.

Table 8: Cost of materials and reagents.

For the CNF production			
Instrument	Price [€/unit]	Units	Total [€]
Hypochlorite acid	20,19	1	20,19
TEMPO	220	1	220
Sodium Bromide	109,39	1	109,39

Sodium Hydroxide	90,89	1	90,89
Novozym 476	99	1	99
Beaker	2,14	4	8,56
Gloves	45	1	45
For the production of gauzes and aerogels			
Infusion starter kit	163,93	1	163,93
Vacuum sealant tape	3,335	20	66,7
Glycerol	9,67	1	9,67
TiO2	38,14	1	38,14
TOTAL REAGENTS AND MATERIALS			871,47

For the cost of the labours, all the hours devoted by each of the resources that have intervened in the work, have been added and subsequently multiplied by the price of the hour they earn. The values are shown in Table 9.

Table 9: Cost of the workforce.

Employer	Duration [h]	Price [€/h]	Total Price [€]
Chemical Engineer	700	15	10.500,00
Subcontracted researchers	8	30	240,00
Subcontracted STR employer	8	25	200,00
TOTAL LABOUR COSTS			10.940,00

For the costs of supplies, it has been considered that they are going to be considered equivalent to 10% of the total labour force. If this 10% is applied to the 10.940€, there is a cost of supplies of 1.641€.

Finally, adding all the values of the different groups described above the global cost of the research rise to 17.222,22€. Specifically, looking to Figure 64, it is possible to see how labour is the most important cost of a project, followed by the annual amortization of the equipment.

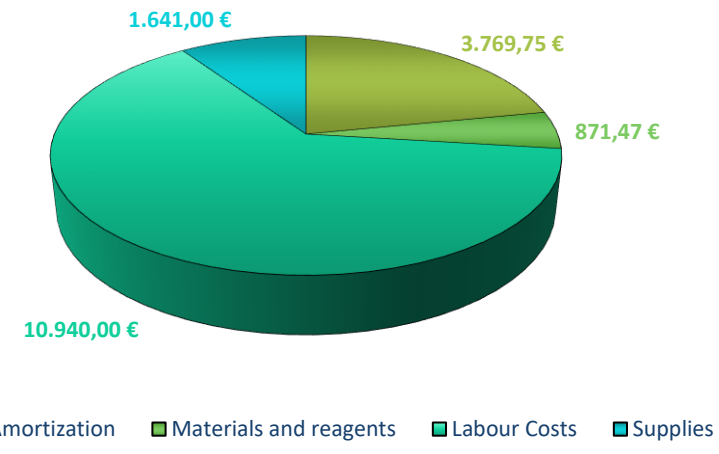

Figure 64: Distribution of the research costs.

7 PLANNING

Finally, amend that any project requires prior planning. In this case, the tool used to carry out the planning of each stage has been the Microsoft Project Professional. The planning has been divided into 8 general sections: the general planning, the literature research, the experimental designs, the samples preparation, the samples analysis and the memory writing. Looking at Figure 65 below, it was planned to start the project on Monday 4th, 2019 and after more than 4 months, on Monday 10th, 2019, it is finished.

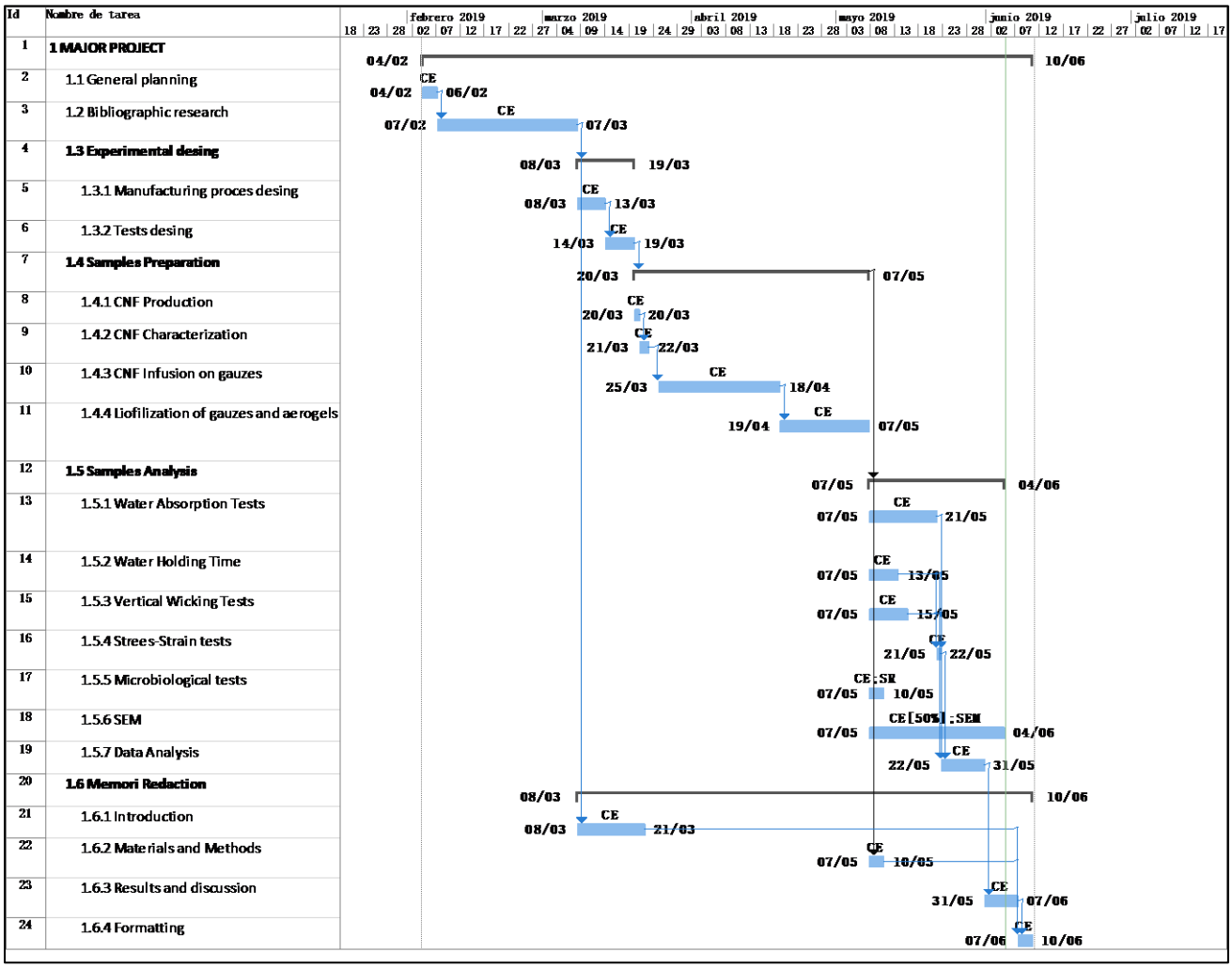

Figure 65: Project planning

.

8 BIBLIOGRAPHY

123RF Limited 2005-2019. (2019). Titanio TiO2. Retrieved June 8, 2019, from https://es.123rf.com/photo_55997298_titanio-tio2-dióxido-de-3d-molécula-aislada-en-blanco.html

Adam, W., Saha-Möller, C. R., & Ganeshpure, P. A. (2001). Synthetic applications of nonmetal catalysts for homogeneous oxidations. *Chemical Reviews*, *101*(11), 3499–3548. https://doi.org/10.1021/cr000019k

Aerogel.org. (2016). Aerogel.org. Retrieved May 26, 2019, from http://www.aerogel.org/

Alibaba. (n.d.). Cementless Femoral Stem Of Hips Prosthesis,Total Hip Replacement,Titanium Hip Stem - Buy Cementless Hips Prosthesis,Cementless Artificial Hips Joint,Artificial Hips Implant Product on Alibaba.com. Retrieved May 14, 2019, from https://www.alibaba.com/product-detail/cementless-femoral-stem-of-hips-prosthesis_60271606425.html

Amazon.in. (2018). Titanium Dioxide Powder. Retrieved June 8, 2019, from https://www.amazon.in/seba-Titanium-Dioxide-Powder-400g/dp/B07D1Z96BD

Arunan, E., Desiraju, G. R., Klein, R. A., Sadlej, J., Scheiner, S., Alkorta, I., … Nesbitt, D. J. (2011). Defining the hydrogen bond. *Pure Appl. Chem*, *83*(8), 1619–1636. https://doi.org/10.1351/PAC-REP-10-01-01

Bailey, W. F., Bobbitt, J. M., & Wiberg, K. B. (2007). Mechanism of the oxidation of alcohols by oxoammonium cations. *Journal of Organic Chemistry*, *72*(12), 4504–4509. https://doi.org/10.1021/jo0704614

Barnhardt Natural Fibers. (2019). *What Is Viscose?* Retrieved from https://www.barnhardtcotton.net/blog/q-and-a-what-is-viscose/?print=pdf

Buettner, K. M., & Valentine, A. M. (2012). Bioinorganic Chemistry of Titanium. *Chemical Reviews*, *112*(3), 1863. https://doi.org/10.1021/cr1002886

Celodev. (2018a). Raffinage enzymatique part 1.

Celodev. (2018b). Raffinage enzymatique partie 2.

Chen, Y., Fan, D., Lyu, S., Li, G., Jiang, F., & Wang, S. (2019). Elasticity-Enhanced and Aligned Structure Nanocellulose Foam-like Aerogel Assembled with Cooperation of Chemical Art and Gradient Freezing. *ACS Sustainable Chemistry and Engineering*, *7*(1), 1381–1388. https://doi.org/10.1021/acssuschemeng.8b05085

Cheng, Q., Wang, S., & Harper, D. P. (2009). Effects of process and source on elastic modulus of single cellulose fibrils evaluated by atomic force microscopy. *Composites Part A: Applied Science and Manufacturing*, *40*(5), 583–588. https://doi.org/10.1016/j.compositesa.2009.02.011

de la Motte, H., Hasani, M., Brelid, H., & Westman, G. (2011). Molecular characterization of hydrolyzed cationized nanocrystalline cellulose, cotton cellulose and softwood kraft pulp using high resolution 1D and 2D NMR. *Carbohydrate Polymers*, *85*(4), 738–746. https://doi.org/10.1016/J.CARBPOL.2011.03.038

Dri, F. L., Hector, L. G., Moon, R. J., & Zavattieri, P. D. (2013). Anisotropy of the elastic properties of crystalline cellulose Iβ from first principles density functional theory with Van der Waals interactions. *Cellulose*, *20*(6), 2703–2718. https://doi.org/10.1007/s10570-013-0071-8

Dugan, J. M., Gough, J. E., & Eichhorn, S. J. (2013). Bacterial cellulose scaffolds and cellulose nanowhiskers for tissue engineering. *Nanomedicine*, *8*(2), 287–298. https://doi.org/10.2217/nnm.12.211

Easy Composites, S. A. (n.d.). Complete Resin Infusion Starter Kit - Easy Composites. Retrieved May 20, 2019, from https://www.easycomposites.co.uk/#!/starter-kits/resin-infusion-starter-kit.html

El Aboussi, S. (2016). *Aplicació de nanofibres lignocel·lulòsiques procedents de residus agrícoles en el procés de producció de paper reciclat*. Universitat de Girona. Retrieved from https://dugi-doc.udg.edu/bitstream/handle/10256/13449/TFG.pdf?sequence=1

Emsley, J. (1980). Very strong hydrogen bonding. *Chemical Society Reviews*, *9*(1), 91. https://doi.org/10.1039/cs9800900091

FARS news agengy. (2014). Enfortiment dels nanofibres de cel·lulosa de Kenaf utilitzats en el paper Kraft. Retrieved June 2, 2019, from http://en.farsnews.com/newstext.aspx?nn=13921206000126

Goldstein, S., & Samuni, A. (2007). Kinetics and mechanism of peroxyl radical reactions with nitroxides. *Journal of Physical Chemistry A*, *111*(6), 1066–1072. https://doi.org/10.1021/jp0655975

Habibi, Y., Lucia, L. A., & Rojas, O. J. (2010). Cellulose Nanocrystals: Chemistry, Self-Assembly, and Applications. *Chemical Reviews*, *110*(6), 3479–3500. https://doi.org/10.1021/cr900339w

Hebeish, A., & Guthrie, J. T. (1981). *The Chemistry and Technology of Cellulosic Copolymers*. Springer Berlin Heidelberg. Retrieved from https://books.google.es/books?hl=ca&lr=&id=I6nxCAAAQBAJ&oi=fnd&pg=PA1&ots=8mj3KXTnlX&sig=SMy4qnCnxtR8MbX2jfDyvW-2Yko&redir_esc=y#v=onepage&q&f=false

Helenius, G., Bäckdahl, H., Bodin, A., Nannmark, U., Gatenholm, P., & Risberg, B. (2006). In vivo biocompatibility of bacterial cellulose. *Journal of Biomedical Materials Research Part A*, *76A*(2), 431–438. https://doi.org/10.1002/jbm.a.30570

Henriksson, M., Henriksson, G., Berglund, L. A., & Lindströ, T. (2007). An environmentally friendly method for enzyme-assisted preparation of microfibrillated cellulose (MFC) nanofibers. https://doi.org/10.1016/j.eurpolymj.2007.05.038

Hsieh, Y. C., Yano, H., Nogi, M., & Eichhorn, S. J. (2008). An estimation of the Young's modulus of bacterial cellulose filaments. *Cellulose*, *15*(4), 507–513. https://doi.org/10.1007/s10570-008-9206-8

ICS, G. de C. (2017). Girona. Institut Català de la Salut. Retrieved May 14, 2019, from http://ics.gencat.cat/ca/lics/memories-dactivitat/memories-territorials/girona/

Isogai, Akira, & Yumiko, K. (1998). Preparation of polyuronic acid from cellulose by TEMPO-mediated oxidation. *Cellulose*, *5*, 153–164.

Isogai, A., Saito, T., & Fukuzumi, H. (2011). TEMPO-oxidized cellulose nanofibers. *Nanoscale*, *3*(1), 71–85. https://doi.org/10.1039/c0nr00583e

Krebs, R. E. (2006). *The history and use of our earth's chemical elements : a reference guide* (2nd ed.). Westport, CT: Greenwood Press. Retrieved from https://books.google.com/books?id=yb9xTj72vNAC

Kroschwitz, J. I., & Seidel, A. (2004). *Kirk-Othmer encyclopedia of chemical technology.* (5th ed.).

KTH, D. de F. i T. dels P. (2019). Tecnologia de fibra i polímers KTH. Retrieved June 1, 2019, from https://www.kth.se/fpt

Li, J., Wan, Y., Li, L., Liang, H., & Wang, J. (2009). Preparation and characterization of 2,3-dialdehyde bacterial cellulose for potential biodegradable tissue engineering scaffolds. *Materials Science and Engineering: C*, *29*(5), 1635–1642. https://doi.org/10.1016/J.MSEC.2009.01.006

Lin, N., & Dufresne, A. (2014a). Nanocellulose in biomedicine: Current status and future prospect. *European Polymer Journal*. https://doi.org/10.1016/j.eurpolymj.2014.07.025

Lin, N., & Dufresne, A. (2014b). Nanocellulose in biomedicine: Current status and future prospect. *European Polymer Journal*, *59*(July), 302–325. https://doi.org/10.1016/j.eurpolymj.2014.07.025

Liu, M., Wu, J., Gan, Y., Hanaor, D. A. H., & Chen, C. Q. (2018). Tuning capillary penetration in porous media: Combining geometrical and evaporation effects. https://doi.org/10.1016/j.ijheatmasstransfer.2018.02.101

Luo, H., Xiong, G., Hu, D., Ren, K., Yao, F., Zhu, Y., … Wan, Y. (2013). Characterization of TEMPO-oxidized bacterial cellulose scaffolds for tissue engineering applications. *Materials Chemistry and Physics*, *143*(1), 373–379. https://doi.org/10.1016/J.MATCHEMPHYS.2013.09.012

Maestre Juanola, N., & Delgado-Aguilar, M. (2016). *Determinació de la viabilitat d'incorporar nanofibres de cel·lulosa com a reforç d'àcid polilàctic*. Girona. Retrieved from https://dugi-doc.udg.edu/bitstream/handle/10256/12818/Nídia Maestre Juanola.pdf?sequence=1

Märtson, M., Viljanto, J., Hurme, T., Laippala, P., & Saukko, P. (1999). Is cellulose sponge degradable or stable as implantation material? An in vivo subcutaneous study in the rat. *Biomaterials*, *20*(21), 1989–1995. https://doi.org/10.1016/S0142-9612(99)00094-0

Medical Market. (2016). Tipos y Usos de Gasas – Blog Medical Market. Retrieved May 26, 2019, from https://blog.medicalmarket.es/tipos-usos-de-gasas/

Meftahi, A., Khajavi, R., Rashidi, A., Sattari, M., Yazdanshenas, M. E., & Torabi, M. (2010). The effects of cotton gauze coating with microbial cellulose. *Cellulose*, *17*(1), 199–204. https://doi.org/10.1007/s10570-009-9377-y

Miyamoto, T., Takahashi, S., Ito, H., Inagaki, H., & Noishiki, Y. (1989). Tissue biocompatibility of cellulose and its derivatives. *Journal of Biomedical Materials Research*, *23*(1), 125–133. https://doi.org/10.1002/jbm.820230110

NET INDUSTRIES. (n.d.). Capillary Action. Retrieved June 2, 2019, from https://science.jrank.org/pages/1182/Capillary-Action.html

Osorio, A., Vásquez, A., Acosta, E., Gil, G., & Bravo, M. (2012). Protocolo para el conteo y recuento de gasas, compresas y otros objetos quirúrgicos. Retrieved June 1, 2019, from https://www.monografias.com/trabajos93/protocolo-conteo-y-recuento-gasas-compresas/protocolo-conteo-y-recuento-gasas-compresas.shtml

Österberg, M., & Cranston, E. D. (2014). Special issue on nanocellulose- Editorial. *Nordic Pulp & Paper Research Journal*, *29*(1), 4–5. https://doi.org/10.3183/npprj-2014-29-01-p004-005

Petersen, N., & Gatenholm, P. (2011). Bacterial cellulose-based materials and medical devices: current state and perspectives. *Applied Microbiology and Biotechnology*, *91*(5), 1277–1286. https://doi.org/10.1007/s00253-011-3432-y

Serra, A., González, I., Oliver-Ortega, H., Tarrès, Q., Delgado-Aguilar, M., & Mutjé, P. (2017). Reducing the amount of catalyst in TEMPO-oxidized cellulose nanofibers: Effect on properties and cost. *Polymers*. https://doi.org/10.3390/polym9110557

Shimotoyodome, A., Suzuki, J., Kumamoto, Y., Hase, T., & Isogai, A. (2011). Regulation of postprandial blood metabolic variables by TEMPO-oxidized cellulose nanofibers. *Biomacromolecules*, *12*(10), 3812–3818. https://doi.org/10.1021/bm2010609

Silberberg, M. S. (Martin S. (2006). *Chemistry : the molecular nature of matter and change* (4th ed.). New York: McGraw-Hill.

Sŏng, S., Younossi, O., Goldsmith, B. W., & United States. Air Force. (2009). *Titanium : industrial base, price trends, and technology initiatives*. RAND Project Air Force. Retrieved from https://books.google.com/?id=tIPFfYW304IC&pg=PA10

Steiner, T. (2002). The Hydrogen Bond in the Solid State. *Angewandte Chemie International Edition*, *41*(1), 48–76. https://doi.org/10.1002/1521-3773(20020104)41:1<48::AID-ANIE48>3.0.CO;2-U

Tarrés, Q., Saguer, E., Pèlach, M. A., Alcalà, M., Delgado-Aguilar, M., & Mutjé, P. (2016). The feasibility of incorporating cellulose micro/nanofibers in papermaking processes: the relevance of enzymatic hydrolysis. *Cellulose*. https://doi.org/10.1007/s10570-016-0889-y

TEXPOL, S. A. (n.d.). Texpol | Productes | Apòsits de gasa estèrils. Retrieved May 14, 2019, from http://www.texpol.com/ca/productos/227/apòsits-de-gasa-estèrils.html

Textile Learner. (2019). Chemical Composition of Cotton Fiber. Retrieved June 8, 2019, from https://textilelearner.blogspot.com/2014/10/chemical-composition-of-cotton-fiber.html

Thomas, B. G. P. (1960). What is Aerogel? Theory, Properties and, 1–3.

Wallace, R., & Venere, E. (2018). cellulose nanocrystals Lab Notes. Retrieved June 2, 2019, from https://www.fpl.fs.fed.us/labnotes/?tag=cellulose-nanocrystals

Wu ', X., Moon ', R. J., Martini, A., Wu, X., Moon, R. J., & Martini, A. (2013). Crystalline cellulose elastic modulus predicted by atomistic models of uniform deformation and nanoscale indentation. *Cellulose*, *20*, 43–55. https://doi.org/10.10071s10570-012-9823-0

Yoshida, E. (2009). Photo-living radical polymerization of methyl methacrylate by 2,2,6,6-tetramethylpiperidine-1-oxyl in the presence of a photo-acid generator. *Colloid and Polymer Science*, *287*(7), 767–772. https://doi.org/10.1007/s00396-009-2023-2

Zhang, X., & Cresswell, M. (2016). Materials Fundamentals of Drug Controlled Release. In *Inorganic Controlled Release Technology* (pp. 17–55). Elsevier. https://doi.org/10.1016/B978-0-08-099991-3.00002-8

ANNEX

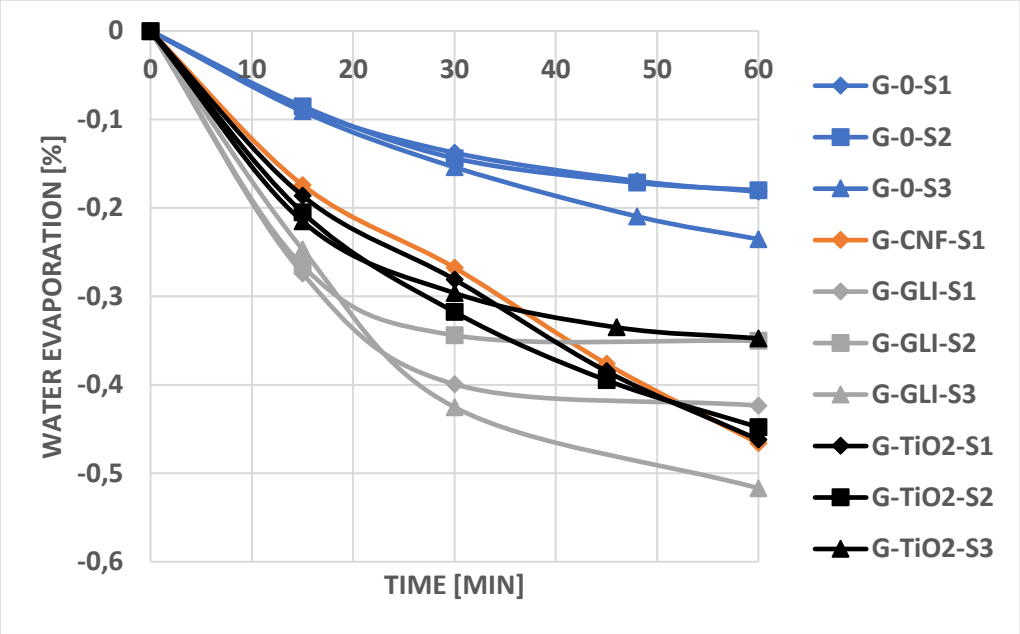

Figure 66: Evolution of evaporation in front of time along the WHT test on JTH gauzes.

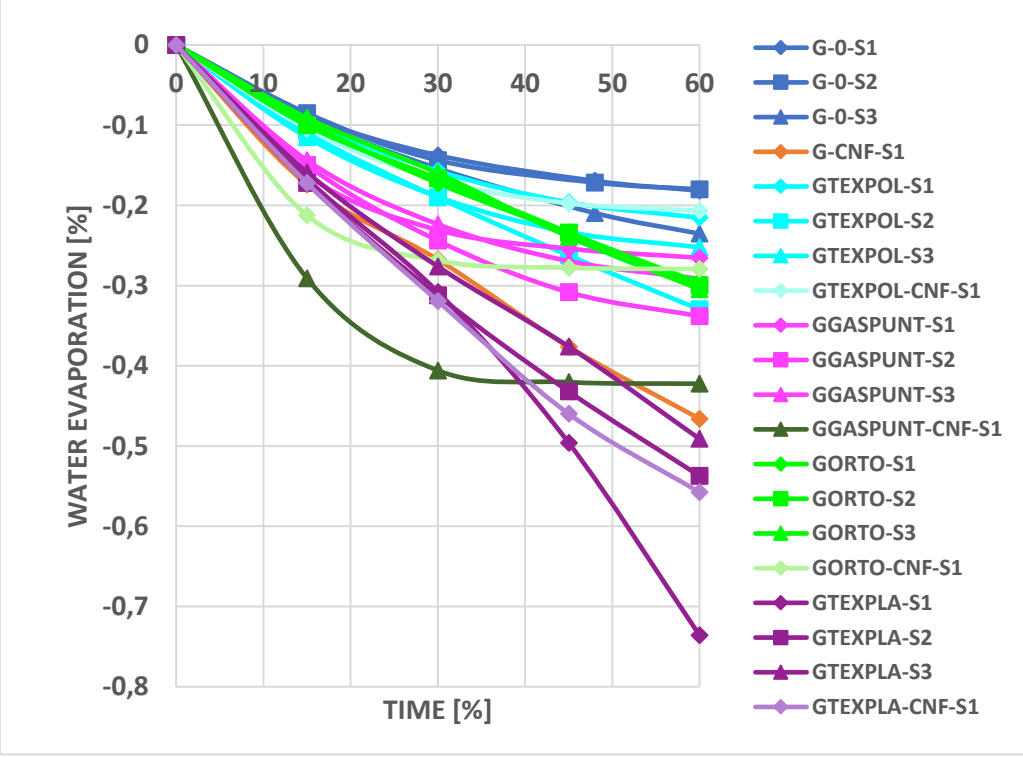

Figure 67: Evolution of evaporation in front of time along the WHT test on gauzes from different suppliers.

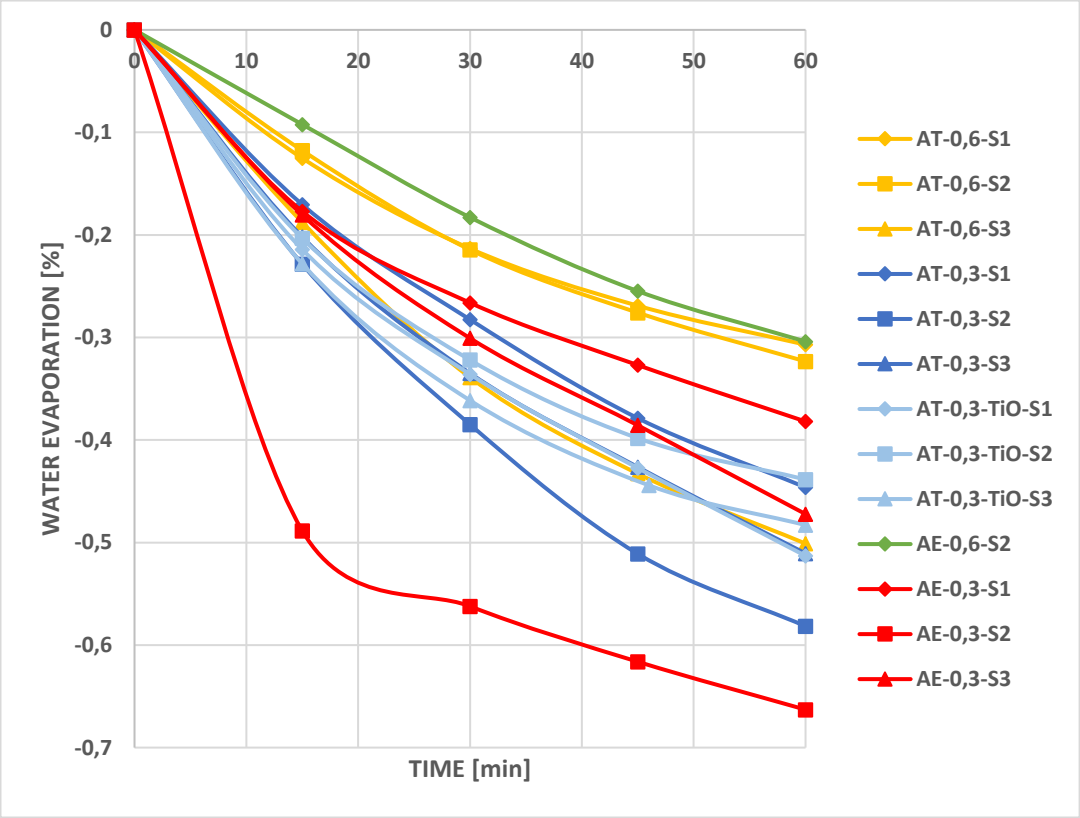

Figure 68: Evolution of evaporation in front of time along the WHT test on aerogels.

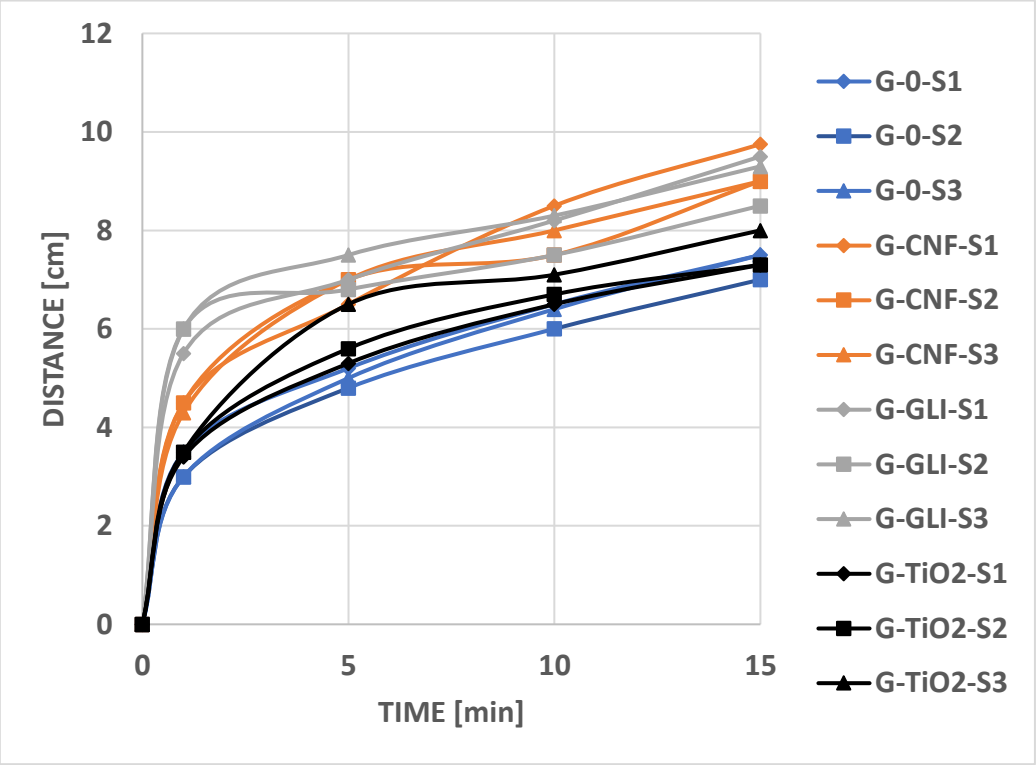

Figure 69: Distance evolution in front of time along the VWT on gauzes from JTH.

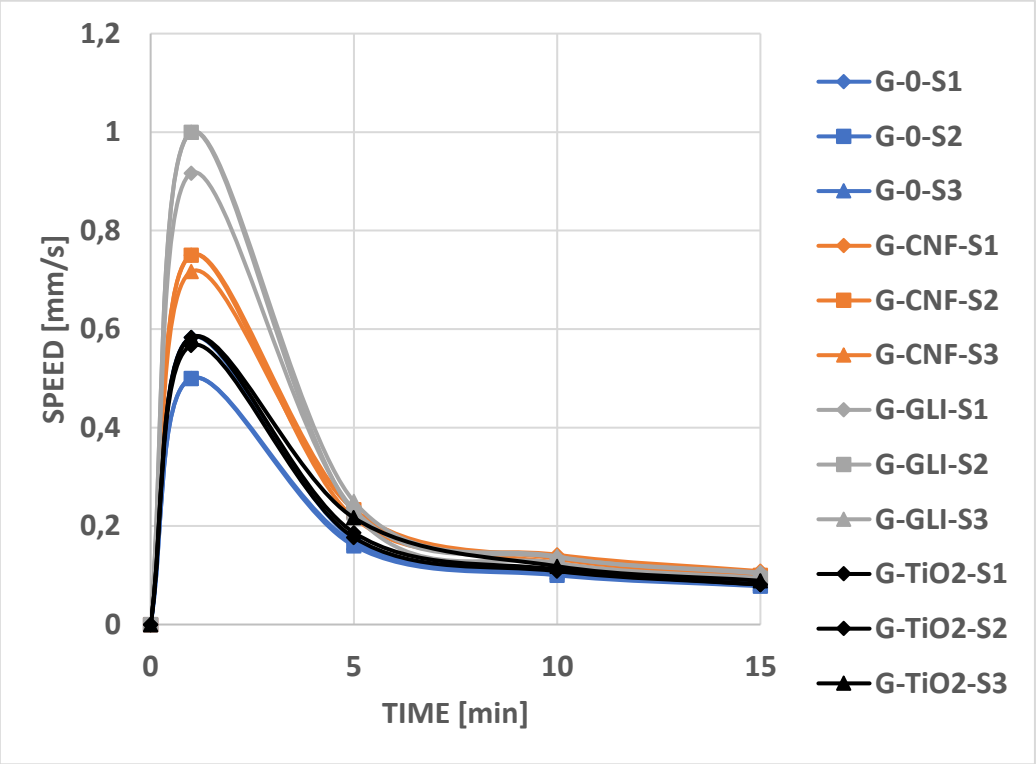

Figure 70: Speed evolution in front of time along the VWT on gauzes from JTH.

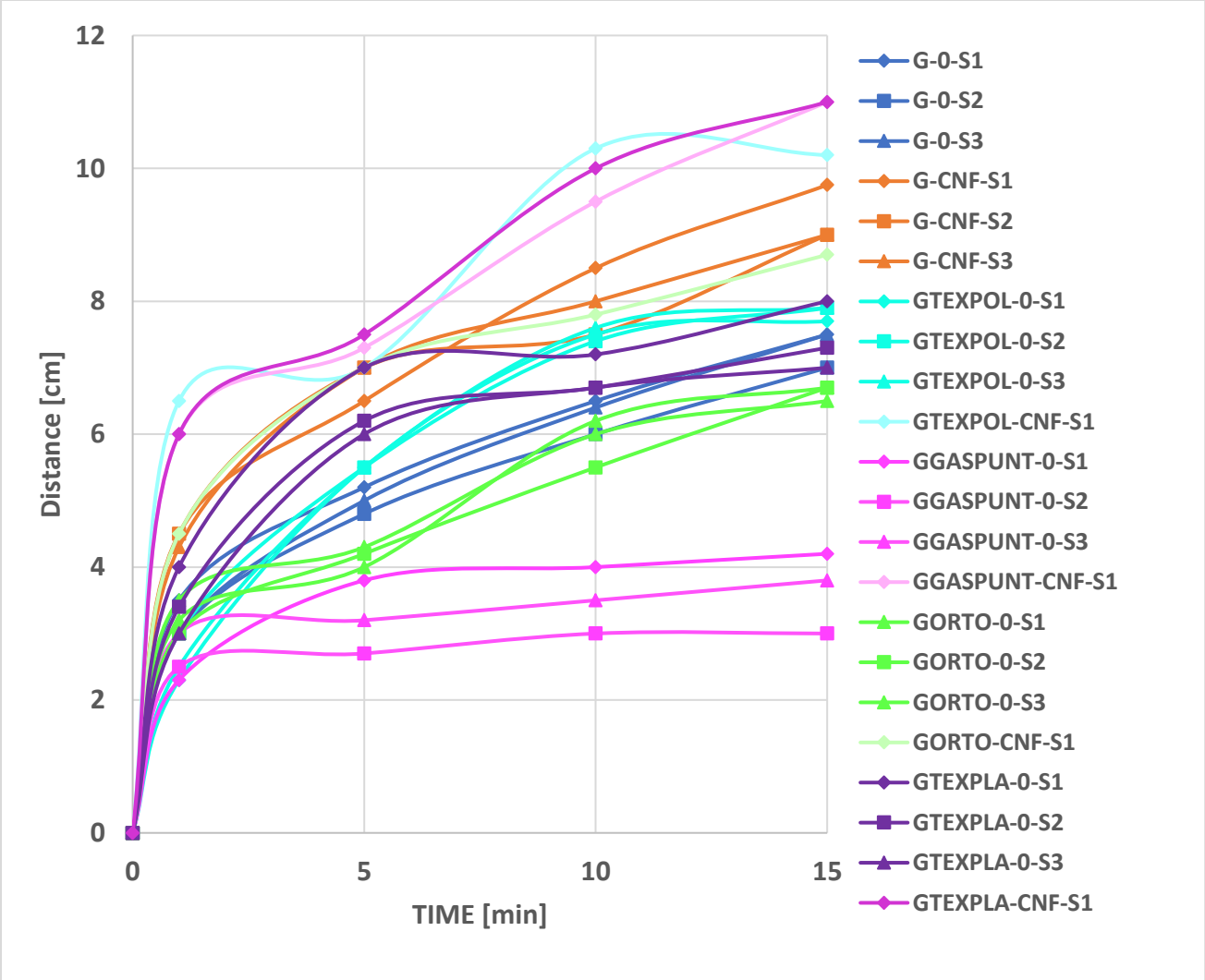

Figure 71: Distance evolution in front of time along the VWT on gauzes from different suppliers.

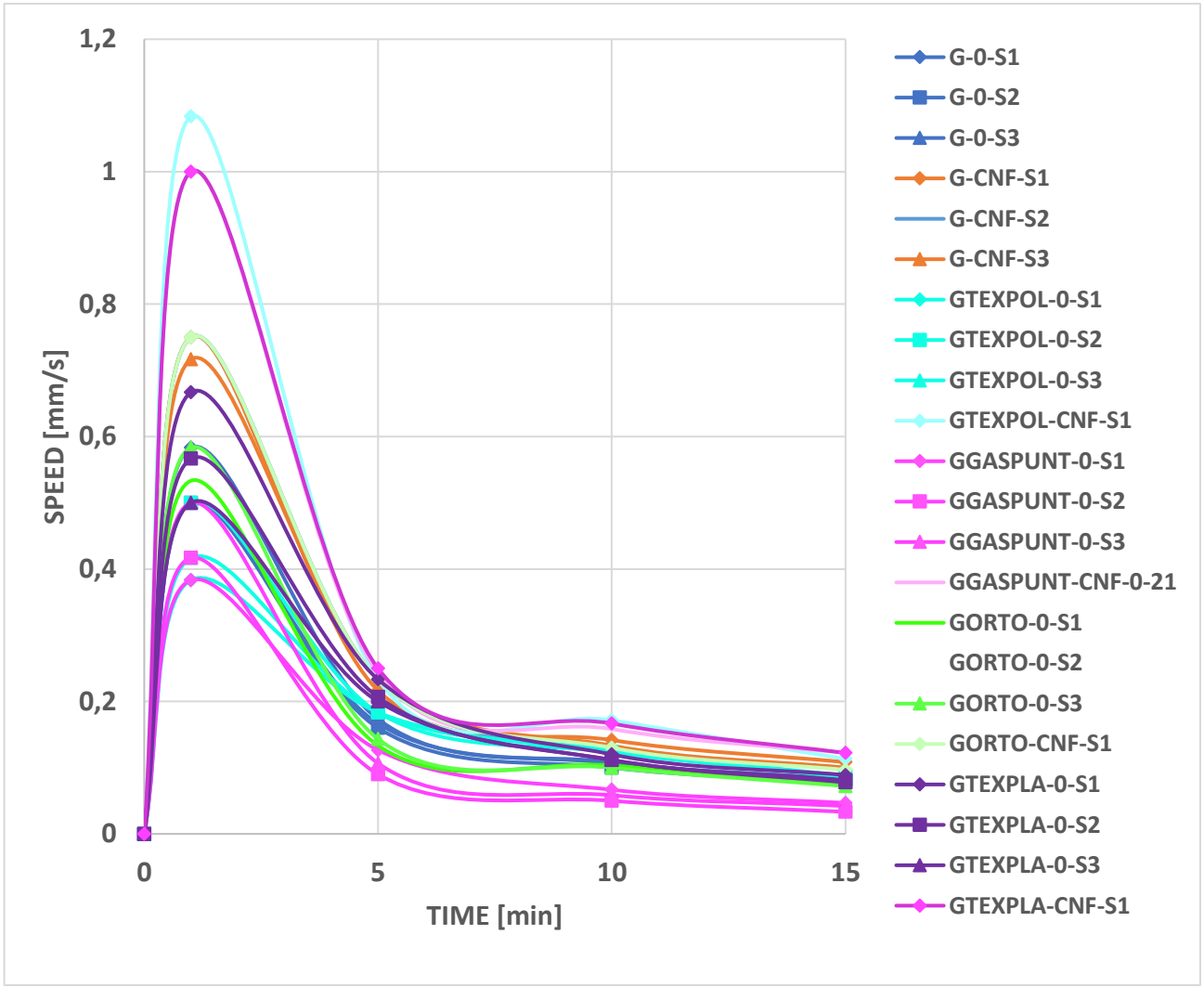

Figure 72: Speed evolution in front of time along the VWT on gauzes from different suppliers.

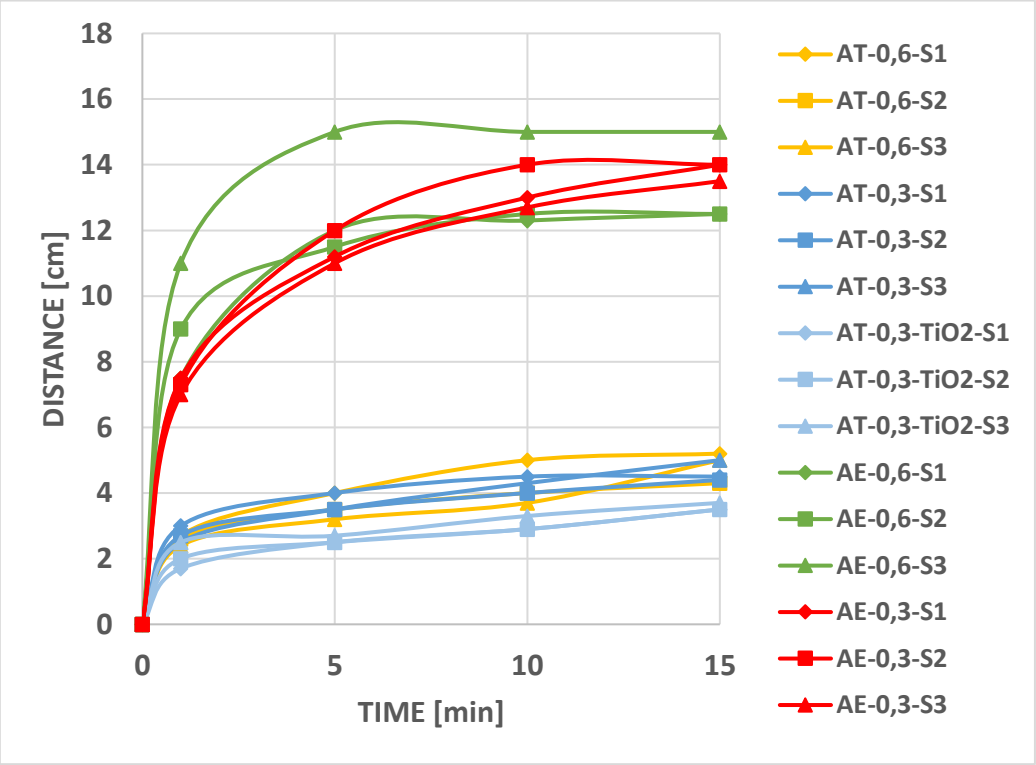

Figure 73: Distance evolution in front of time along the VWT on aerogels.

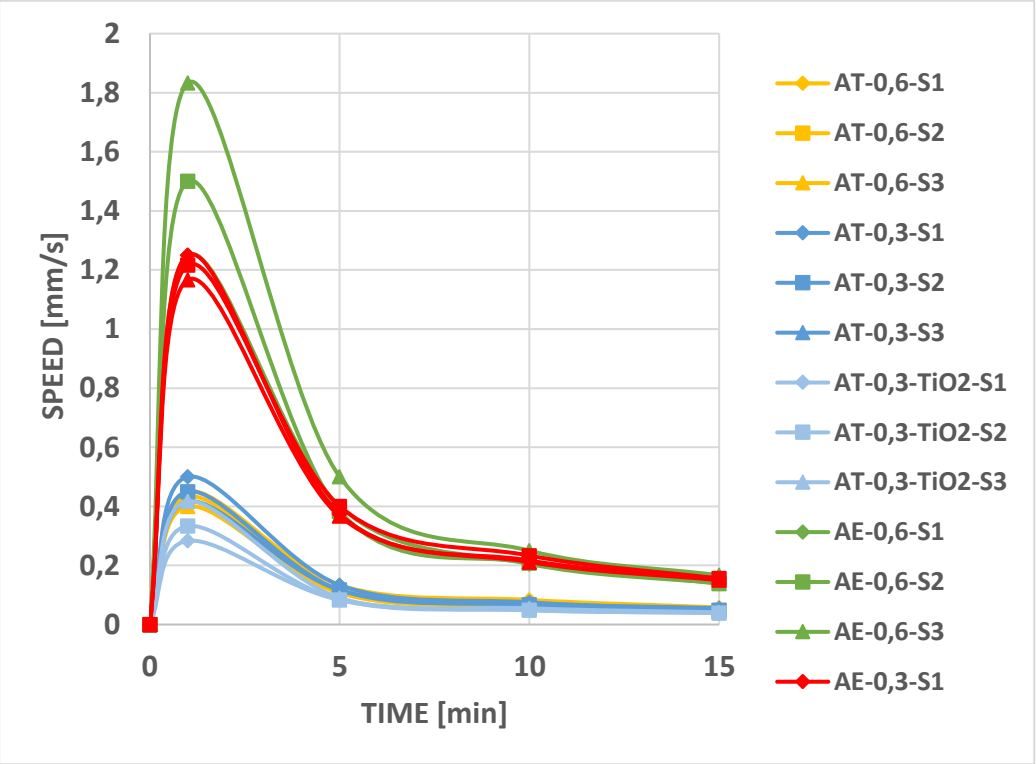

Figure 74: Speed evolution in front of time along the VWT on aerogels.